

**Real-Time Monitoring of Resin Transfer Molding
Using a Grid of Dielectric Sensors**

by

Bekir Yenilmez

**A Thesis Submitted to the
Graduate School of Engineering
in Partial Fulfillment of the Requirements for
the Degree of**

**Master of Science
in
Mechanical Engineering**

Koc University

September, 2008

Koc University
Graduate School of Sciences and Engineering

This is to certify that I have examined this copy of a master's thesis by

Bekir Yenilmez

and have found that it is complete and satisfactory in all respects,
and that any and all revisions required by the final
examining committee have been made.

Committee Members:

Assist. Prof. E. Murat Sözer

Assist. Prof. Mehmet Sayar

Assist. Prof. Erdem Alaca

Date:

ABSTRACT

A grid of fifty dielectric sensors is embedded in mold walls to monitor the Resin Transfer Molding (RTM) process. The capacitance of each sensor increases as resin occupies the space between the upper and lower sensor plates, making it possible to monitor mold filling. After complete mold filling, the same sensors are used to monitor the cure level of the resin since the capacitance decreases with curing. Monitoring of mold filling can be used as an in-situ data for a process control to prevent dry spots in the part; and monitoring of resin cure level can be used to determine the minimum time required before de-molding the part once the green strength and stiffness are achieved. In previous studies, a small number of dielectric sensors were used in an entire mold cavity. As experimentally shown in this study, these large-plate or lineal dielectric sensors may mislead the user since a sensor measures the total fraction of the sensor's plate area occupied by resin but not the resin's whereabouts on the sensor. To avoid ambiguity and yet maintain detailed flow monitoring, a grid of smaller dielectric sensors was used in this study. The grid was made at the projections of vertical and horizontal electrodes embedded in the two opposite mold lids, to avoid the complexity of embedding separate sensors. The developed sensor operation system eliminated the tedious and costly manufacturing of conventionally shielded sensors. The success of the developed sensor system was demonstrated in RTM experiments for several different case studies.

ÖZETÇE

Kalıp içine monte edilmiş ızgara şeklindeki elli dielektrik algılayıcı ile Reçine Tranfer Kalıplama (RTM) üretim usulü izlenmiştir. Her bir algılayıcının alt ve üst plakaları arası reçine ile doldukça, algılayıcının elektrik kapasitesi artmaktadır; bu sayede kalıp içindeki reçine akışının izlenmesi mümkün olmaktadır. Kalıp tamamen dolduktan sonra, aynı algılayıcılar reçinenin kürleşme seviyesinin izlenmesinde kullanılırlar, çünkü kür seviyesi arttıkça reçinenin elektrik kapasitesi düşmektedir. Reçine akışının izlenmesi, üretim usulünün kontrolünde gerçek zamanlı veri olarak kullanılır; kür seviyesinin izlenmesi de kompozit parçanın yeterli mukavemet ve bükülmezlik değerlerine eriştikten sonra kalıbın ne zaman açılarak parçanın çıkartılmasına karar vermek için kullanılır. Daha önceki çalışmalarda, az sayıda dielektrik algılayıcısı tüm kalıp içinin izlenmesinde kullanılmıştır. Bu çalışmada deneysel olarak gösterilmiştir ki, geniş plakalı ya da doğrusal dielektrik algılayıcıları kullanıcıyı yanlış yönlendirebilir, çünkü bir algılayıcı ancak yüzey alanının ne kadarının reçine ile kaplandığını ölçebilir, reçinenin kalıp içinde nerede olduğunu algılayamaz. Bu yanlış anlama durumunu yok etmek ve yine de yeterince detaylı akış izlenmesine olanak vermesi için, bu çalışmada ızgara şeklindeki ufak dielektrik algılayıcıları kullanılmıştır. Izgaranın oluşturulmasında, uğraştırıcı bir usul olan her bir algılayıcının tek tek kalıba monte edilmesi yerine, dikey ve yatay elektrotlar kalıbın karşılıklı iki plakasına yerleştirilmiştir. Geliştirilen algılayıcı çalıştırma sistemi sayesinde, uğraştırıcı ve masraflı konvensiyonel yalıtılmış algılayıcı üretimine gerek kalmamıştır. Bazı RTM deneylerinde kullanılarak, geliştirilen algılayıcı sisteminin başarısı gösterilmiştir.

ACKNOWLEDGEMENTS

I would like to thank my supervisor Murat Sözer for all his guidance, efforts and continued support. Additionally, I wish to extend my gratitude to the members of my thesis committee for their critical reading and invaluable comments.

I also wish to offer my sincerest thanks to my colleagues whose friendship have made the years in Koc University a most memorable time in my life.

Many thanks are also due to TUBITAK (The Scientific and Technical Research Council of Turkey) for their scholarship at Koc University, Istanbul, Turkey.

Finally, I would like to thank to my family for their endless love and support, especially Nihan Hudson, Teymur Tahseen and Tuna Türkbey for all their help in writing this thesis.

TABLE OF CONTENTS

List of Tables	x
List of Figures	xi
Nomenclature	xiii
Chapter 1: Introduction	1
1.1 Resin Transfer Molding (RTM) Process	1
1.2 Previous Sensor Systems for Flow and Cure Monitoring	2
1.3 Objective.....	5
Chapter 2: Dielectric Sensors	6
2.1 Comparison between Resistive (Voltage) and Dielectric (Capacitive) Sensors	6
2.2 Theory	7
2.3 A Single Dielectric Sensor.....	10
2.3.1 Shielding	11
2.3.2 Grounding	12
2.4 Proposed Method, “Modified Grounded”	13
2.5 The Major Issue of Using a Single Dielectric Sensor.....	15
2.6 Comparison of the Dielectric Sensor Configurations	18

Chapter 3: The Mold	20
3.1 The Experimental Setup	22
Chapter 4: The Electrical System for Operation of Sensors and DAQ	25
4.1 System Operation.....	27
4.2 Circuit Description.....	28
Chapter 5: Experiments	31
5.1 Monitoring of Mold Filling	31
5.2 Monitoring of Resin Cure	37
5.3 Using the Sensor System as Point-Resistive Sensors and Dielectric Sensors	37
Chapter 6: Summary and Conclusions	40
Bibliography	42
Vita	47

Appendix A: RTM material specifications	48
A.1 Datasheet of the resin.....	48
A.2 Injection machine.....	50
A.3 Fabric preform material	51
A.4 RTM process steps overview.....	51
Appendix B: Dielectric Mold	52
B.1 Mold technical drawings.....	52
B.2 Mold 3D visualizations.....	56
B.3 Mold photos	58
Appendix C: Experiment Results	62
C.1 Results of Experiment 6.....	62
C.2 Results of Experiment 11.....	64
C.3 Results of Experiment 12.....	66
C.4 Results of Experiment 14.....	68
C.5 Results of Experiment 15.....	70
C.6 Results of Experiment 16, Case Study 1	72
C.7 Results of Experiment 17, Case Study 2	73

Appendix D: LabVIEW Diagram	74
Appendix E: Electronic Circuit	75
E.1 Amplifier stage calibration data.....	75
E.2 Capacitance versus voltage output data.....	75
E.3 Electronic circuit part list.....	76
E.4 Electronic circuit schematics	78
E.5 Electronic circuit printed circuit board	83
Appendix F: Electronic Component Datasheets	86
F.1 iUSBDAQ-U120816 DAQ card	86
F.2 LF347 operational amplifier	90
F.3 CD4066 grounding switch.....	93
F.4 CD4051, CD4052 analog multiplexer	97

LIST OF TABLES

Table 1: Circuit schematics, diagrams and formulas for different dielectric configurations	14
Table 2: Capacitance measurement using a single large dielectric sensor	16
Table 3: Measurement of empty sensor capacitance for two different sensors	19

LIST OF FIGURES

Figure 1: Electrical circuit of a dielectric sensor	8
Figure 2: Frequency response of Equation (1)	9
Figure 3: Fringing effect on a parallel-plate capacitor	11
Figure 4: (a) Shielding and (b) grounding of multiple sensors (only two are shown for simplicity)	12
Figure 5: The RTM mold.....	21
Figure 6: Experimental setup for RTM	23
Figure 7: Top view of the mold cavity with a grid of 50 embedded dielectric sensors	24
Figure 8: Diagram of the entire monitoring system	26
Figure 9: Electrical circuit schematic of the signal conditioner	29
Figure 10: The relative permittivity, ϵ_r of the fifty sensors (A1, A2, ..., E9, E10) during the mold filling stage of Case Study 1. In each graph, the five row sensors (A, B, C, D and E) were plotted for the corresponding column	33
Figure 11: The relative permittivity, ϵ_r of the fifty sensors during the mold filling stage of Case Study 2	34
Figure 12: The flow front contours at different times using the recorded data of the fifty sensors for Case Study 1	35
Figure 13: The flow front contours at different times using the recorded data of the fifty sensors for Case Study 2	35

Figure 14: The user interface for monitoring the mold filling in Case Study 2. The relative permittivities of the sensors are used to show what regions of the mold cavity are filled/empty at the current time 36

Figure 15: The average of relative permittivities, of the fifty sensors during the resin cure stage of Case Study 2 38

Figure 16: The data of a sensor (C5) when it is operated as a point-resistive sensor (dashed, blue) and a dielectric sensor (solid green)..... 39

NOMENCLATURE

A	area of a sensing plate, [m ²]
$C_{analytical}$	capacitance of a dielectric sensor using the analytical formula, $\epsilon A / d$, which is valid for infinitely long parallel plates, [F]
C_m	capacitance of a mold, [F]
C_{ref}	reference capacitance used in the electric circuit, [F]
C_{sens}	capacitance of a sensor, [F]
d	separation of two parallel sensing plates, [m]
i	imaginary unit, $\sqrt{-1}$
Q	resin flow rate, [cc/min]
R_{sens}	resistance of a sensor, [Ω]
R_{ref}	reference resistance used in the electric circuit, [Ω]
V_{in}	alternating excitation voltage, [V]
V_o	amplitude of alternating excitation voltage, [V]
V_m	DC offset of alternating excitation voltage, [V]
$V_{sens,A}$	amplitude of sensor voltage in form A, [V]
$V_{sens,B}$	amplitude of sensor voltage in form B, [V]
Z_{ref}	reference impedance used in the circuit, $[(1/R_{ref}) + i\omega C_{ref}]^{-1}$
Z_{sens}	impedance of the medium between the sensor plates, $[(1/R_{sens}) + i\omega C_{sens}]^{-1}$
ϵ_R	relative permittivity
ϵ_{air}	permittivity of air, [F/m]
ϵ_{resin}	permittivity of resin, [F/m]
ϵ_{sens}	permittivity of the sensor (medium within the plates), [F/m]
ϵ_{vacuum}	permittivity of vacuum, [F/m]
ω	frequency of alternating excitation voltage [rad/s] or [Hz]

Chapter 1

INTRODUCTION

1.1 Resin Transfer Molding (RTM) Process

RTM is commonly used to manufacture advanced composite materials with a high fiber content and a good surface finish. In this process, a fabric preform is placed in a mold cavity and thermoset resin is injected into the mold to fill the empty spaces between the fibers of the fabric. After complete filling, the mold is kept closed until the resin cures to a certain level so that enough strength and rigidity of the part are achieved. Complete mold filling may not be repeatable due to the variations in the fabric preform preparation (cutting, stacking and placement) and variation in the fabric compaction and nesting. Since these variations affect the permeability distribution of the fabric preform, the resin flow pattern may significantly deviate from the originally designed pattern, and hence macro size voids (dry spots) may remain in the part. To avoid this problem, resin flow should be monitored using sensors as a part of the process control. If the resin propagates unexpectedly, injection parameters (such as injection and ventilation locations, resin pressure or flow rate) can be changed with a control scheme to correct the flow pattern [1,2].

Besides being used for monitoring mold filling, the sensors are also used for monitoring the resin cure level. This is needed to determine the optimal de-molding time. If the mold is opened too early, the part may not gain its green strength and stiffness and it may warp or deform [3]. On the other hand, if the mold is opened too late, the manufacturing cycle time will be unnecessarily long.

1.2 Previous Sensor Systems for Flow and Cure Monitoring

Various monitoring systems have been developed in the literature. Commonly used sensor types are point and lineal resistive (a.k.a. voltage) [4-6], SMARTweave [7-9], ultrasonic [10,11], fiberoptic [12,13], temperature [14], pressure [15], electric time-domain reflectometry (E-TDR) [16,17] and dielectric [15,18-26] sensors.

Resistive sensors [4-6] use either point or lineal conductor probes to detect arrival and curing of the resin. When the resin reaches the sensor, electrical resistance between the probes decreases significantly. This results in an increase in the voltage across the probes which can be measured from a DAQ system. Moreover, the resistance of the resin increases as it cures and therefore allows the level of curing to be monitored. However, the resistance of typical RTM resin between the probes is in the order of hundreds of MegaOhms corresponding to a typical probe size. Thus, the voltage change upon the resin arrival can be so low that electrical noise caused by other equipments can interfere with the measurements.

SMARTweave [7-9] uses an approach similar to the resistive sensors, except that the probes are the junctions of a grid of conductive wires separated by nonconductive dry

fabric layers. The conductivity between a pair of orthogonal wires increases when resin reaches that junction, and consequently resin filled sections can be monitored. Nonetheless, the wires remain in the composite part after curing, which reduces the overall strength due to stress concentration; and a new wire set must be prepared again for the next part, which is time-consuming.

Ultrasonic sensors [10,11] detect sound waves generated by an impulse generator on the opposite side of the mold. With varying media, the speed and damping of the sound changes, and consequently resin inside the mold can be detected by using the phase and the magnitude change of the reflected sound wave. The arrival of the resin at a sensor will cause a significant decrease in the travel time of the impulse and a further decrease as it cures.

Fiberoptic sensors [12,13] transmit infrared light and monitor the intensity of the light at the opposite end of the sensors. As resin reaches the sensor, the light starts to refract and the monitored intensity decreases. However, the optical properties of the resin change so slightly with curing, that it is difficult to observe.

Temperature sensors (thermocouples) [14] measure the temperature of the mold cavity which changes due to (i) the arrival of the resin to a sensor if the inlet resin is either cooler or hotter than the mold walls, and/or (ii) the exothermic reaction which occurs with resin curing. However, the response rate and accuracy of these sensors depend on the thermal properties of the mold material and the resin, temperature difference between the inlet resin and the mold walls, and the flow rate [11].

Pressure sensors [15] can be used for flow monitoring but not for curing. As the resin reaches a sensor location the pressure at that point rises to the fluid pressure plus the initial static compaction pressure.

Electric time-domain reflectometry (E-TDR) method is used to measure the wetted regions of sensor wire by applying high speed pulses to the wire and recording the reflection signals [16,17]. The reflections change as the impedance of the sensing medium changes during the RTM or VARTM process. This method is capable of sensing multiple and separate wetted regions so that multiple flow fronts can be monitored. In [16], resin covered regions were measured with an accuracy of +/-30 mm for sensor lengths up to 1 m. A newer algorithm was used in [17] to improve the accuracy to +/-7 mm, however online processing had not been done due to long processing time (in the order of minutes). Moreover, this technique requires costly high speed equipment since reflections occur in the order of nanoseconds.

Dielectric sensors [13,18-26] measure the capacitance of the media between the sensor plates. In the literature, two types of sensing plates have been used: (1) parallel-plate sensors placed on both sides of a mold [18,19]; and (2) co-planar sensors (fringing effect field, FEF) placed on only one side of the mold [20-23]. Besides being used in RTM, co-planar sensors were also used in VARTM [22-23]. In Skordos' study [24], a lineal sensor was used to monitor mold filling by measuring the total length of the region covered with resin on the sensor. Mounier et al. [25] used two parallel carbon fiber tows as electrodes of a lineal dielectric sensor to measure resin flow in glass fabric preform. Three large parallel-plate sensors were used in Hegg et al. [19] and Rowe et al. [23] to monitor three different regions in the mold. Similar to resistance, the capacitance of resin changes as it cures which permits monitoring of resin cure [18,20,21]. Vaidya et al. [22] used dielectric sensors for

localized cure monitoring. Since dielectric sensors have no need for direct contact with the resin, one side of the sensor can be placed over a nonmetallic mold lid as in [19], and with this approach sensors do not degrade the surface finish of the manufactured part. Nonetheless, the mold may need maintenance more often due to the nonmetallic material used.

1.3 Objective

In the aforementioned studies, dielectric sensors have been used to monitor the fraction of the mold cavity filled with resin. In the following section, the drawbacks of such a monitoring approach will be discussed using several case studies. To improve the conventional dielectric sensor system, the resolution was increased as follows: ten vertical narrow plates were embedded in the lower mold wall and five horizontal narrow plates in the upper mold wall, thus a grid of fifty dielectric sensors was formed. The aim was to have more informative and detailed monitoring by using these multiple sensors, and also to permanently embed these sensors in the mold for use in mass production. Several RTM case studies were done to show the response rate, reliability and performance of the sensor system on a lab-scaled mold.

Chapter 2

DIELECTRIC SENSORS

Both resistive and dielectric sensors function by measuring the electrical properties (resistance and capacitance, respectively) of the resin, however they have some dissimilarity which shall be discussed in this section. The drawbacks of the resistive and conventional dielectric sensors shall also be reviewed. A new form of the dielectric sensor system will be proposed and then applied in an RTM mold. By using this enhanced sensor system, monitoring of both resin flow and cure can be achieved successfully for several case studies in Section 5.

2.1 Comparison between Resistive (Voltage) and Dielectric (Capacitive) Sensors

Durable and low-cost resistive sensors have been successfully used for flow monitoring, and they can also be used for cure monitoring if the electrical resistivity of the resin versus the degree of cure has already been collected in databases as mentioned in [4]. However, it is essential that the user be cautious of potential problems with such sensors; (1) the electrical resistivity of the resin should be much lower than that of the fabric preform; (2)

pre-impregnated preforms may cause a false resin arrival signal; (3) the response of the sensor is in the order of its noise level for some RTM resin systems such as polyester used in [4] due to its very high resistivity; (4) high gain (typically in the order of hundreds) is necessary for trouble-free flow monitoring, however this high gain results in low precision in monitoring the degree of cure; and (5) some mold release agents and/or oxidation of sensor plates induce additional resistance to the sensor's circuit, thus the sensors are required to be calibrated frequently to prevent false triggering.

Dielectric sensors are not affected (or, less affected) by the mentioned drawbacks of the resistive sensors, which shall be further discussed later.

2.2 Theory

Dielectric means non-conducting material (insulator) in an alternating electric field. Since the resistivity of an RTM resin is usually very high and difficult to measure, dielectrics become a better alternative to monitor both resin flow and curing.

The parallel-plate dielectric sensor version is schematically described in Figure 1. The two plates are separated by a distance of d , and each plate has an area of A . The plates are connected to the electrical circuit in series. The alternating excitation voltage, V_{in} has an amplitude of V_o , frequency of ω and DC offset of V_m . Z_{ref} is the known reference impedance of the circuit. The sensor medium (dry or wet preform) is modeled as a resistor and a capacitor in parallel configuration [27]. $Z_{sens} = [(1/R_{sens}) + i\omega C_{sens}]^{-1}$ is the impedance of the medium between the sensor plates. The resistance, R_{sens} and the

capacitance, C_{sens} of the medium are unknown and to be calculated indirectly after

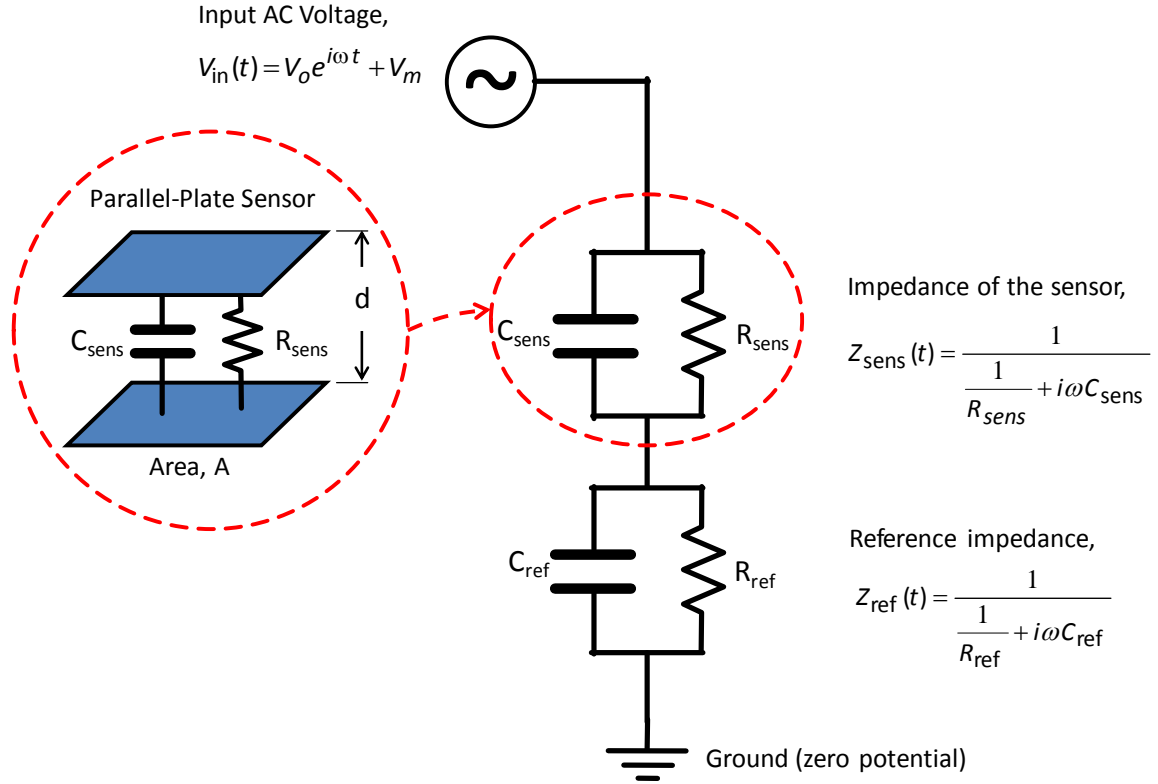


Figure 1. Electrical circuit of a dielectric sensor.

measuring sensor voltage, V_{sens} . By using Ohm's law, the voltage ratio is written as follows in complex form:

$$\frac{V_{sens}}{V_{in}} = \frac{Z_{ref}}{Z_{ref} + Z_{sens}} \quad (1)$$

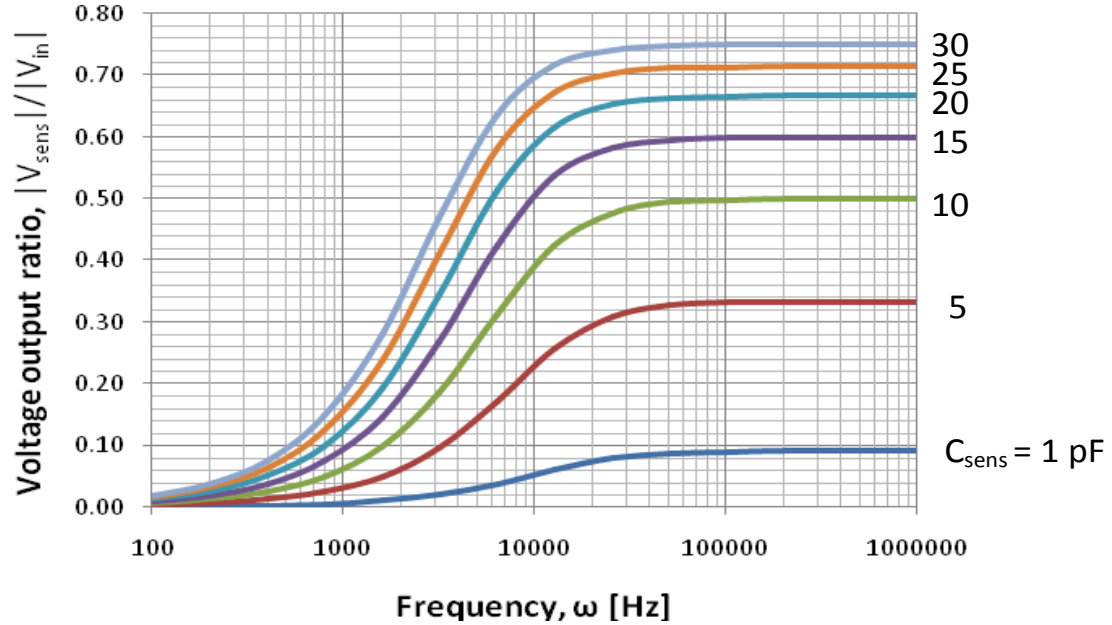


Figure 2. Frequency response of Equation (1).

Typically, the order of magnitudes of the reference capacitance and resistance should be selected as close to the sensor values as possible. For $C_{ref} = 10 \text{ pF}$, $R_{ref} = 1 \text{ M}\Omega$ and $R_{sens} = 100 \text{ M}\Omega$ values, the frequency response was plotted in Figure 2 for a range of expected sensor capacitance values to see the effect of the excitation frequency, ω . As seen in the figure, the output ratio does not change above 100 kHz. Thus, Equation (1) reduces to the following asymptotic form which is not a complex but a real number:

$$C_{sens} = C_{ref} \frac{V_{sens}}{V_{in} - V_{sens}} \quad (2)$$

This way, C_{sens} can be calculated directly from Equation (2) since all the terms on the right hand side are either known or measured. Note that the resistance terms, R_{sens} and R_{ref} do not appear in this equation.

Equation (2) is valid for high frequencies only. In another extreme case, as ω goes to zero (DC excitation), Equation (1) reduces to the following form

$$R_{sens} = R_{ref} \frac{V_{in} - V_{sens}}{V_{sens}} \quad (3)$$

where the system functions as a resistive sensor. So, this sensor can be used as either a resistive or a capacitive sensor if ω is zero or infinite. In this study, ω was set to 150 kHz for capacitive measurements.

2.3 A Single Dielectric Sensor

For an infinitely long parallel-plate sensor, the capacitance can be calculated as [28]

$$C_{sens} = \frac{\epsilon_{sens} A}{d} \quad (4)$$

where ϵ_{sens} is the permittivity of the medium within the plates, A is the area of each sensor plate and d is the separation between the plates. However, for a finite sized sensor the capacitance of the sensor deviates from Equation (4) due to the fringing effect that occurs

at the edges of the plates where the electric field bends [28] as schematically illustrated in Figure 3a.

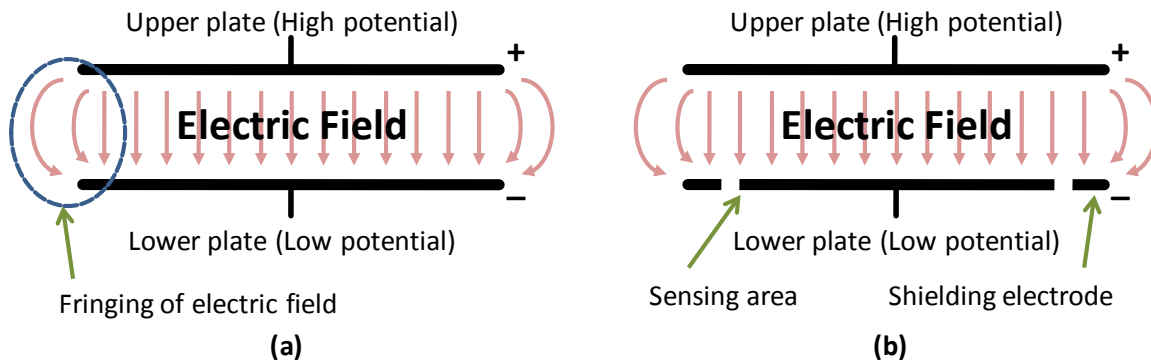


Figure 3. Fringing effect on a parallel-plate capacitor.

2.3.1. Shielding

Besides the fringing effect, the sensor is vulnerable to the external electric field. To eliminate both the edge and external effects, the sensor must be properly shielded by (i) adding an electrode surrounding the sensing area and the back side of the plate; and (ii) keeping the potential of the shielding electrode the same as the sensor [29]. Thus the electric field will not be distorted within the entire sensing area (Figure 3b).

Shielding not only removes the fringing effect but also eliminates the interference between the sensors. This allows the use of multiple sensors on the same mold, but it requires an additional electrode for each sensor which occupies an additional area. This may not be a major problem for a single sensor, but it is very tedious and costly to manufacture a mold with multiple embedded sensors.

2.3.2 Grounding

While using multiple sensors, a much simpler approach to avoid interference is to add a common ground electrode for all the sensors as shown in Figure 4b instead of shielding each sensor separately as in Figure 4a. Since typical RTM molds are made of metal, multiple sensors can be easily grounded.

Grounding instead of shielding however, reveals the following major problems: (1) the sensors have different potential than the ground (= zero potential), causing a non-uniform electric field between the sensor plates and thus they may lead to incorrect measurements; (2) the electrical circuit of the sensor shown in Figure 1 will change unexpectedly due to the capacitance, C_m of the insulator between the sensor and the ground electrode. This altered electrical circuit is shown in Table 1c. C_{ref} in Equation (2) has to be replaced with $C_{ref} + C_m(t)$ where $C_m(t)$ is unknown and varying with time since it is affected by the flowing resin.

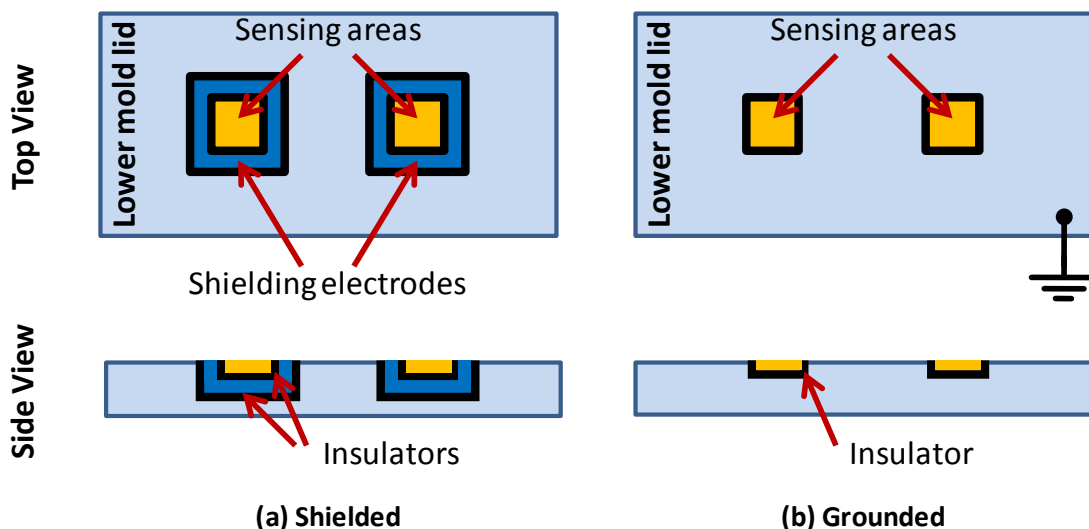


Figure 4. (a) Shielding and (b) grounding of multiple sensors (only two are shown for simplicity).

2.4 Proposed Method, “Modified Grounded”

A simpler dielectric sensor system is proposed here. As illustrated in Table 1d, two measurements are taken at each time-step: (1) in Form A (the same circuit of the “grounded” configuration), the voltage output, $V_{sens,A}$ is recorded; (2) in Form B, the places of C_{ref} and C_{sens} in the electrical circuit are switched by the DAQ system, and then $V_{sens,B}$ is recorded. The voltage output ratios for these two forms A and B are given below:

$$\text{Form A:} \quad \frac{|V_{sens,A}(t)|}{|V_{in}|} = \frac{C_{sens}(t)}{C_{sens}(t) + C_{ref} + C_{mold}(t)} \quad (5a)$$

$$\text{Form B:} \quad \frac{|V_{sens,B}(t)|}{|V_{in}|} = \frac{C_{ref}}{C_{sens}(t) + C_{ref} + C_{mold}(t)} \quad (5b)$$

in which $C_{mold}(t)$ is the unknown capacitance of the mold which varies with time. This unknown $C_{mold}(t)$ can be eliminated by combining the two equations. Thus C_{sens} can be calculated in terms of the known C_{ref} and the voltage outputs $V_{sens,A}$ and $V_{sens,B}$ of the two circuit forms which are measured at each time step:

$$\frac{\frac{|V_{sens,A}(t)|}{|V_{in}|}}{\frac{|V_{sens,B}(t)|}{|V_{in}|}} = \frac{\frac{C_{sens}(t)}{C_{sens}(t) + C_{ref} + C_{mold}(t)}}{\frac{C_{ref}}{C_{sens}(t) + C_{ref} + C_{mold}(t)}}} \longrightarrow C_{sens}(t) = C_{ref} \frac{V_{sens,A}(t)}{V_{sens,B}(t)} \quad (6)$$

Table 1. Circuit schematics, diagrams and formulas for different dielectric configurations.

	Circuit schematic	Diagram	Formula
(a) Unshielded			$\frac{ V_{sens} }{ V_{in} } = \frac{C_{sens}}{C_{ref} + C_{sens}}$
(b) Shielded			$\frac{ V_{sens} }{ V_{in} } = \frac{C_{sens}}{C_{ref} + C_{sens}}$
(c) Grounded			$\frac{ V_{sens} }{ V_{in} } = \frac{C_{sens}}{C_{ref} + C_{sens} + C_m}$
(d) Proposed method	Form A		<p>Form A:</p> $\frac{ V_{sens,A} }{ V_{in} } = \frac{C_{sens}}{C_{ref} + C_{sens} + C_m}$
	Form B		<p>Form B:</p> $\frac{ V_{sens,B} }{ V_{in} } = \frac{C_{ref}}{C_{ref} + C_{sens} + C_m}$ <p style="text-align: center;">↓</p> $\frac{ V_{sens,A} }{ V_{sens,B} } = \frac{C_{sens}}{C_{ref}}$

As a summary, the benefits of using this proposed method are the followings:

- Embedded multiple sensors operated by this method will not pose major difficulty as in the “shielded” version. The metal mold is simply connected to the ground instead of using a separate shielding electrode for each sensor, which also requires a separate circuitry.
- C_{sens} can be directly calculated, recall that the “grounded” version miscalculated C_{sens} since Equation (2) does not represent the actual electrical circuit in which $C_{mold}(t)$ exists.


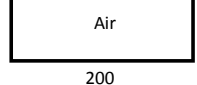





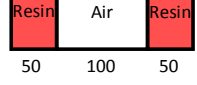

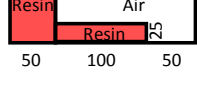
2.5 The Major Issue of Using a Single Dielectric Sensor

A parallel-plate dielectric sensor was made using two copper plates each with a sensing area of 200 mm X 100 mm separated by a distance of $d = 5$ mm. The measured voltage, V_{sens} and the corresponding capacitance of the sensor, C_{sens} were found to be 3.86 V and 34.2 pF respectively when the medium of the sensor is air only. For the measurement technique, the “shielded” configuration was used. C_{sens} deviated only 3.4 % from the analytical value,

$$C_{analytical} = \frac{\epsilon_{air} A_{air}}{d} = \frac{(8.85 * 10^{-12} \text{ F/m})[(0.200 \text{ m})(0.100 \text{ m})]}{(0.005 \text{ m})} = 35.4 * 10^{-12} \text{ F} = 35.4 \text{ pF} \quad (7)$$

where ϵ_{air} is the permittivity of air taken from [30].

Table 2. Capacitance measurement using a single large dielectric sensor.

Case Study	Sensing Medium	Sensing Area of the Dielectric Sensor (all dimensions are in [mm])		Analytical Capacitance, $C_{\text{analytical}}$ [pF] $= \frac{\epsilon_{\text{air}} A_{\text{air}}}{d} + \frac{\epsilon_{\text{resin}} A_{\text{resin}}}{d}$	Measured Voltage, V_{sens} [V] ($V_{\text{in}}=20$ V)	Measured Capacitance, C_{sens} [pF] $= C_{\text{ref}} \frac{V_{\text{sens}}}{V_{\text{in}} - V_{\text{sens}}}$
		Side view	Top view			
A	100 % air	5 		35.4	3.86	34.2
B	100 % resin	5 		---	11.36	188.3
C	50 % resin + 50 % air	5 		111.9	8.76	111.6
D	25 % resin + 50 % air + 25 % resin	5 		111.9	8.84	113.4
E	50 % resin + 50 % air (Non-uniform channel: A representative of racetracking channel)	5 		111.9	8.80	112.5

Next, the sensor was filled with the thermoset resin (Poliya Polipol™ 336-RTM), V_{sens} and C_{sens} were measured as 11.36 V and 188.3 pF respectively as tabulated in Table 2. Equation (4) was used to calculate the permittivity of the resin used:

$$C_{\text{sens}} = \frac{\epsilon_{\text{resin}} A_{\text{resin}}}{d}$$

$$\epsilon_{\text{resin}} = \frac{C_{\text{resin}} d}{A_{\text{resin}}} = \frac{(188.3 \text{ pF})(0.005 \text{ m})}{[(0.200 \text{ m})(0.100 \text{ m})]} = 47.08 \text{ pF/m}. \quad (8)$$

Upon measuring the permittivity of the resin, it was possible to conduct three case studies (C, D and E) in which half of the sensing area was filled with resin while the other half with air. In C, the resin filled only the first half; in D, the resin filled the first and last 25% of the sensing area; and in (E), the resin filled a non-uniform region which represents a resin flow affected by racetracking channels in the RTM process. As shown in Table 2, the three measured capacitance values (111.6, 113.4 and 112.5 pF) were quantitatively similar, and agree with the analytical value,

$$C_{sens} = \frac{\epsilon_{air} A_{air}}{d} + \frac{\epsilon_{re\ sin} A_{re\ sin}}{d}$$

$$= \frac{(8.85 * 10^{-12} \text{ F/m})(0.0100 \text{ m}^2)}{(0.005 \text{ m})} + \frac{(47.08 * 10^{-12} \text{ F/m})(0.0100 \text{ m}^2)}{(0.005 \text{ m})} = 111.9 \text{ pF} \text{ (9)}$$

within a maximum error of only 1.4 %. This was anticipated to be due to the experimental errors such as inaccuracies in the resin filled areas and the separation of the plates, d .

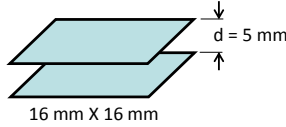
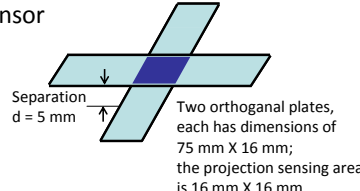
It can be concluded that large parallel-plate dielectric sensors can measure the total fraction of the sensor's plate area occupied by resin but cannot detail the resin's whereabouts on the sensor. This characteristics of the sensor may mislead the user particularly when an unpredicted flow pattern develops in the mold, which is likely to occur in the RTM process. This may be the result of the process disturbances such as racetracking channels, non-uniform fabric compaction and nesting effects. Taking into account the drawback of a single, or a small number of, sensors in the mold as illustrated in the previous studies, a grid of multiple (fifty) sensors was embedded in the mold walls for an unambiguous but yet detailed monitoring.

2.6 Comparison of the Dielectric Sensor Configurations

Instead of manufacturing and embedding fifty separate parallel-plate sensors in the mold walls, a much simpler approach will be used here, similar to the sensor grid used by SMARTweave. However, the feasibility of this approach was checked first by investigating the change in the measured capacitance value when a pair of rectangular plates formed a cross shape instead of using identical square parallel-plates. A square and a cross-shaped dielectric sensor were made as shown in Table 3. The two rectangular plates were placed orthogonal to each other making a cross, and separated with a distance of $d = 5$ mm (see Table 3). The projected area of the cross-sensor was the same as the sensing area of the square sensor. The capacitances of the sensors were measured and averages are recorded in all versions mentioned so far: (1) unshielded, (2) shielded, (3) grounded, (4) proposed method, and to compare these values with (5) the analytical value. Table 3 reveals the following: (1) the unshielded configuration gives unreliable readings for both sensors; (2) the shielded configuration is very accurate; (3) the grounded configuration has an error of 29.5 % for the square sensor, and 29.7 % for the crossed sensor; (4) the proposed method is very accurate for the square sensor, and has an error of 20.5 % for the cross sensor. High error in unshielded configuration is mainly due to the external effects rather than fringing. Measurement must be done in an environment insulated from external electric fields. This unshielded measurement is done to show magnitude of error if it is not done properly. The error in the proposed method is assumed to be due to the fringing effects as explained in Figure 3 when the cross-shaped sensor is used mainly due to different plate geometries or basically orientation. Even though the cross sensor has a significant error, it is relatively much easier to manufacture and embed them in mold walls than embedding the shielded sensors. As a direct consequence, in order to facilitate the study, they will be used. The error will be reduced by measuring the capacitance ratio C_{sens} / C_{air} instead of C_{sens}

during actual injections. As will be illustrated in the following sections, the results of several case studies are extremely satisfactory.

Table 3. Measurement of empty sensor capacitance for two different sensors.

Circuit configuration $V_{in} = 20\text{ V}$ $C_{ref} = 143.2\text{ pF}$	Square sensor 			Cross sensor 		
	V_{sens} [mV]	C_{sens} [pF]	Error in C_{sens} [%]	V_{sens} [mV]	C_{sens} [pF]	Error in C_{sens} [%]
Analytical	---	$= \frac{\epsilon_{air} A}{d}$ $= \frac{(8.859)(0.016)(0.016)}{0.005}$ $= 0.454$	---	---	$= \frac{\epsilon_{air} A}{d}$ $= \frac{(8.859)(0.016)(0.016)}{0.005}$ $= 0.454$ (using projected area)	---
Unshielded	1720	13.5	2874	1336	10.25	2158
Shielded	63.2	0.454	0.0	66.4	0.477	5.07
Grounded	44.6	0.320	29.5	44.0	0.319	29.7
Proposed method ("modified grounded")	$V_A = 44.6$ $V_B = 14080$	0.454	0.0	$V_A = 44.0$ $V_B = 11520$	0.547	20.5

Chapter 3

THE MOLD

The mold was designed to manufacture rectangular composite panels with in-plane dimensions of 300 mm x 140 mm. The lower and upper mold lids are made of UNS 301 steel. A variety of spacer frames allow the manufacturing of panels with different thicknesses (in this study, only $h = 3$ mm). There are ten vertical conductive electrodes (copper plates with a face thickness of 16 mm) on the lower mold lid, and five horizontal conductive electrodes on the upper mold lid as shown in Figure 5. Delrin plastic bars were machined for the housing and insulation of the copper plates from the conductive mold. After the copper plates and plastic insulator housings were tightly fitted in the mold lids, the surface of the mold lids were finish cut on a milling machine (by Bayrak Plastik, Bursa, Turkey) to level the surfaces of the copper plates and the mold lids and to reduce the surface roughness. On both sides of the spacer frame, o-ring silicon seals the mold cavity, and thin nylon films electrically insulate the metal frame from the mold lids. Six latches are used manually to compact the fabric preform and close the mold cavity. A resin inlet gate and ventilation (exit) port are located such that empty pools exist within the mold cavity between the left and right edges of the fabric preform and the mold walls; thus these inlet and exit pools function as a linear inlet and exit in practice.

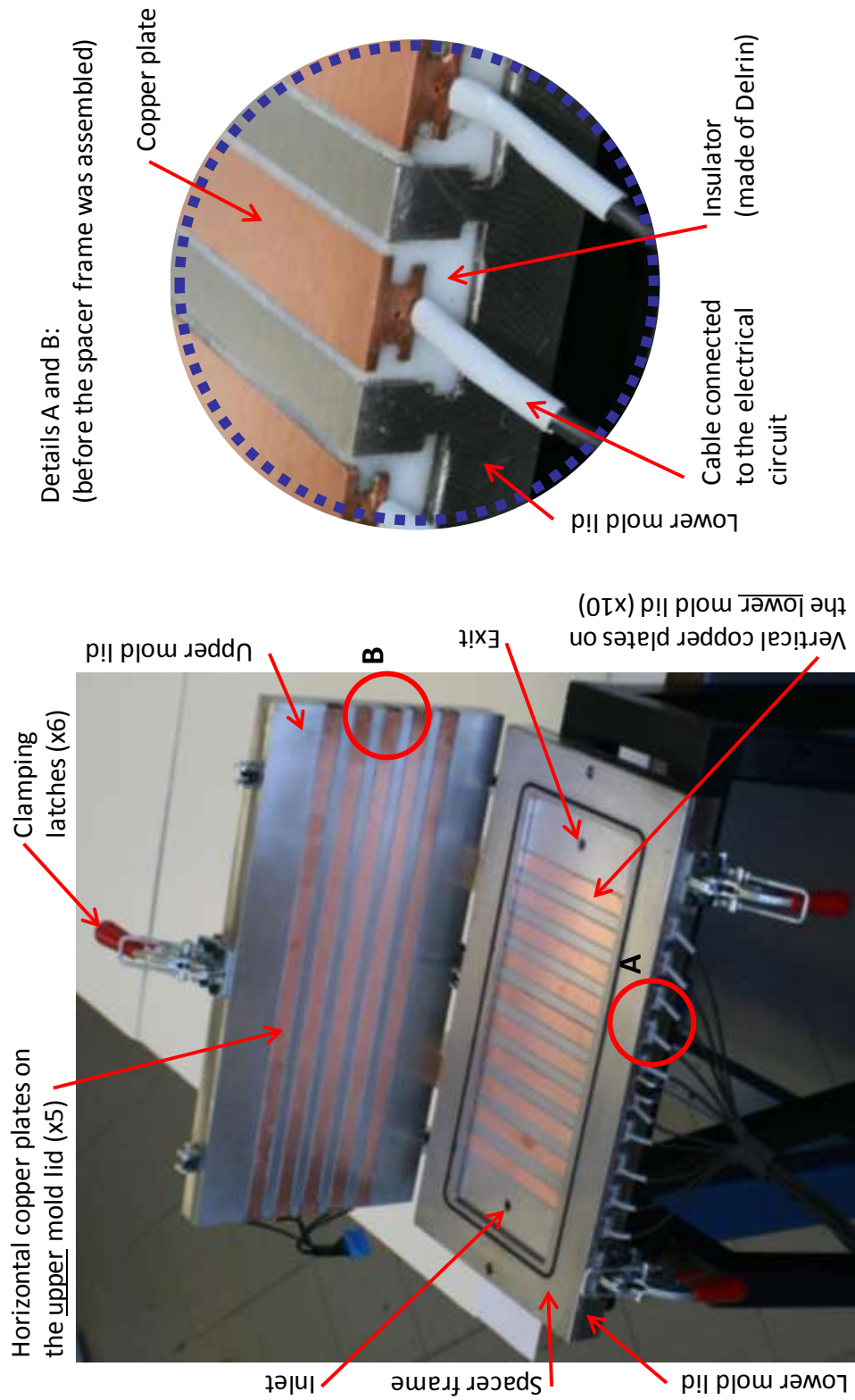


Figure 5. The RTM mold

3.1 The Experimental Setup

Figure 6 shows the experimental setup for the RTM injection and in-situ sensor data evaluation. A flow-rate controlled injection machine (Radius Engineering RTM 2100 cc) transfers thermoset resin (Poliya Polipol™ 336-RTM) to the mold cavity in which a fabric preform (5 layers of stitched random e-glass fabric by Fibroteks with 500 g/m² superficial density per layer) was compacted previously. The projected intersections of the horizontal electrodes (A,B,...,E) and the vertical electrodes (1,2,...,10) form fifty sensors (A1,A2,...,E10) as shown in Figure 7. The grid of 50 dielectric sensors is connected to the electrical circuit and monitored on the computer. Flow front positions and empty/filled regions can be monitored on-line during the injection, and the level of cure can be monitored by using the “permittivity versus cure level” database, during the cure stage of the process.

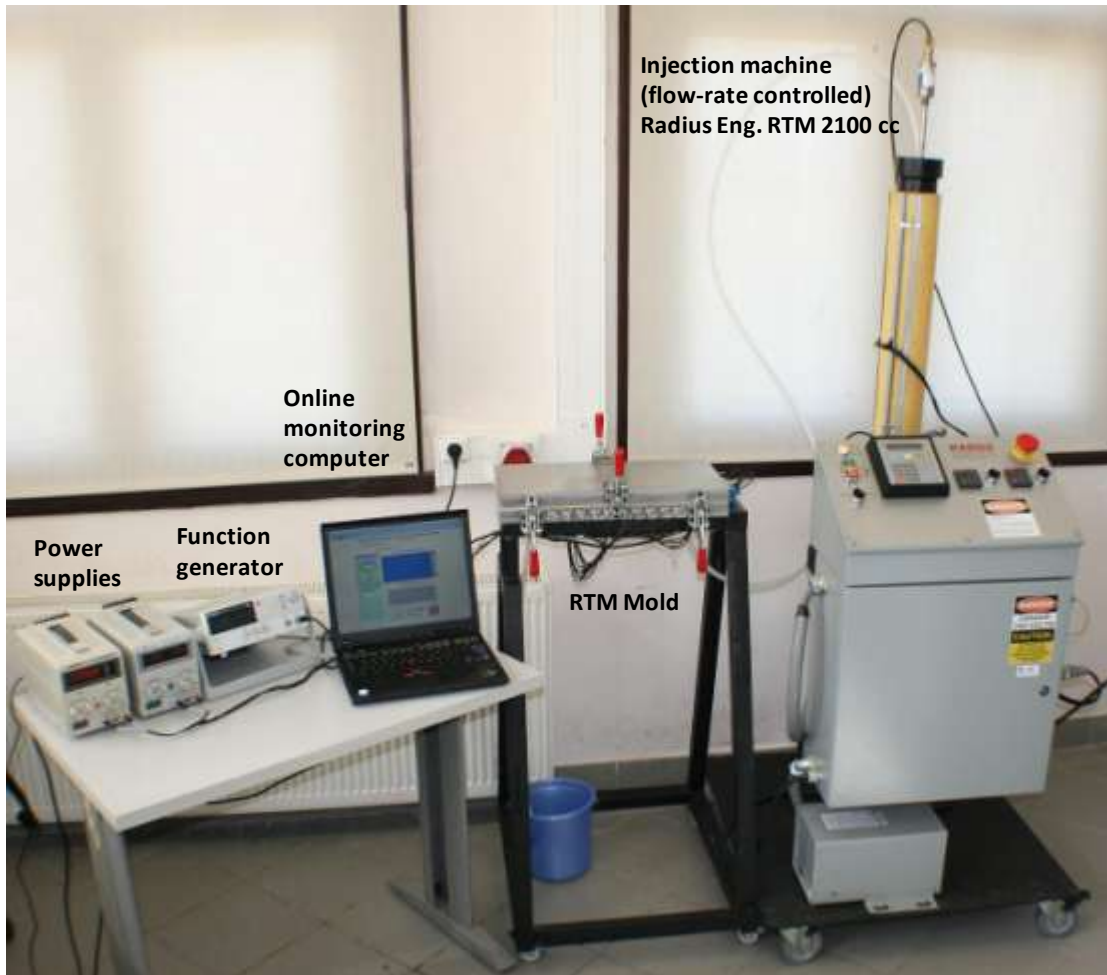


Figure 6. Experimental setup for RTM.

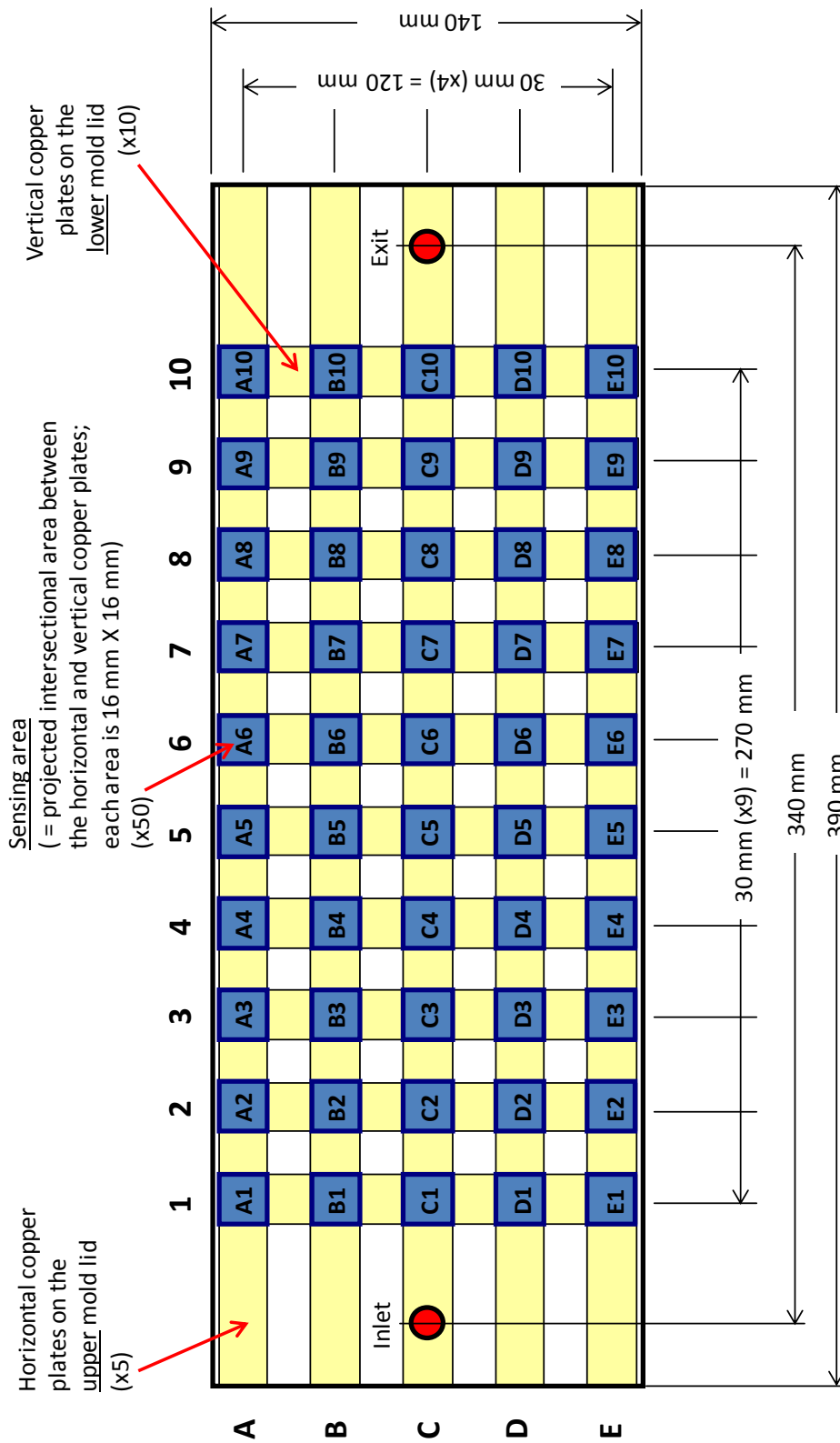


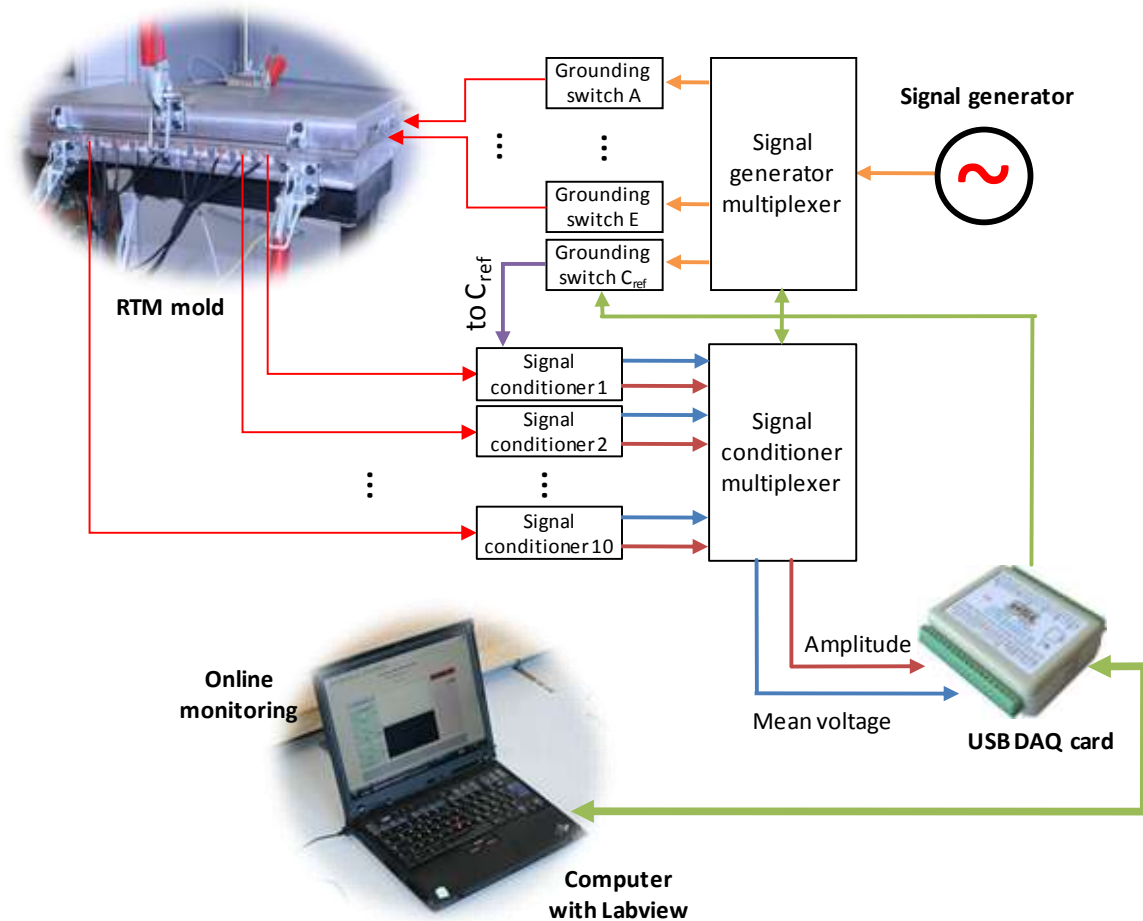
Figure 7. Top view of the mold cavity with a grid of 50 embedded dielectric sensors.

Chapter 4

THE ELECTRICAL SYSTEM FOR OPERATION OF SENSORS AND DAQ

The electrical system consists of a circuit board, a signal generator, a USB data acquisition card and a computer running LabVIEW. The diagram of the overall system can be seen in Figure 8.

The circuit board consists of multiplexers, grounding switches and signal conditioners. The signal generator used in this study is Gwinstek SFG-2004 DDS function generator, which can be replaced with any signal generator capable of generating sine waves. For controlling the circuit board and data acquisition, iUSBDAQ – U120816 card is used due to its low cost and easy implementation to LabVIEW. This card is capable of capturing analog inputs at 32 kSamples/s with 12-bit resolution. It is connected to an IBM compatible computer running LabVIEW software for online monitoring. The software controls the multiplexers and processes the voltage data to calculate the capacitances. Relative permittivities are displayed both in numerical and contour map formats. The data is also recorded for later inspection.



- Multiplexers and switches are controlled by DAQ card.
- Only one horizontal electrode is connected to the signal generator at a time and the rest are connected to the ground.
- C_{ref} is connected as an horizontal electrode because of the similar operation.
- Signals from the lower mold lid electrodes are amplified and decoupled with signal conditioners and are fed to the DAQ card via a multiplexer.

Figure 8. Diagram of the entire monitoring system.

4.1 System Operation

As explained in Section 2, a dielectric sensor works by applying an alternating current to the sensor which is connected serially to a reference capacitor, C_{ref} . By measuring the voltage across C_{ref} and using the known value of C_{ref} in Equation (2), the unknown sensor capacitance C_{sens} , can be calculated. For a single sensor this process is straightforward, however it becomes more complicated for a grid of sensors, as shown in this study. Figures 7 and 8 explain how the grid sensors can be used to measure the capacitances, C_{sens} at all junctions: (1) The first horizontal plate (A) is connected to the signal generator, and other horizontal channels (B-E) and C_{ref} are connected to the ground. (2) The amplitude and average of the voltage at all vertical plates (1-10) are measured and recorded. (3) Steps 1 and 2 are repeated for the other horizontal plates (B-E) sequentially, and the corresponding voltages are recorded. (4) C_{ref} is connected to the signal generator and all of the horizontal plates (A-E) are connected to the ground. (5) Voltage amplitudes at all vertical plates are recorded. (6) For each vertical plate, the ratio of the amplitudes recorded at Step 2 ($V_{sens,A}$) and Step 5 ($V_{sens,B}$) are multiplied with C_{ref} of the corresponding plate as in Equation (5). (7) The relative permittivity of each sensor is calculated by using

$$\epsilon_{R,sens} = \frac{\epsilon_{sens}}{\epsilon_{vacuum}} = \frac{\epsilon_{sens}}{\epsilon_{air}} \frac{\epsilon_{air}}{\epsilon_{vacuum}} = 1.00059 \frac{C_{sens}}{C_{air}} \quad (10)$$

where C_{air} is the capacitance of each sensor recorded when there is only air present, and the relative permittivity of air is taken from [30] as $\epsilon_{air} / \epsilon_{vacuum} = 1.00059$.

4.2 Circuit Description

The circuit can be divided into three sections: (i) driver for horizontal plates, (ii) signal conditioner, and (iii) DAQ multiplexer.

Driver for Horizontal Plates: This circuit consists of grounding switches and a multiplexer for each channel. The signal generator is directly connected to a CD4051 8-channel analog multiplexer. One CD4066 bilateral switch is used to connect each output channel to the ground. By using logic gates, multiplexer's channel selector and switches are connected together so that non-selected channels will be connected to the ground. Channel selection is handled by LabVIEW software through the DAQ card. For the mentioned mold setup, five channels are used for the mold's horizontal electrodes (A, B, ... , E) and one channel for the reference capacitor.

Signal Conditioner: This part of the circuit is used to measure the voltage of electrodes at lower mold plate. Even if C_{ref} is selected as close to the expected sensor capacitance, the effect of the C_{mold} in the grounded configuration causes the voltage V_{sens} , to decrease and require amplification for accurate readings.

The circuit is divided into parts and shown with representative signals at various stages in Figure 9. The voltages are measured as follows: (i) The circuit is directly connected to the sensor in the voltage divider as explained in the previous section. (ii) To avoid saturation at the op-amps, the amplification is conducted in two steps. The 1st amplifier consists of an op-amp in a non-inverting amplifier configuration with a gain of 52. (iii) The signal is separated into DC and AC components by using a low-pass and a high-pass filter, respectively. (iv) The low-pass filtered signal, labeled as "Mean", is connected to the DAQ

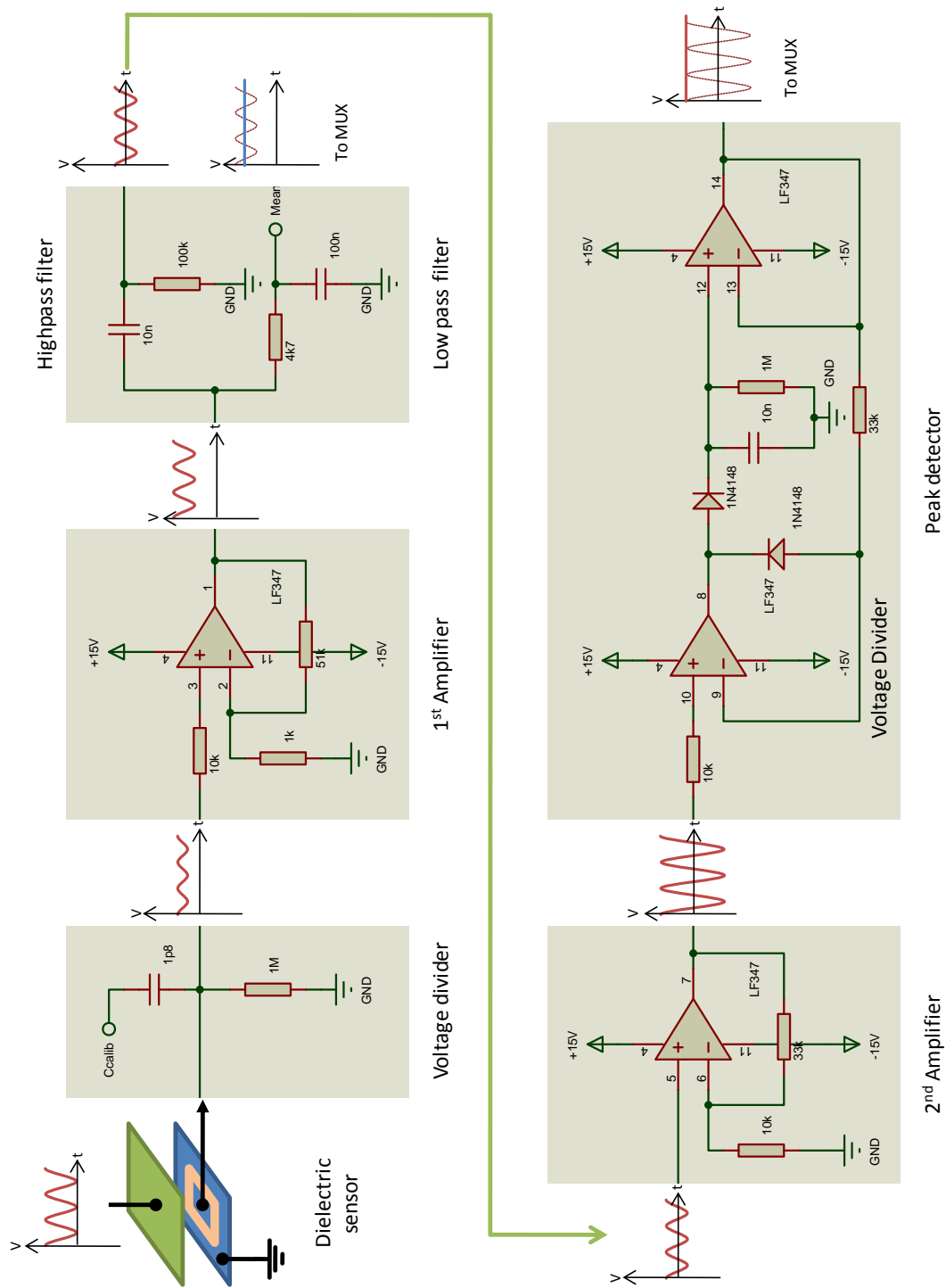


Figure 9. Electrical circuit schematic of the signal conditioner.

multiplexer. (v) The AC signal is further amplified by using the 2nd amplifier for higher sensitivity. The gain of the 2nd amplifier is set to 4.3 which brings the signal level between 0.5 V and 3.8 V. (vi) The last part of the circuit is the peak voltage detector which is used to measure the magnitude of the AC component of the signal [31]. The output of this part is also fed to the DAQ multiplexer.

The op-amps selected for this circuit are LF347. It has a high slew rate (13V/ μ s) which is required for high frequency signals, and also has high input impedance of 10 T Ω . This high input impedance permits the neglecting of the op-amps in voltage divider calculations.

DAQ Multiplexer: The limited number of channels on the DAQ card can be compensated for by adding multiplexers to the system. The only drawback of multiplexing is the decrease in the sampling rate. Since the resin flow develops slowly in RTM, this is not considered a critical issue.

Three CD4052 2x4 channel analog multiplexers are used to feed twenty voltage values (ten for mean and ten for amplitude) to six channels of the DAQ card. Similarly, the channels of the multiplexers are selected from LabVIEW via the DAQ card. At each measurement step, (i) the channel is selected, (ii) three mean and three amplitude values are read, (iii) the second step is repeated for channels 2 to 4, and (iv) voltage values for the ten vertical plates are recorded.

Chapter 5

EXPERIMENTS

To verify the reliability and accuracy of the proposed sensor system, many RTM experiments were done, two of those experiments will be presented here for brevity and the rest are included in the Appendix C. These case studies are RTM mold fillings with (1) approximately 1D resin flow; and (2) 2D resin flow induced by a racetracking channel along the bottom edge of the preform. The resin cure stage of one case study was also monitored until the de-molding time and its evaluation will be done later in this section.

5.1 Monitoring of Mold Filling

In both case studies, curing agent and accelerator were added to Poliya Polipol™ 336-RTM thermoset resin so that the pot life (gelation time) was adjusted to approximately 15 minutes at room temperature. The fabric preform was prepared by stacking five layers of stitched random e-glass fabric (by Fibroteks) with superficial density of 500 g/m² per layer. The preform was compacted to the mold thickness of 3mm, which resulted in a fiber volume fraction of 32.8 %. Injections were performed at a constant flow rate of $Q = 15$

cc/min. As previously explained, the resin filled the empty rectangular pool around the inlet seen in Figure 5, and then it propagated through the porous fabric preform. In Case Study 1, the preform's width was cut with precision so that there was no significant racetracking channel between itself and the mold walls. In Case Study 2, the preform's width was cut approximately 2 mm shorter than the mold width (140 mm), and it was placed in the mold cavity so that the racetracking channel was formed only along the bottom edge.

As explained in the previous section, initially the sensor capacitances were measured and recorded when the mold cavity was empty (i.e., only air existed in it, thus $C_{sens} = C_{air}$). After placing the preform and closing the mold, the sensors measured the capacitance of the medium (dry fabric and air). During the mold filling, the sensors measured the capacitance of the wetted fabric.

In Figures 10 and 11, the relative permittivities of the sensors, ϵ_R are plotted during the entire injection of Case Studies 1 and 2. Each sensor's reading was approximately 1.8 before the arrival of resin to that sensor. After the resin reached the sensor (with a sensing area of 16 mm X 16 mm), the reading started to increase gradually as seen in the two figures. Due to almost 1D flow in Case Study 1, the rate of increase in the readings was almost constant. The readings remained constant (approximately $\epsilon_R = 6.5$) after the preform was saturated completely in the sensor. The arrival times to the sensors along each column (for example A1,B1,...,E1 for the first column, and so on) were quantitatively similar. However, they deviated very significantly in Case Study 2 showing that the flow was not 1D. When the relative permittivity of a sensor reached its mid value, $0.5(\epsilon_{R,final} - \epsilon_{R,initial})$, the sensor was considered to be 50 % filled. The corresponding times of all fifty sensors were used at their central coordinates to plot the flow front contours in Figures 12 and 13. The user interface of the LabVIEW program is given in Figure 14 which monitors the current relative permittivities and the location of the flow front when the mold was partially filled at $t = 418.8$ s.

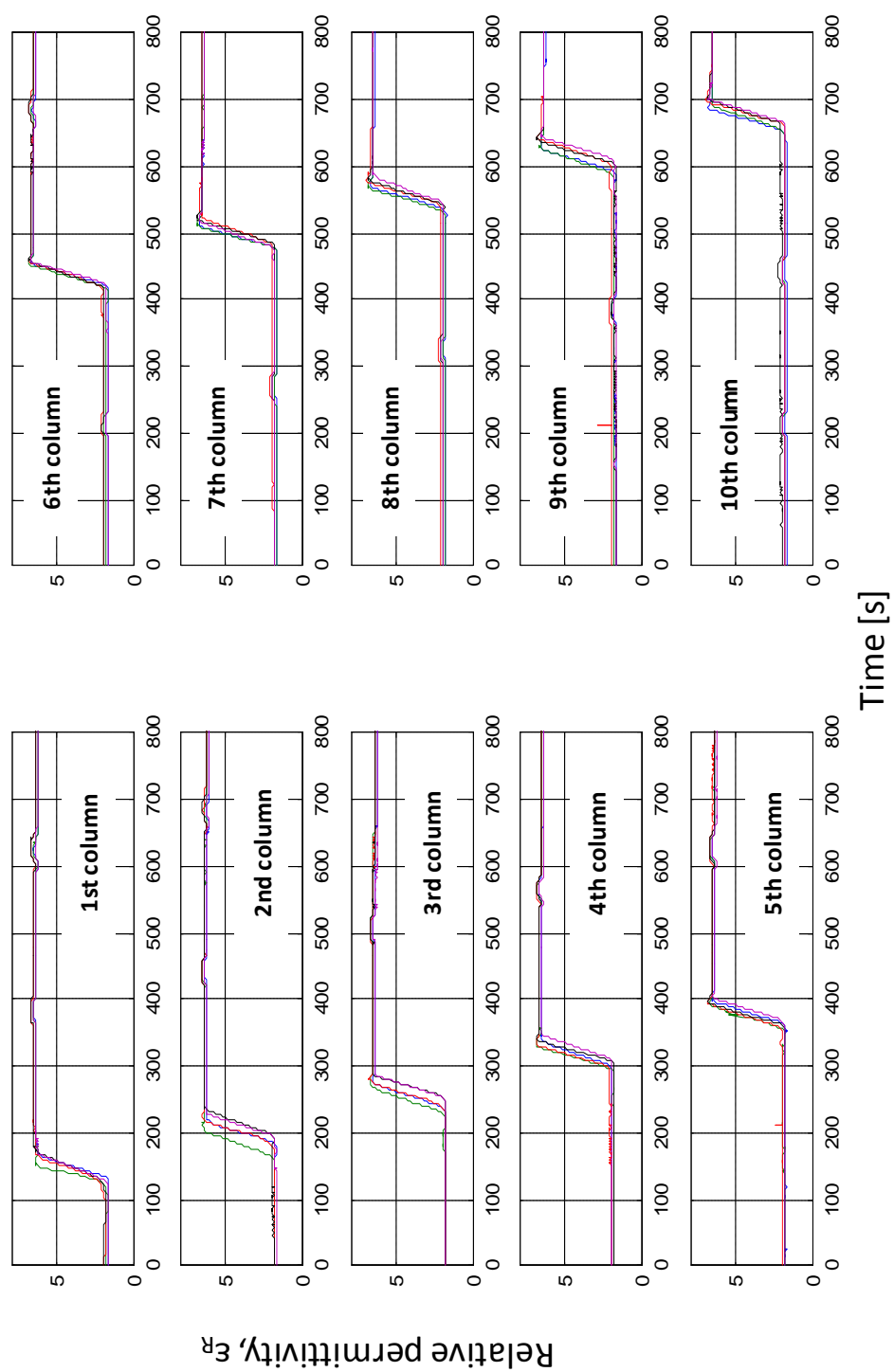


Figure 10. Figure 10. The relative permittivity, of the fifty sensors (A1, A2, ..., E9, E10) during the mold filling stage of Case Study 1. In each graph, the five row sensors (A, B, C, D and E) were plotted for the corresponding column.

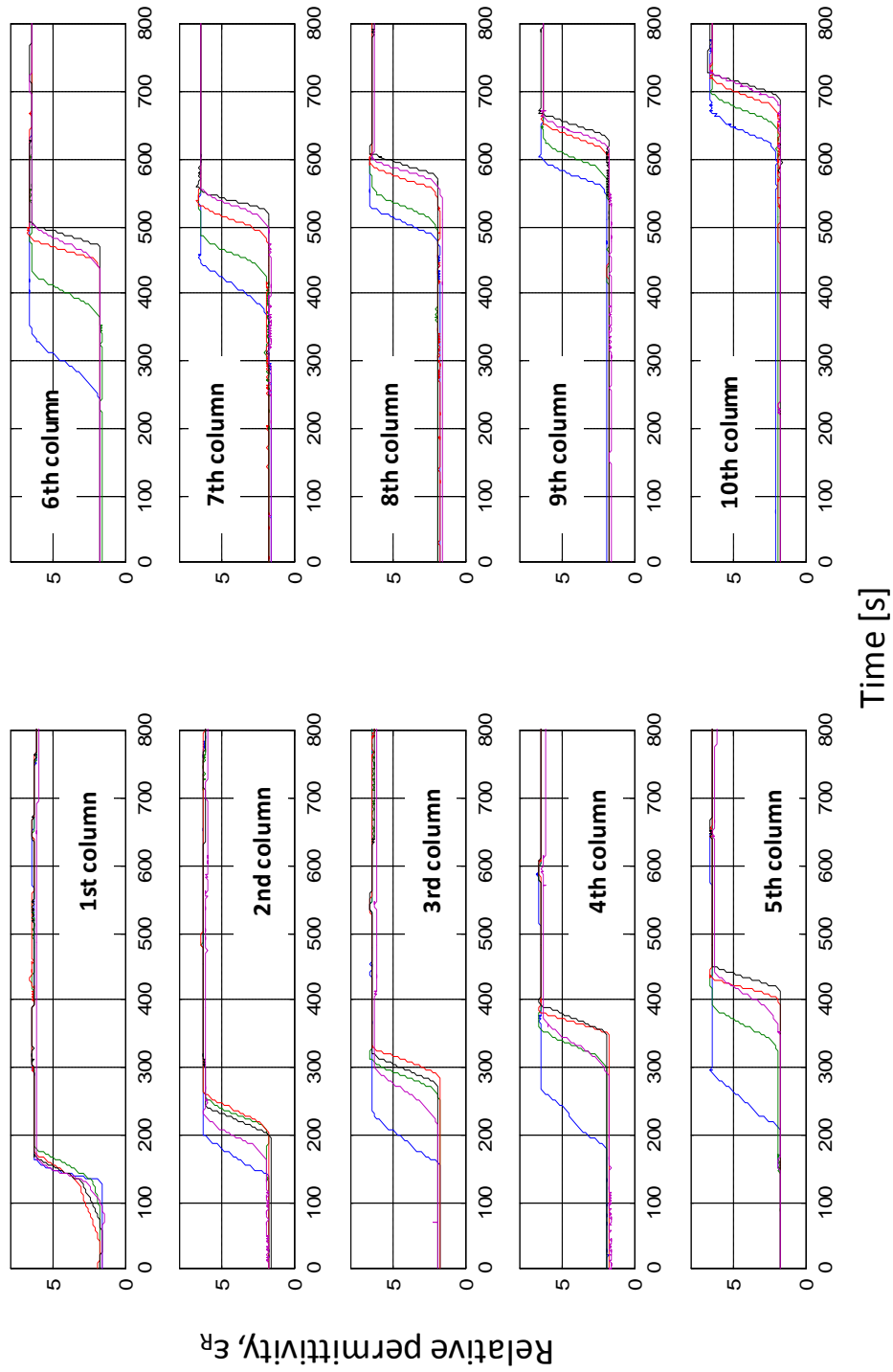


Figure 11. The relative permittivity, ϵ_r of the fifty sensors during the mold filling stage of Case Study 2.

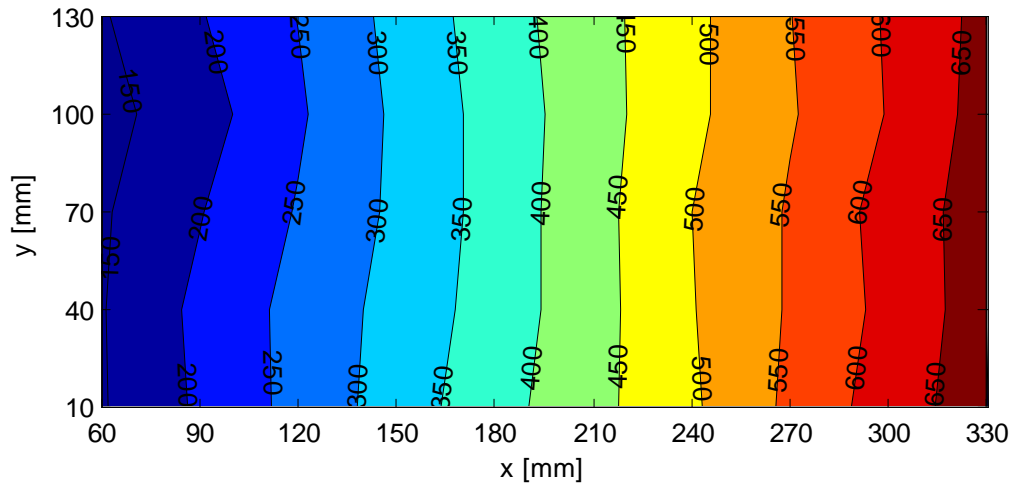


Figure 12. The flow front contours at different times using the recorded data of the fifty sensors for *Case Study 1*.

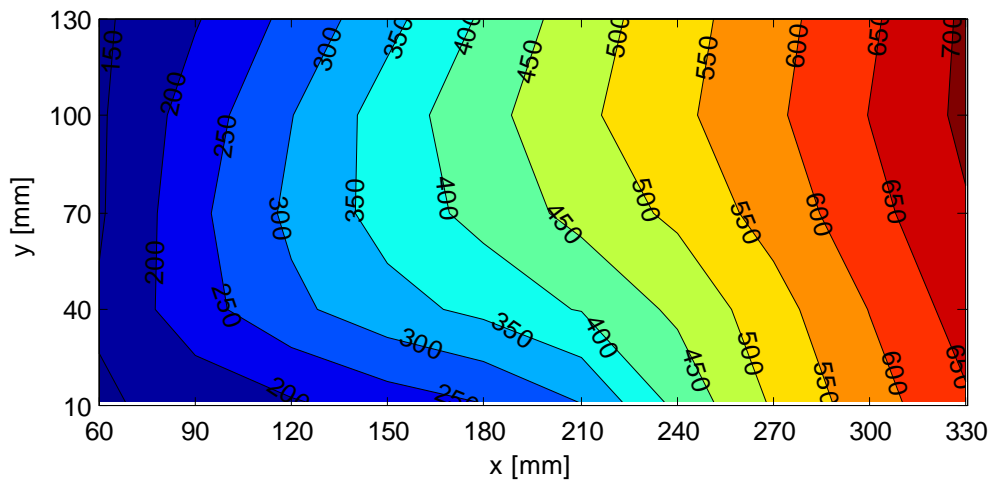


Figure 13. The flow front contours at different times using the recorded data of the fifty sensors for *Case Study 2*.

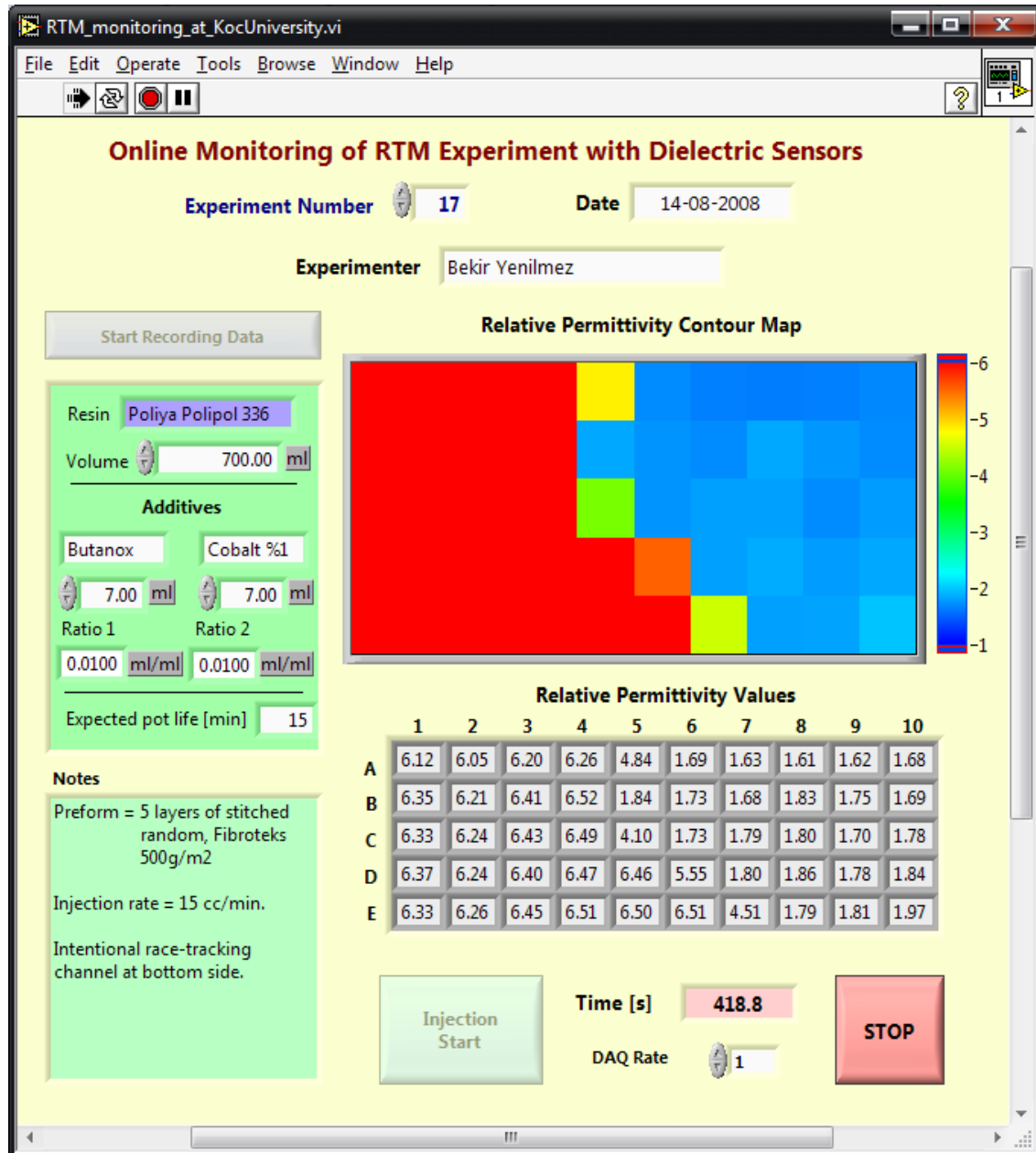


Figure 14. The user interface for monitoring the mold filling in Case Study 2. The relative permittivities of the sensors are used to show what regions of the mold cavity are filled/empty at the current time.

5.2 Monitoring of Resin Cure

The curing stage of Case Study 2 is shown in Figure 15. As the level of resin cure increased with time, the relative permittivity decreased. As mentioned in the first section, for an optimum de-molding time, one ideally needs a database which relates the mechanical properties (strength and stiffness) of the composite part to the relative permittivity. The part should be de-molded after the green strength and stiffness of the composite part are high enough so that no warpage occurs during and after the part is taken out of the mold. In this study and [26], no complete database was used, however no significant deformation was observed during and after the de-molding of the part following approximately 4 hours of curing, for the resin system used in this study. For this room-temperature curable resin type, Figure 15 suggests that the composite part's relative permittivity level should be equal or less than 4.5 at the time of de-molding. This could be much shorter if a different resin system was used and/or the mold was kept in an autoclave during the partial curing stage.

5.3 Using the Sensor System as Point-Resistive Sensors and Dielectric Sensors

To investigate how differently the mold filling and resin cure would be monitored if fifty resistive sensors were used instead of the fifty dielectric sensors, one more case study was performed. The sensors' electric system was operated in exactly the same way as before (i.e., running the alternating input voltage at a frequency of 150 kHz), except that after recording the sensor data at each time step, the input voltage was converted to DC form (by setting the excitation frequency, ω to zero) and the corresponding data was separately recorded as resistive sensor data. For brevity, only one sensor's (C5) response

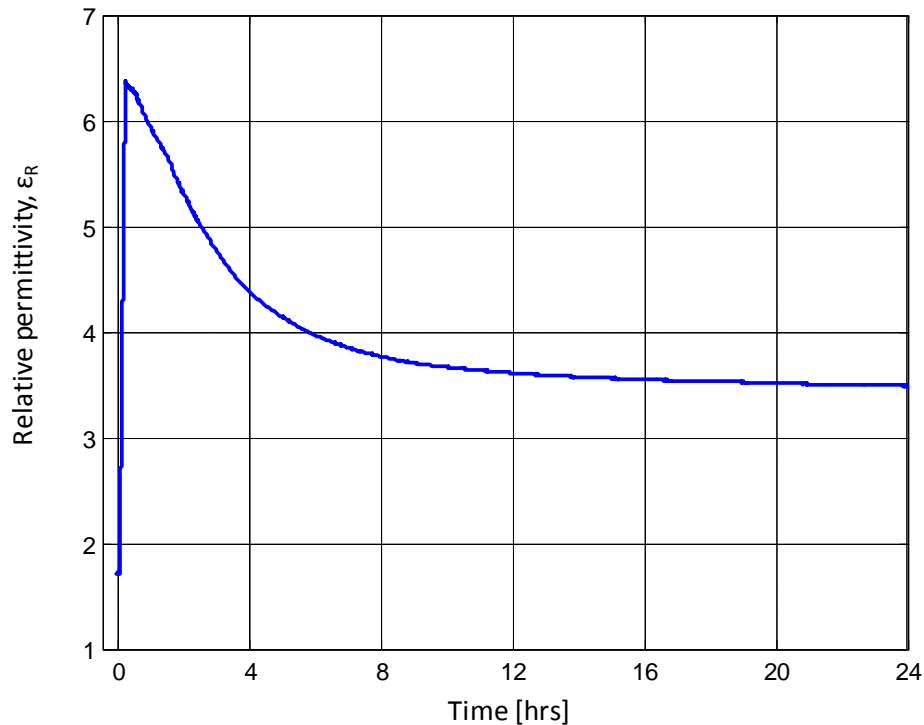


Figure 15. The average of relative permittivities, ϵ_R of the fifty sensors during the resin cure stage of Case Study 2.

was plotted in Figure 16. As seen in the figure, the resistive sensor responded as an almost step function upon the resin arrival to that sensor. In other words, the output voltage increased to its saturated value even when a small fraction of the sensor's surface was filled with resin. This is due to the high gain used in the circuit. Recall that using a much lower gain would not have this problem (sudden increase in the output voltage). However, the system then would be very vulnerable to the external noise. When the gain is set to a low value, the sensors may even give false resin arrival signals unless the threshold value is set low enough [4]. This though is very difficult to do especially when the high electrical resistivity of typical RTM resins are considered.

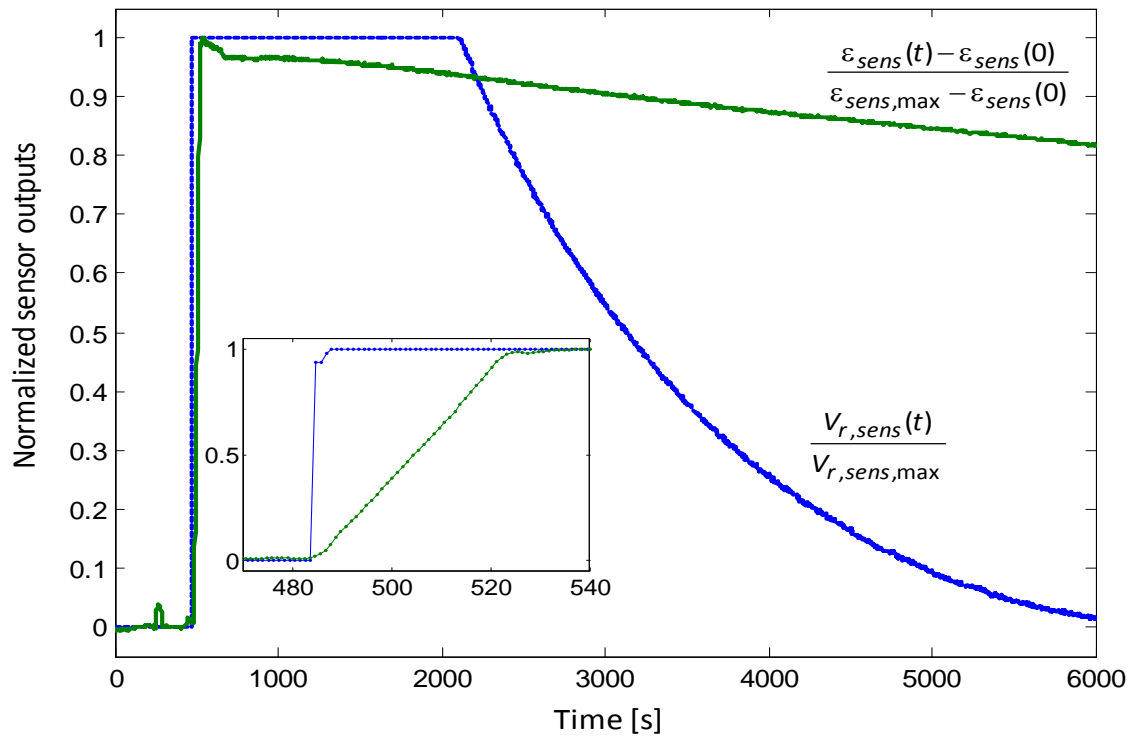


Figure 16. The data of a sensor (C5) when it is operated as a point-resistive sensor (dashed, blue) and a dielectric sensor (solid green).

Chapter 6

SUMMARY AND CONCLUSIONS

It was shown that previously used dielectric sensor systems can only measure the fraction of the sensors filled with the flowing resin, but not the resin's whereabouts in the mold cavity. The monitoring results of these previous studies may be ambiguous and cause false control of the RTM process. A grid of fifty dielectric sensors were embedded in RTM mold walls so that much more detailed and accurate monitoring could be achieved. Each of these sensors gives the local saturation, and the multiple sensor data can be used to monitor the flow front position with a higher certainty than the previous applications. These sensors were permanently embedded to the mold by machining the mold surface after assembling the copper-plate electrodes and the insulator housings to the mold walls tightly. This study also reviews the four different alternatives for parallel-plate dielectric sensor configurations: unshielded, shielded, grounded and "modified grounded" (the proposed method of this study) by comparing these sensors' output with the analytical value. The most accurate choice is the shielded configuration. However it is tedious and costly to embed multiple shielded sensors as mentioned earlier. The modified version of the grounded configuration enabled the measuring of the relative permittivity of the medium (dry or wetted fabric preform) by eliminating the unknown and time-varying mold

capacitance from the system equations. Instead of having fifty separate parallel-plate sensors, an easier approach was used, in which a grid was formed by having five horizontal and ten vertical electrodes and by considering the projected areas as the sensing areas. Several RTM case studies were presented here to validate the success of the proposed dielectric sensor system.

BIBLIOGRAPHY

- [1] Sozer EM, Bickerton S, Advani SG. "On-line strategic control of liquid composite mould filling process," *Composites Part A: Applied Science and Manufacturing* 2000;31(12):1383-1394.
- [2] Lawrence JM, Hsiao KT, Don RC, Simacek P, Estrada G, Sozer EM, Stadtfeld HC, Advani SG, "An approach to couple mold design and on-line control to manufacture complex composite parts by resin transfer molding," *Composites Part A: Applied Science and Manufacturing* 2002;33(7):981-990.
- [3] Advani SG, Sozer EM. *Process modeling in composites manufacturing*. Elsevier Marcel Dekker Inc. 2003.
- [4] Danisman M, Tuncol G, Kaynar A, Sozer EM. "Monitoring of resin flow in the resin transfer molding (RTM) process using point-voltage sensors", *Composites Science and Technology* 2007;67(3-4):367-379.
- [5] Barooah P, Berker B, Sun JQ. Lineal sensors for liquid injection molding of advanced composite materials, *J. Mater. Process Manuf. Sci.* 1999; 6(3): 169-184.
- [6] Lawrence JM, Hsiao K, Don RC, Simacek P, Estrada G, Sozer EM, Stadtfeld HC, Advani SG. An approach to couple mold design and on-line control to manufacture complex composite parts by resin transfer molding. *Composites Part A: Applied Science and Manufacturing* 2002; 33(7), 981-990.

-
- [7] Walsh S. In-situ sensors method and device, U.S. Patent 5,210,499, May 1993.
- [8] Fink BK, Walsh SM, DeSchepper DC, Gillespie Jr. JW, McCullough RL, Don RC, Waibel BJ. Advances in resin transfer molding flow monitoring using SMARTweave sensors. In: Proceedings of ASME, International Mechanical Engineering Congress and Exposition. San Francisco, CA; 1995; 69(II): 999-1015.
- [9] Bradley JE, Diaz-Perez J, Gillespie Jr. JW, Fink BK. On-line process monitoring and analysis of thick-section composite parts utilizing SMARTweave in situ sensing technology. In: Proceedings of International SAMPE Symposium and Exhibition; 1998. p 254-67.
- [10] Rath M, Doring J, Stark W, Hinrichsen G. Process monitoring of moulding compounds by ultrasonic measurements in a compression mould. NDT&E International 2000;33:123-130.
- [11] Schmachtenberg E, Schulte J zur Heide, Topker J. Application of ultrasonics for the process control of Resin Transfer Moulding (RTM). Polymer Testing 2005;24(3):330-338.
- [12] Lim ST, Lee W. An analysis of the three-dimensional resin-transfer mold filling process. Composites Science and Technology 2000;60:961-975.
- [13] Dunkers JP, Lenhart JL, Kueh SR, van Zanten JH, Advani SG, Parnas RS. Fiber-optic flow and cure sensing for liquid composite molding. Opt. Lasers Engineering 2001;35(2):91-104.

-
- [14] Tuncol G, Danisman M, Kaynar A, Sozer EM. Constraints on monitoring resin flow in the resin transfer molding (RTM) process by using thermocouple sensors. *Composites Part A: Applied Science and Manufacturing* 2007;38(5):1363–1386.
- [15] Heider D, Don R, Thostensen ET, Tackitt K, Belk JH, Munns T. Cure monitoring and control. *ASM Handbook, Vol. 21. Composites*; 2001; 692-698.
- [16] Dominauskasa A, Dirk Heider D, Gillespie JW. Electric time-domain reflectometry sensor for online flow sensing in liquid composite molding processing. *Composites Part A: Applied Science and Manufacturing* 2003;34 67–74.
- [17] Dominauskasa A, Dirk Heider D, Gillespie JW. Electric time-domain reflectometry distributed flow sensor. *Composites Part A: Applied Science and Manufacturing* 2003;38 138-146.
- [18] McIlhagger A, Brown D, Hill B. The development of a dielectric system for the online cure monitoring of the resin transfer molding process. *Composites Part A: Applied Science and Manufacturing* 2000;31:1373-1381.
- [19] Hegg MC, Ogale A, Mescher A, Mamishev AV, Minaie B. Remote monitoring of resin transfer molding processes by distributed dielectric sensors. *Journal of Composite Materials*, Vol. 39, No. 17/2005.
- [20] Kim HG, Lee DG. Dielectric cure monitoring for glass/polyester prepreg composites. *Composite Structures* 2002;57:91-99.

-
- [21] Bang KG, Kwon JW, Lee DG, Lee JW. Measurement of the degree of cure of glass fiber epoxy composites using dielectrometry. *Journal of Materials Processing Technology* 2001;1113:209-214.
- [22] Vaidya UK, Jadhav NC, Hosur MV, Gillespie JW, Fink BK. Assessment of flow and cure monitoring using direct current and alternating current sensing in vacuum-assisted resin transfer molding. *Smart Mater. Struct.* 2000; 9 : 727–736.
- [23] Rowe GI, Yi JH, Chiu KG, Tan J, Mamishev AV, Minaie B. Fill-front and cure progress monitoring for VARTM with auto-calibrating dielectric sensors. *SAMPE 2005 Symposium & Exhibition*, May 2005.
- [24] Skordos AA, Karkanas PI, Partridge IK. A dielectric sensor for measuring flow in resin transfer moulding. *Meas. Sci. Technol.* 2000; 11 : 25–31.
- [25] Mounier AL, Binétruy C, Krawczak P. Multipurpose carbon fiber sensor design for analysis and monitoring of the resin transfer molding of polymer composites. *Polymer Composites* 2005; 26(5): 717 – 730.
- [26] Yenilmez B, Sozer EM. Real-time monitoring of resin transfer molding (RTM) using grid of dielectric sensors. Submitted to *Composites A: Manufacturing and Technology*, August 2008.
- [27] Basics of measuring the dielectric properties of materials, Application Note 1217-1, Hewlett-Packard Inc.

- [28] Nishiyama H, Nakamura M. Form and capacitance of parallel-plate capacitors. IEEE transactions on components, packaging, and manufacturing technology, Part A, 1994; 17(3).

- [29] Blythe T, Bloor D. Electrical properties of polymers. Cambridge University Press, 2005. p159.

- [30] Ball J, Moore AD. Essential physics for radiographers. Blackwell publishing, 1997. p32.

- [31] Novak G. Electronics tutorial, peak detector. Nov55, <http://nov55.com/amr/tu.html>, retrieved on 13.08.2008.

VITA

BEKIR YENILMEZ was born in Ankara, Turkey on August 2, 1984. He received his B.Sc. degree in Mechanical Engineering from Middle East Technical University, Ankara in 2006. Since then, he has enrolled in the M.Sc program in Mechanical Engineering at Koc University, Istanbul with full TUBITAK scholarship, as both a teaching and research assistant. His most recent thesis, “Real-Time Monitoring of Resin Transfer Molding Using A Grid of Dielectric Sensors” acts as a complement to his numerous other RTM and VARTM related works. He published a journal paper in Composite Science and Technology. Upon completion of his Masters Degree, Bekir plans to study further, with a view to achieving a PhD.

Appendix A.1. Datasheet of the resin. [www.poliya.com.tr]

Polipol™ 336-RTM

SIVI HALDEKİ ÖZELLİKLERİ
PROPERTIES OF LIQUID FORM

TEST TEST	METOD METHOD	DEĞER VALUE
Renk Colour	ISO 2211 -	max. 100 Hazen
Yoğunluk Density	ISO 1675 ±%5	1,094 gr/cm ³
Kırılma Indisi Refraction Index	ISO 0489 ±%5	1,532
Asit Değeri Acid Value	ISO 2114 ±%10	23 mg KOH/gr
Viskozite ¹ Brookfield® Viscosity Brookfield®	ISO 2555 ±%30	300 cp
Tiksotropi Thixotropy	- ±%30	N/A
Jel Süresi ² Gel Time	ISO 2535 ±%40	14'
Monomer Oranı Monomer Content	- ±%12	37 %
Parlama Noktası Flash Point	Abel-Pernsky -	28 °C
Raf Ömrü Shelf life in months	- -	4 ay

1 23 °C de, 4 uç, 50 devir ile ölçülmüştür.
It is measured at 23 °C, 50 rpm with spindle 4.

2 23 °C de, % 1 ml % 1 lik Co, % 1 ml Mek-p (Butanox M 60) ile ölçülmüştür.
It is measured at 23 °C added 1 % ml Co (1 % con.) and 1 % ml Mek-p (Butanox M 60).

SERTLEŞME VERİLERİ³
CURING DATA

TEST TEST	METOD METHOD	DEĞER VALUE
t _{65°C → 90°C} t _{65°C → 90°C}	ISO 0584 ±%10	6'13"
t _{65°C → T_{make}} t _{65°C → T_{max}}	ISO 0584 ±%10	8'38"
t _{make} t _{max}	ISO 0584 ±%10	11'36"
T _{make} T _{max}	ISO 0584 ±%10	222 °C

3 Reçine 80 °C sıcaklığındaki banyoda, %2 oranında %50 lik Benzoil Peroksit Pasta (Lucidol BT-50,Akzo) ile sertleştirilmiştir.
Resin cured in 80 °C bath with 2% Benzoyl Peroxide Paste (50% con,Lucidol BT-50,Akzo)

SERTLEŞMİŞ REÇİNENİN ÖZELLİKLERİ ⁴

PROPERTIES OF CURED RESIN

TEST TEST	METOD METHOD		DEĞER VALUE
Yük Altında Eğilme Sıcaklığı (HDT) Heat Deflection Temperature (HDT)	ISO 0075-A ISO 0075-B	±%10	77 °C 91 °C
Su Absorbsiyonu Water Absorption	ISO 0062	±%10	0,185 %
Barkol Sertliği (Barcol 934-1) Barcol Hardness (Barcol 934-1)	ASTM-D 2583	±%10	44
Toplam Hacimsel Çekme Total Volume Shrinkage	ISO 2114	±%10	9,04 %

SERTLEŞMİŞ REÇİNENİN MEKANİK ÖZELLİKLERİ ⁵

MECHANICAL PROPERTIES OF CURED RESIN

TEST TEST	METOD METHOD		SAF REÇİNE DEĞERİ PURE RESIN VALUE
Eğilme Dayanımı Flexural Strength	ISO 0178	±%10	113 MPa
Elastiklik Modülü Flexural Modulus	ISO 0178	±%10	3110 MPa
Kopmadaki Uzama Elongation at Break	ISO 0178	±%10	4,3 %
Çekme Dayanımı Tensile Strength	ISO 0527	±%10	64 MPa
Elastiklik Modülü Modulus of Elasticity in Tensile	ISO 0527	±%10	2801 MPa
Kopmadaki Uzama Elongation at Break	ISO 0527	±%10	2,8 %
İzod Darbe Dayanımı Izod Impact Strength	ISO 0180	±%10	9 kJ/m ²

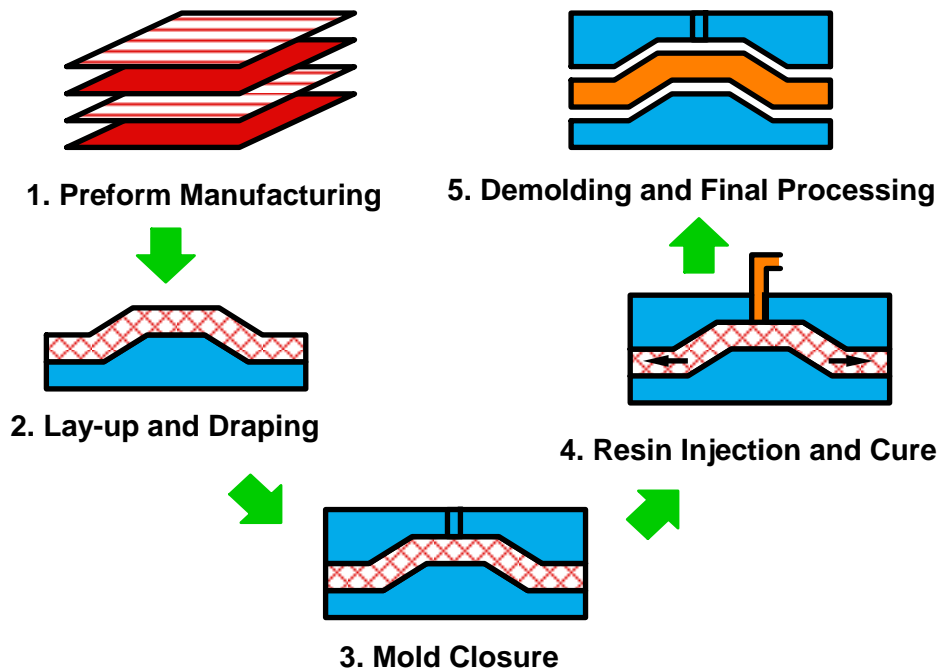
4 **5** Sertleşmiş reçinenin testleri için reçine sertleştikten sonra post-kür işlemine tabi tutulmuştur.
Before the mechanical tests, the cured resin is post-cured.

Appendix A.2. Injection Machine.[www.radiuseng.com]

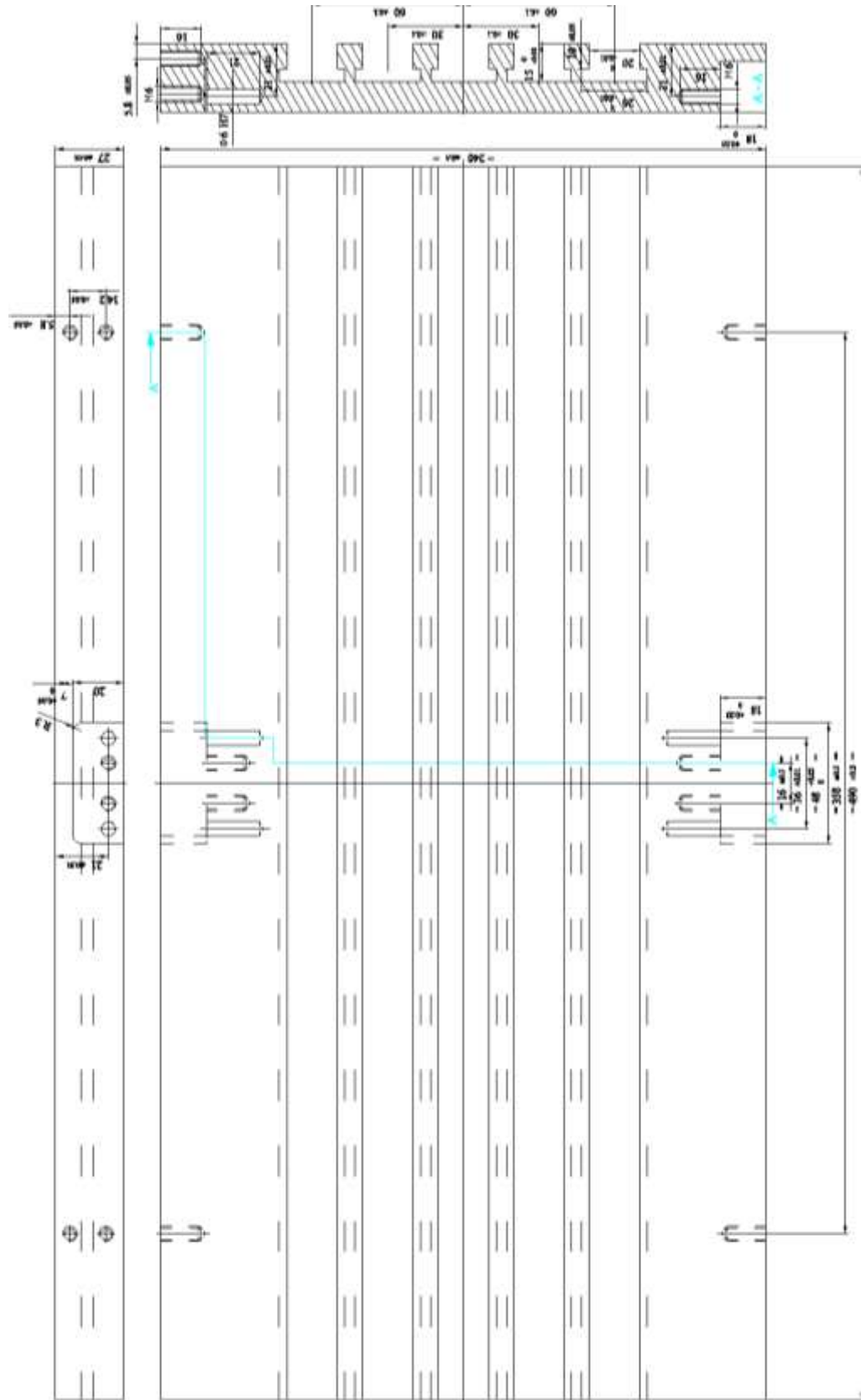
Manufacturer:	Radius Engineering Inc., Utah, USA (RADIUS)
Model:	Radius 2100 cc Electric RTM Injection Cylinder Version 5.17.2001
Capacity of polymer:	2100 cc
Polymer types:	Thermoset (applicable to RTM)
Maximum injection pressure:	27.5 bar (= 2.7 MPa = 400 psi)
Heating system:	Electrical heater around injection cylinder and tubes
Maximum temperature:	176°C (= 350°F)
Control:	PID temperature control Flowrate control Injection pressure set points
Power:	4.8 kW (240 V, 20 amp)

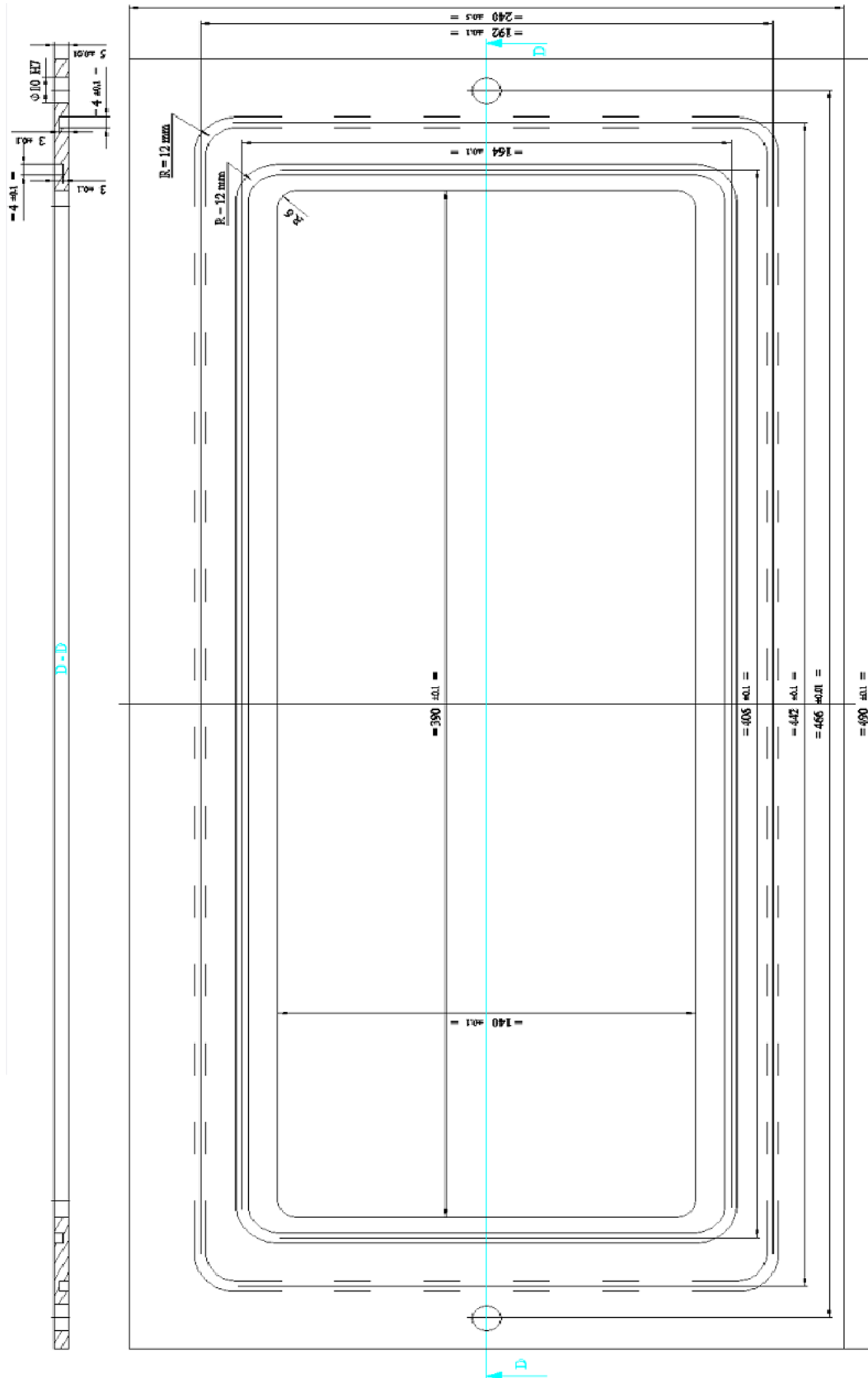
Appendix A.3. Fabric preform material.

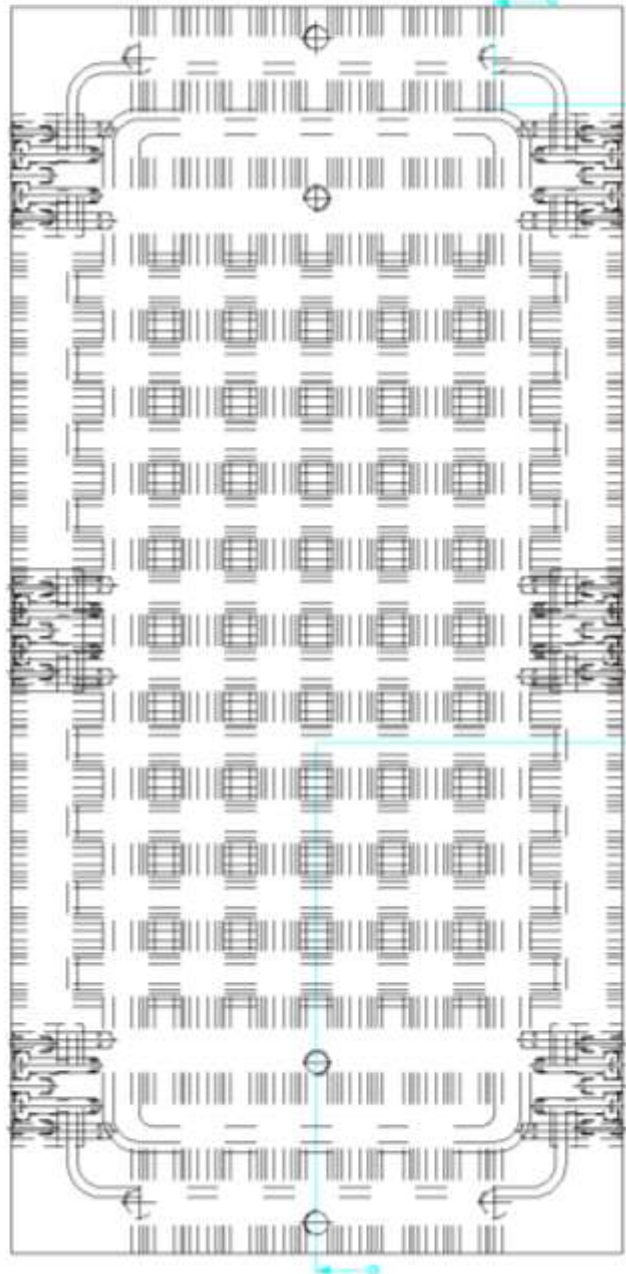
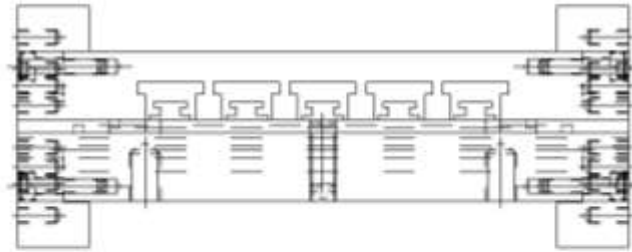
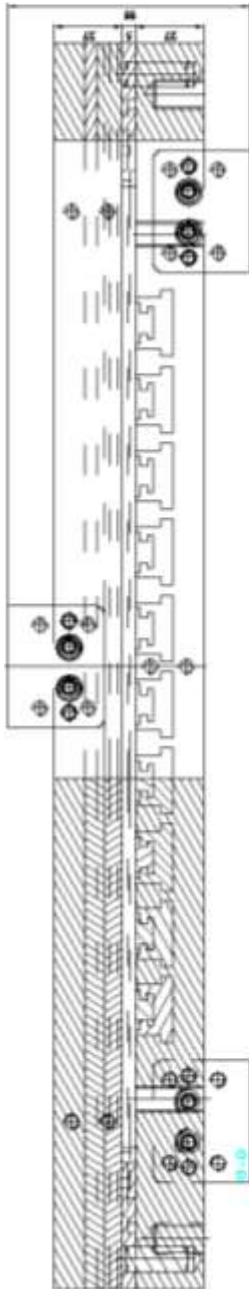
Fibroteks
Stitched Random
450 gram/m²

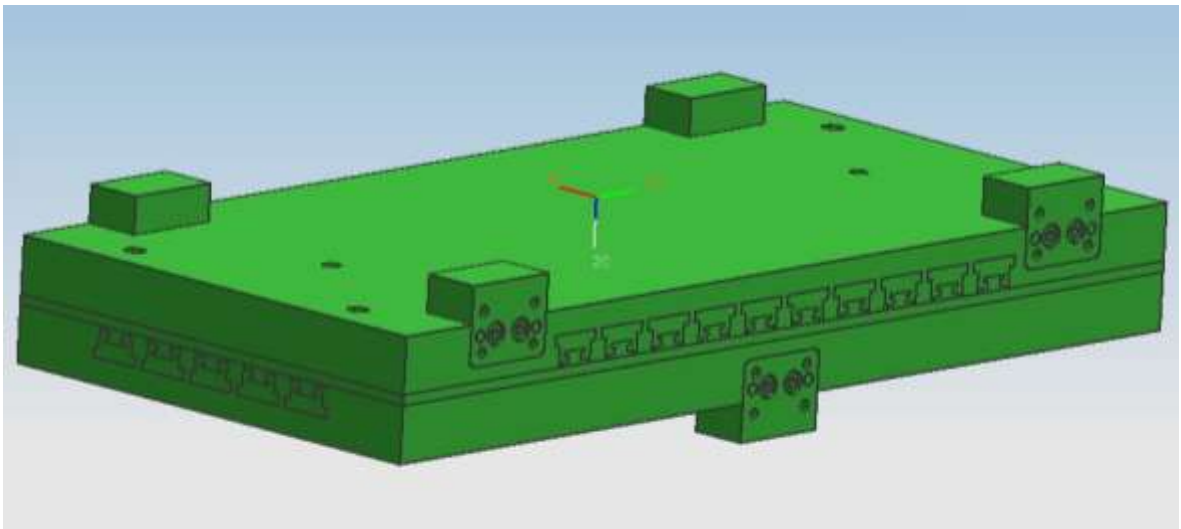
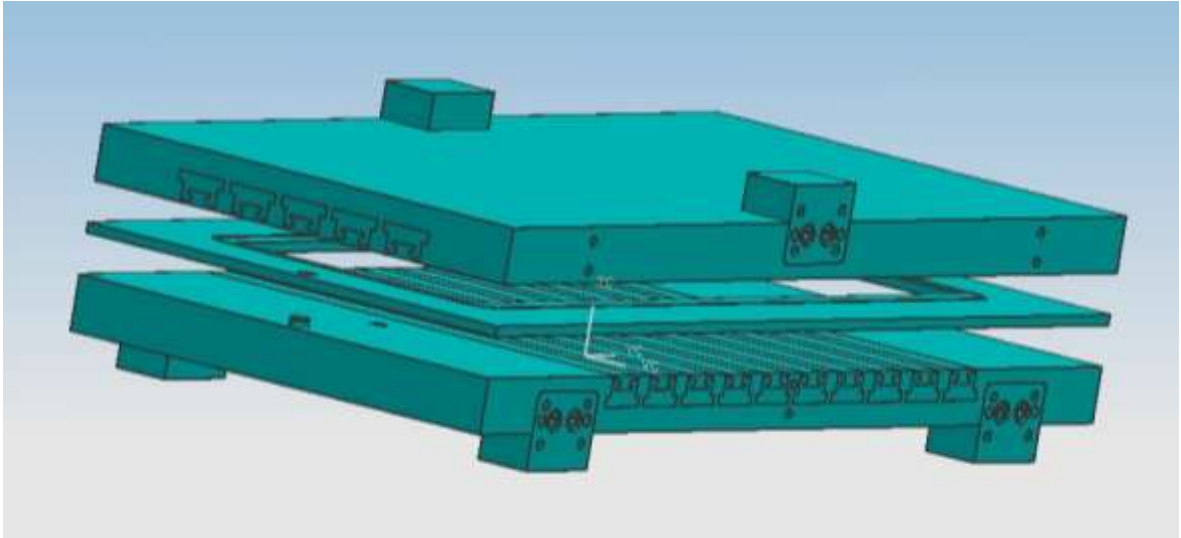
Appendix A.4. RTM process steps overview [14]

Appendix B.1. Mold technical drawings.

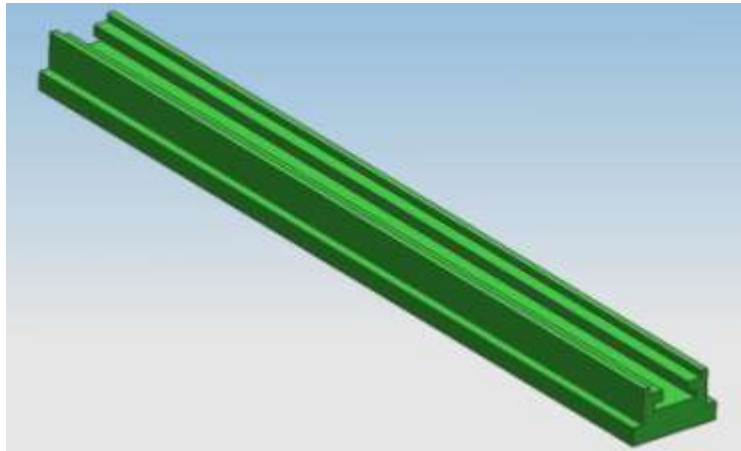




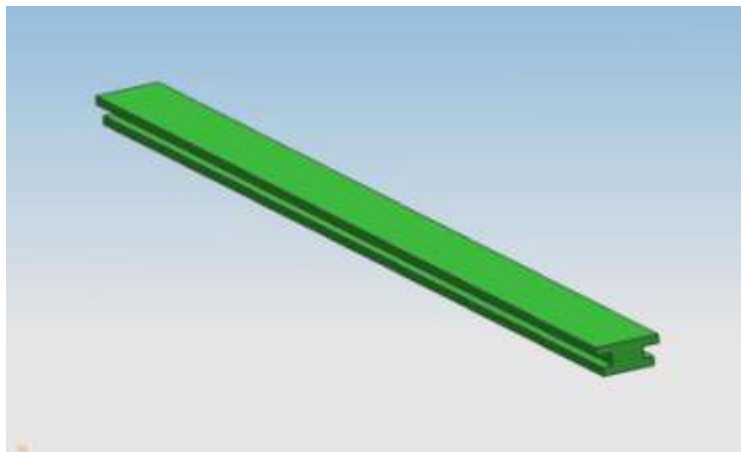


Appendix B.2. Mold 3D Visualitions.

Open/Closed view of the entire mold.



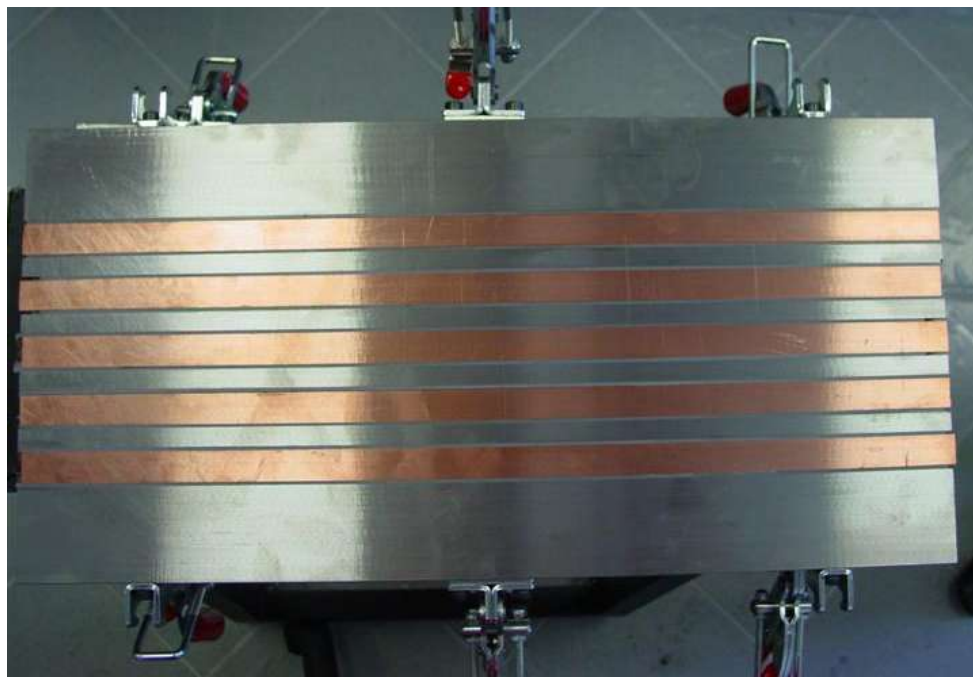
Insulator made from delrin



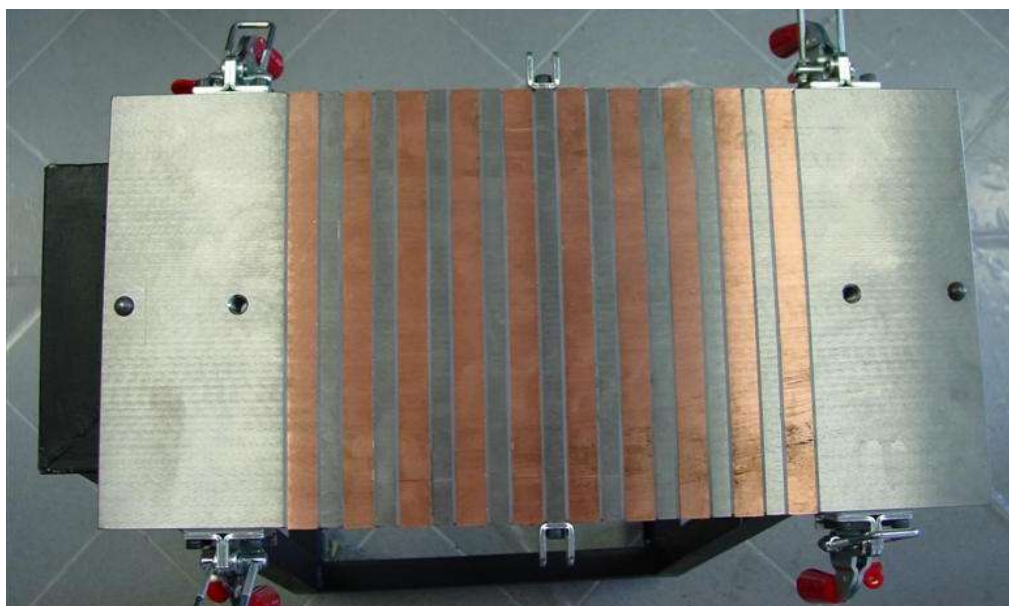
Sensing plates made of copper.

Appendix B.3. Mold Photos.

Entire mold, without circuit board.



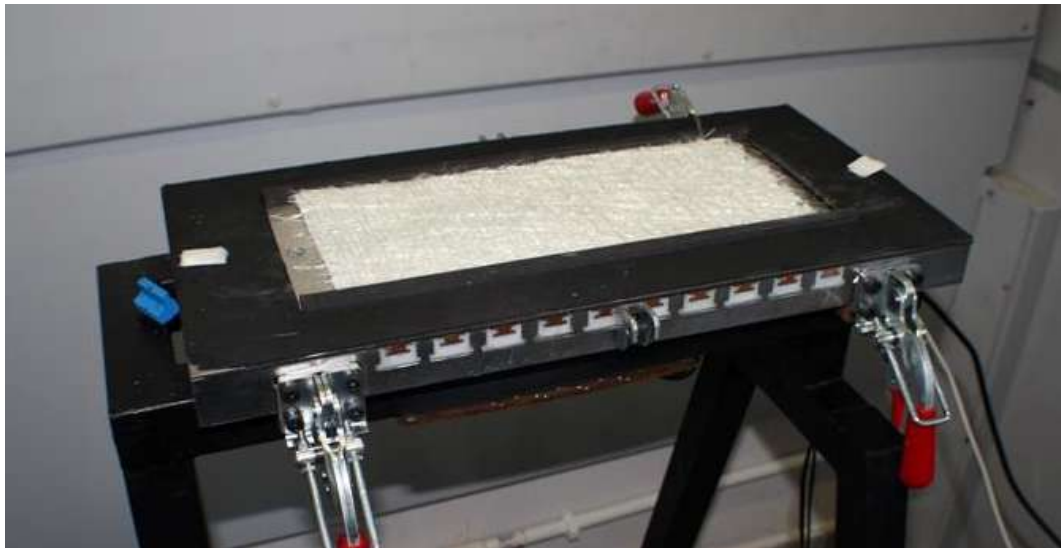
Upper mold plate.



Lower mold plate



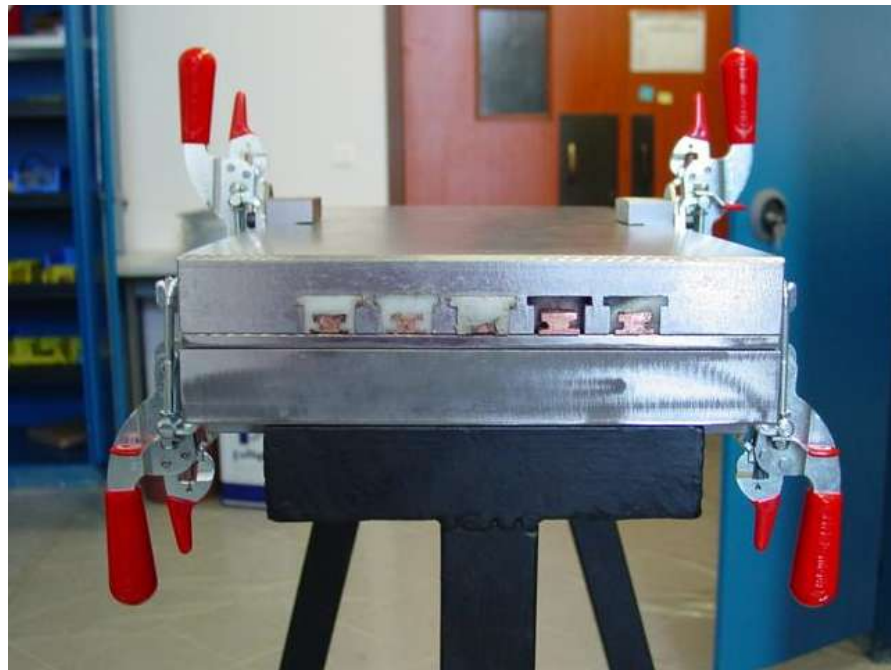
Lower mold plated with 6mm spacer frame.



Fabric placed and mold is ready to be closed.

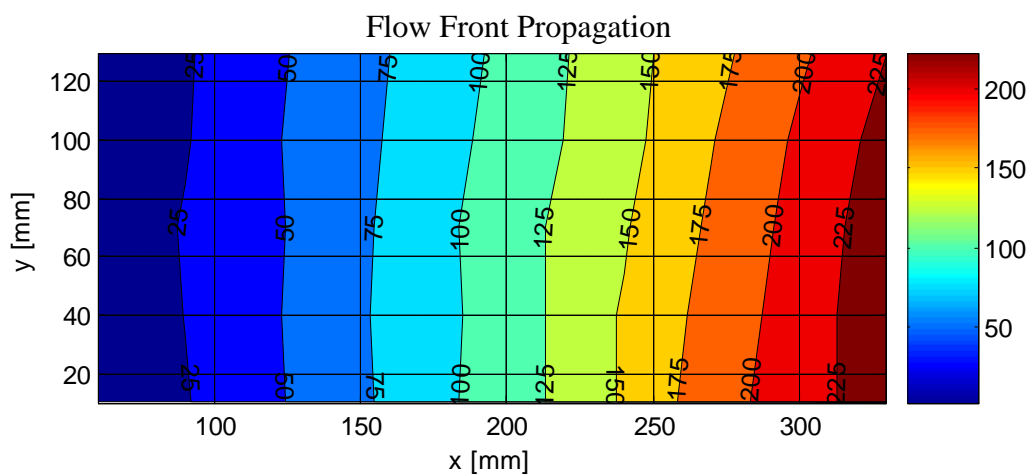
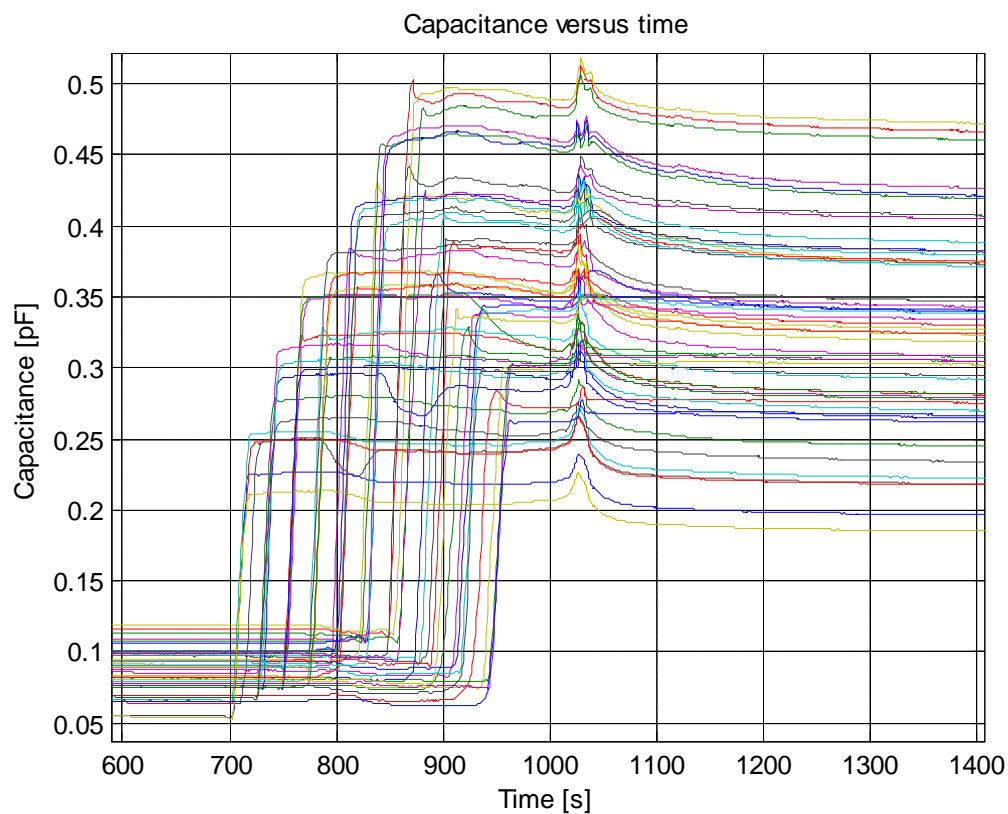


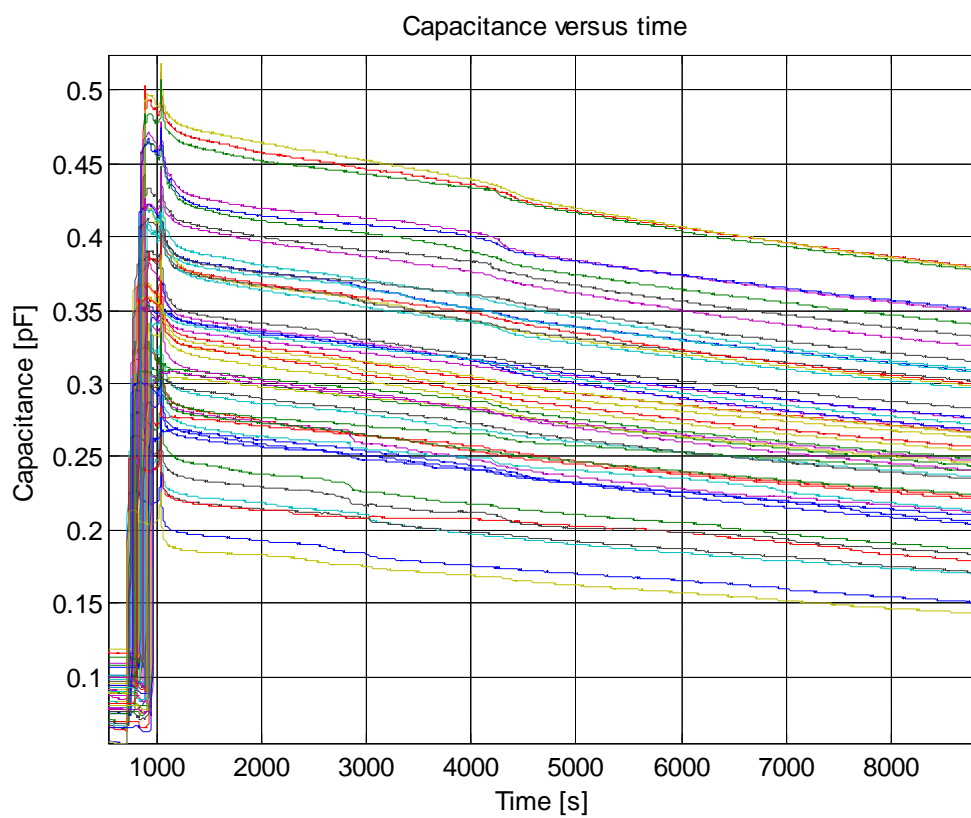
Mold with latches closed. Isometric view.



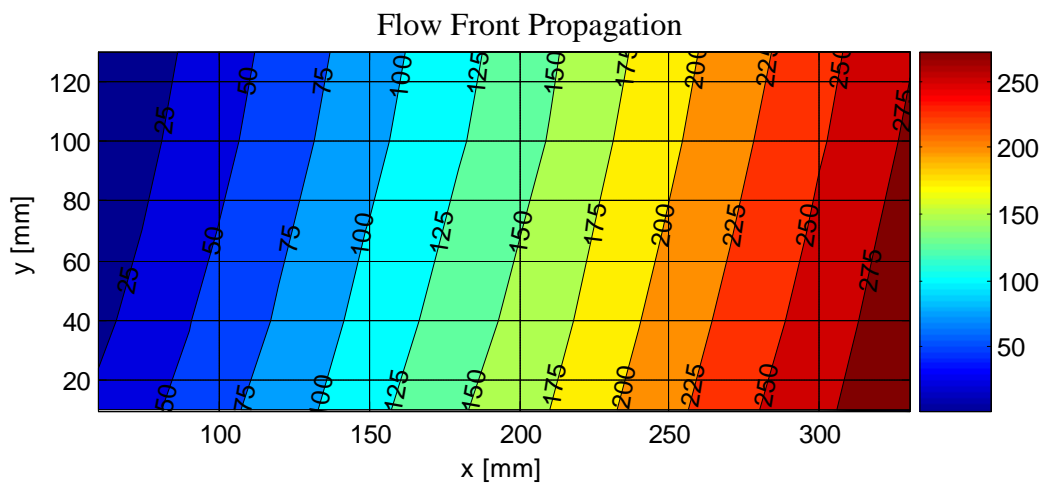
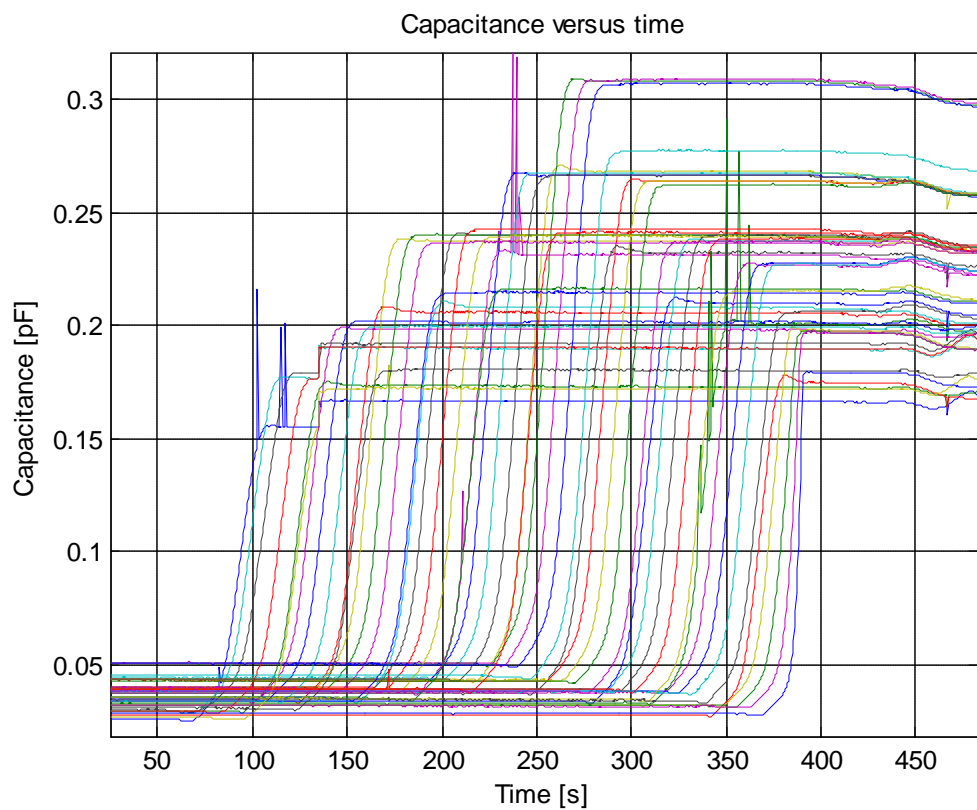
Mold with latches closed. Side View

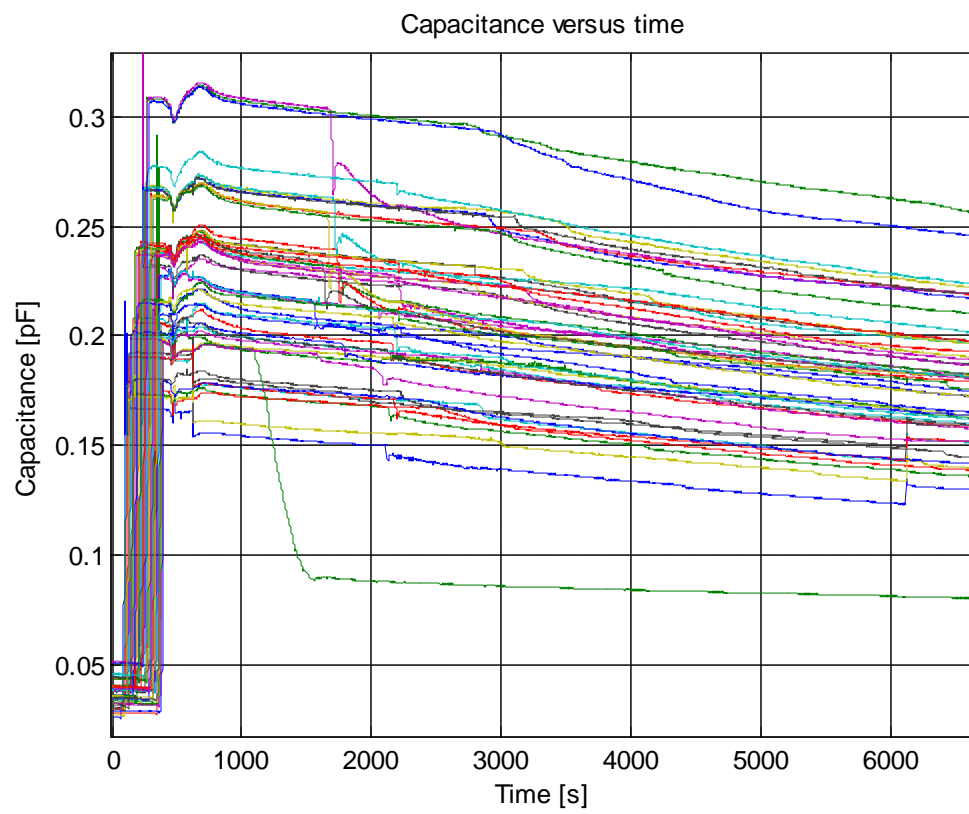
Appendix C.1. Results of Experiment 6. With grounded configuration.



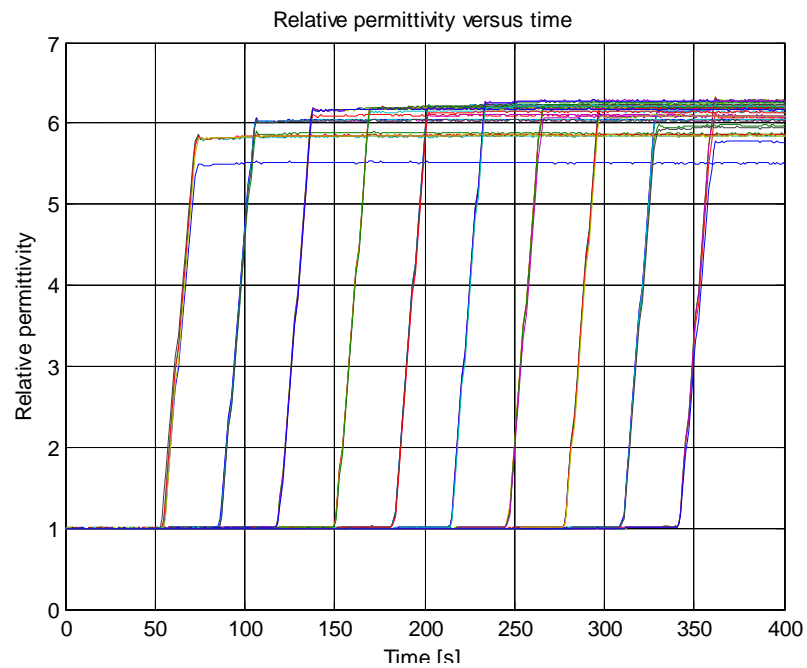
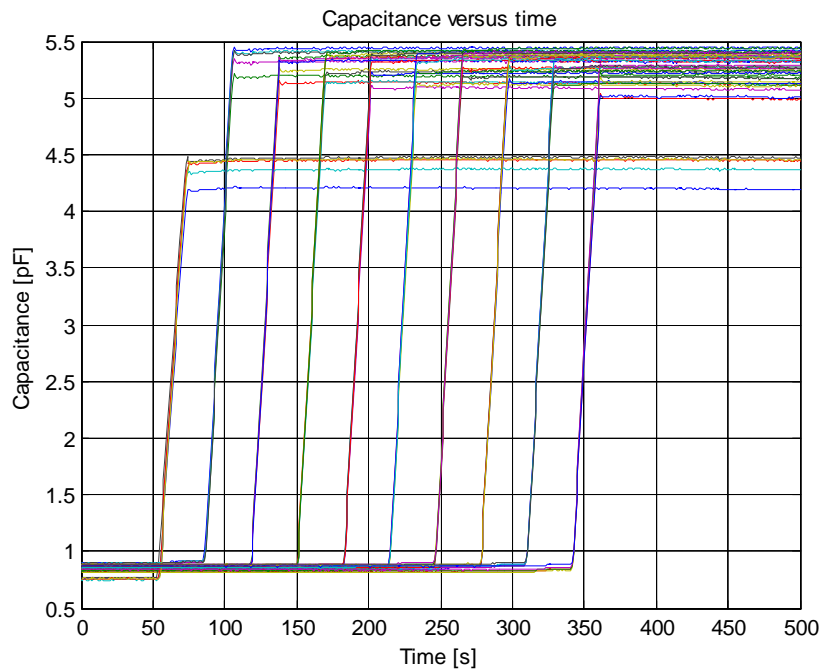


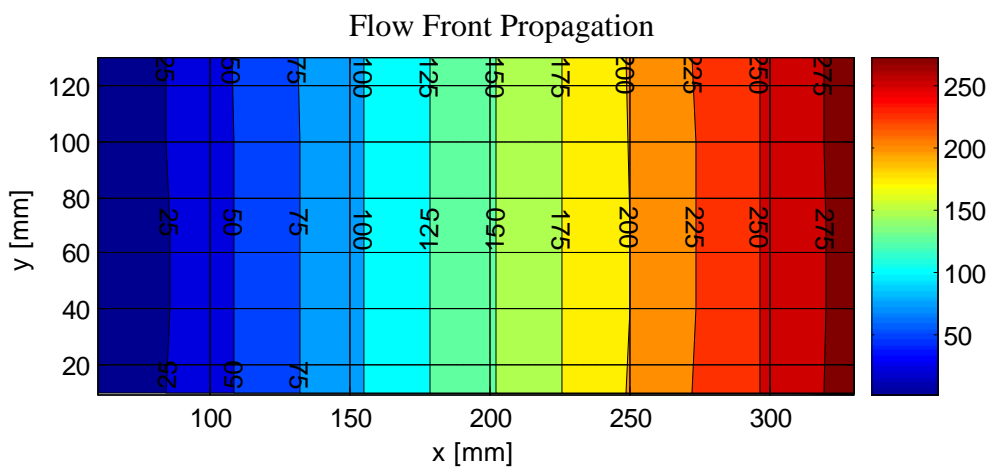
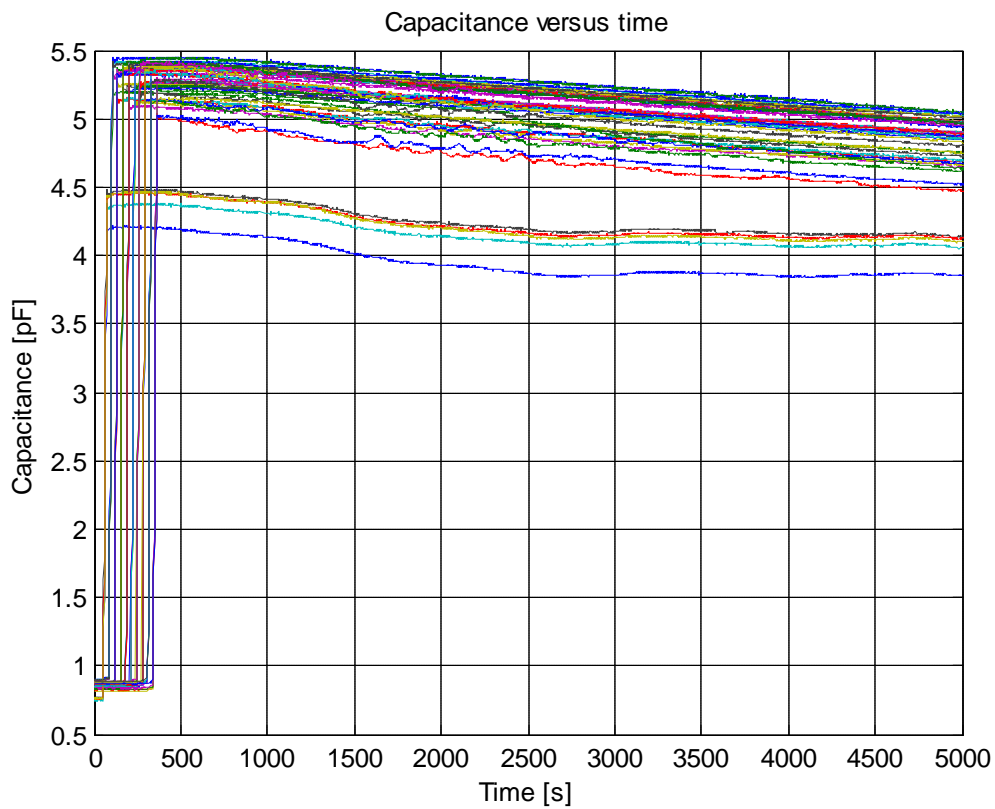
Appendix C.2. Results of Experiment 11. With grounded configuration.

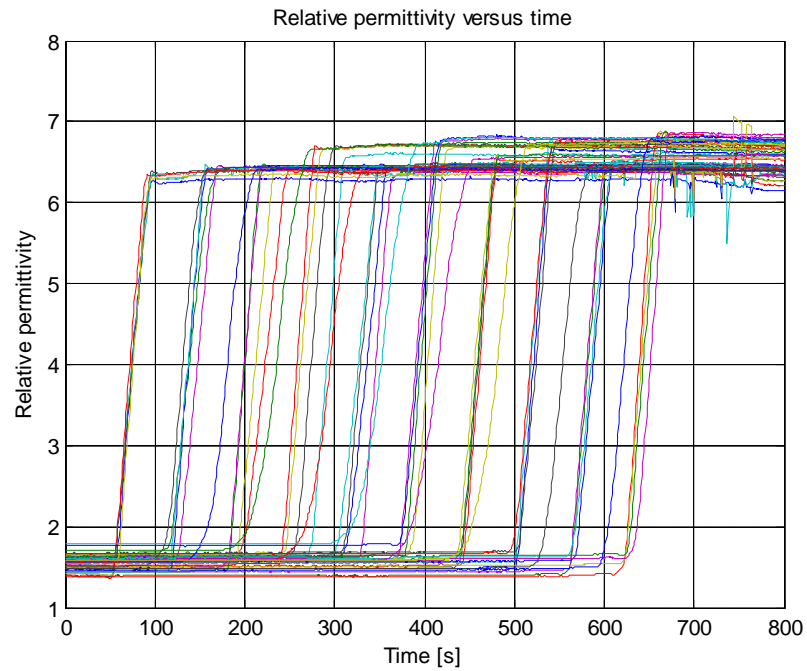
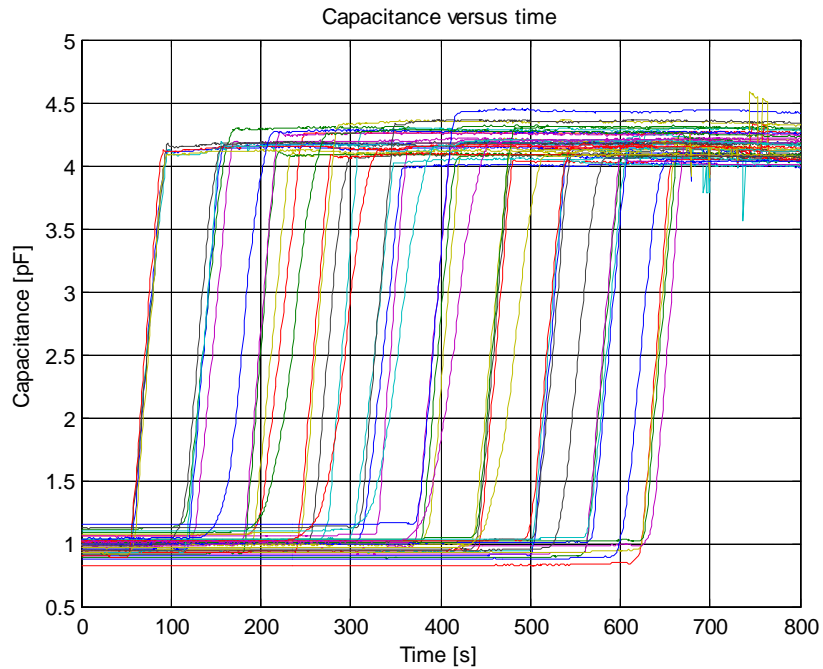


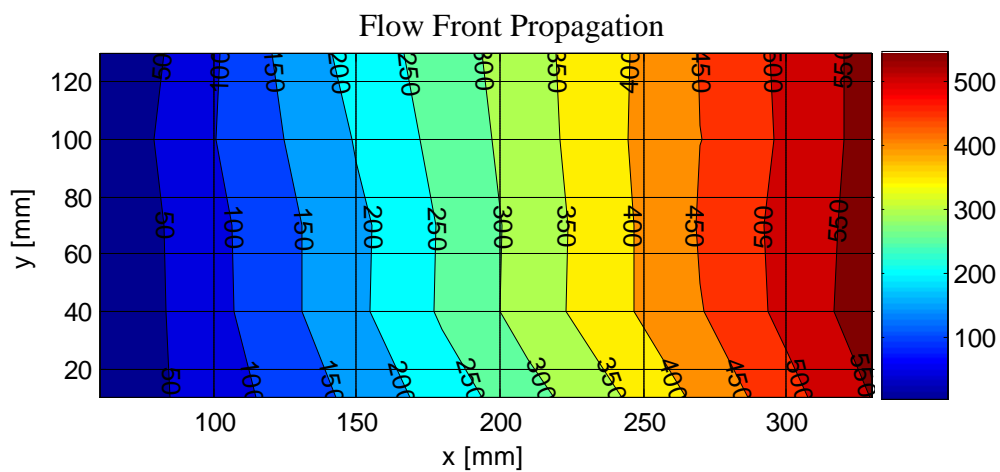
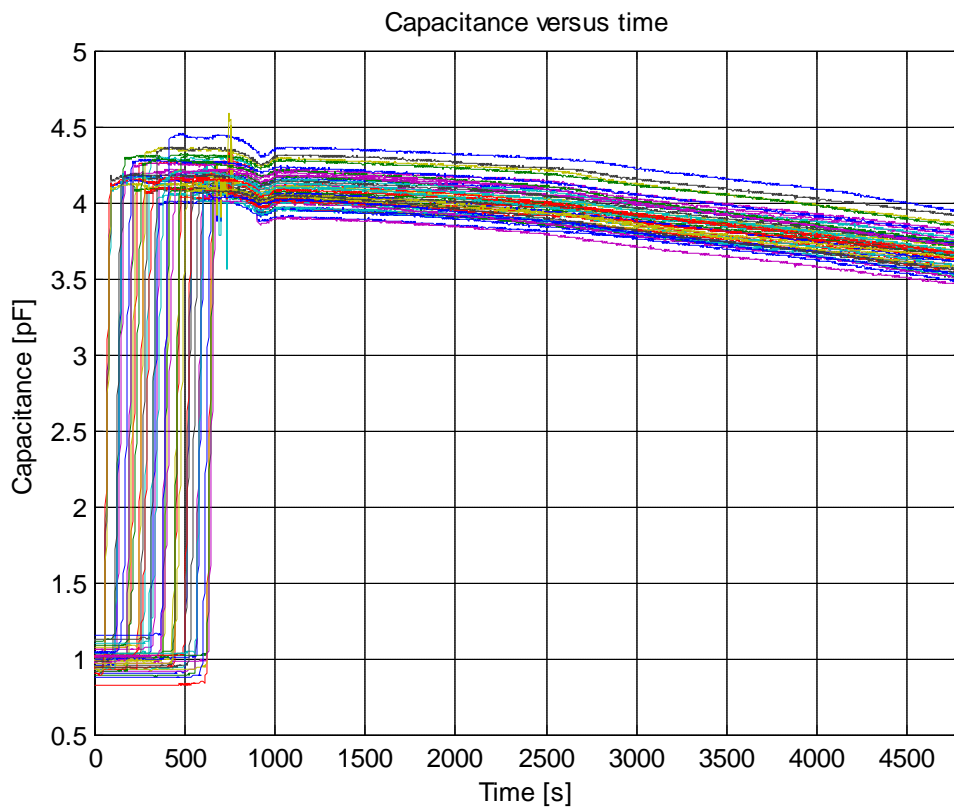


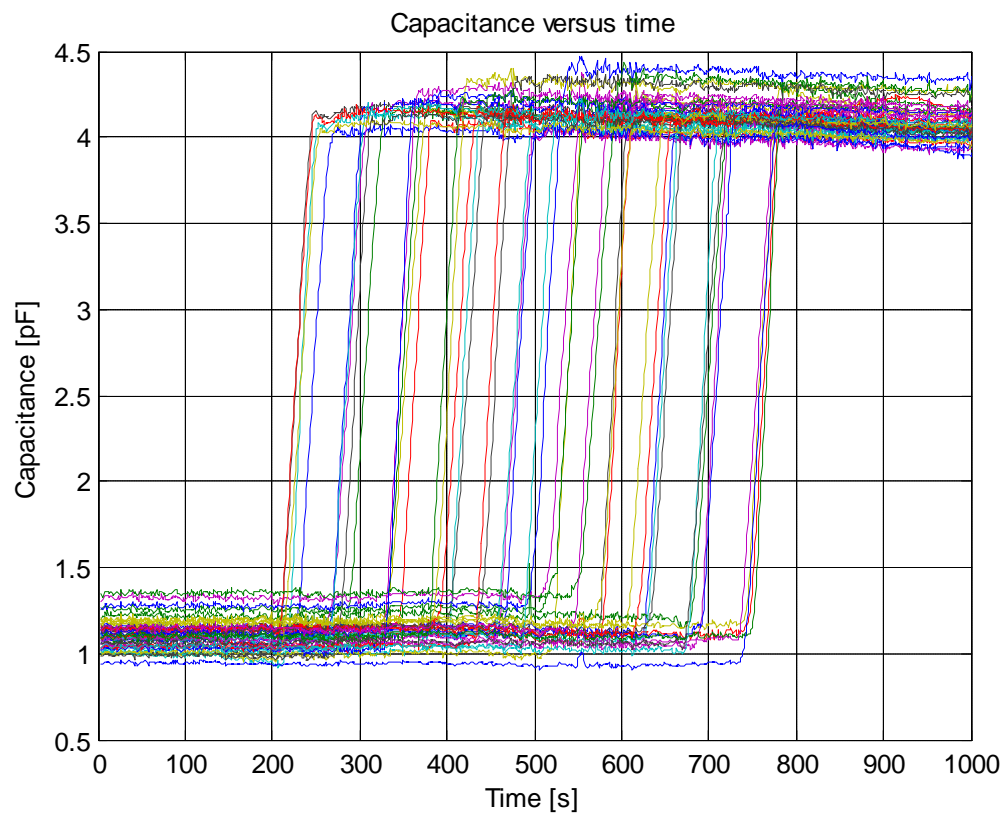
Appendix C.3. Results of Experiment 12. With modified grounded configuration.No fabric, mould placed vertically for a perfect 1-D flow

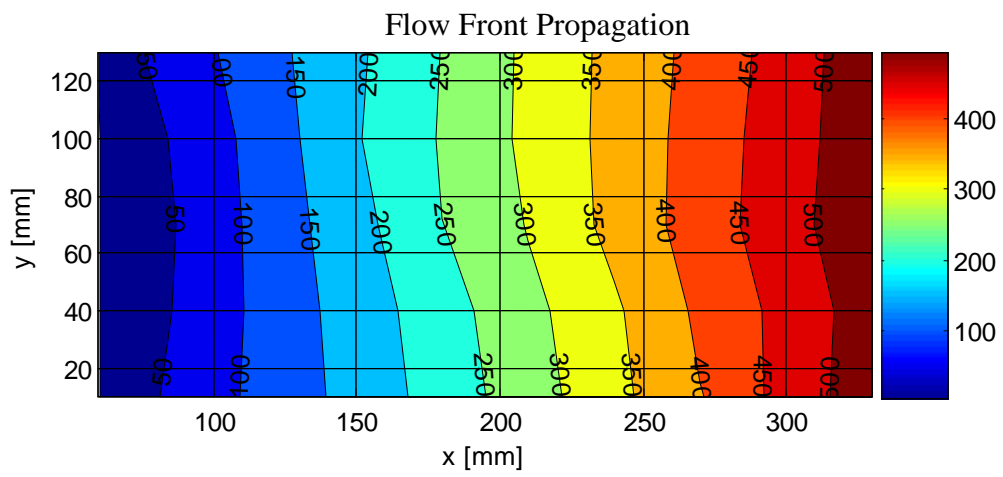
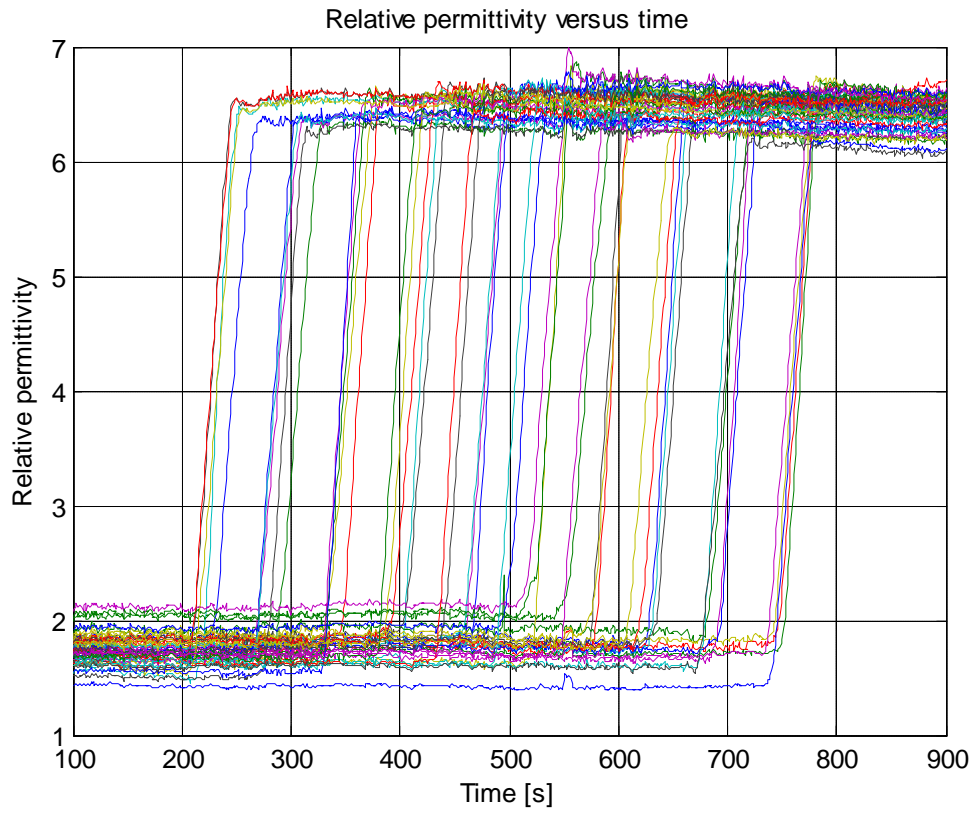


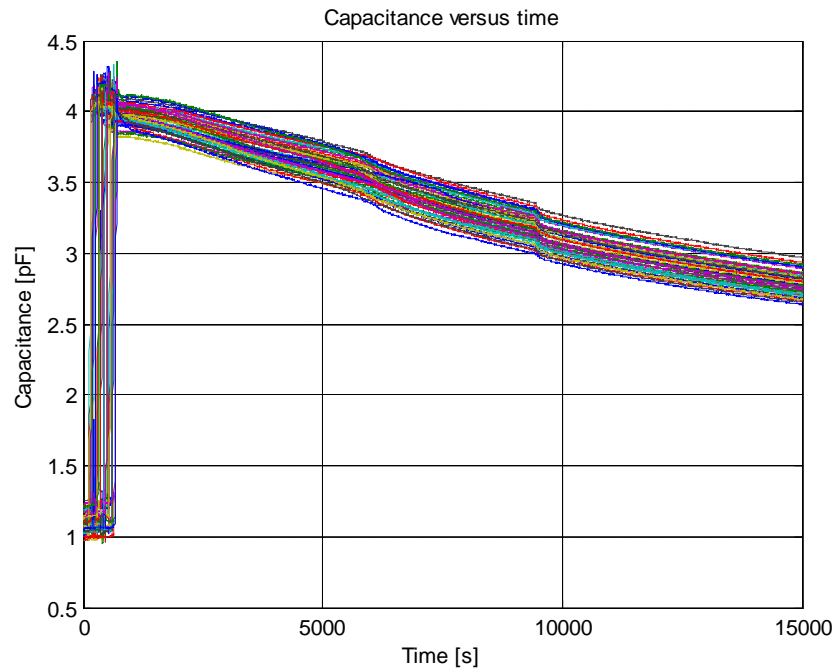
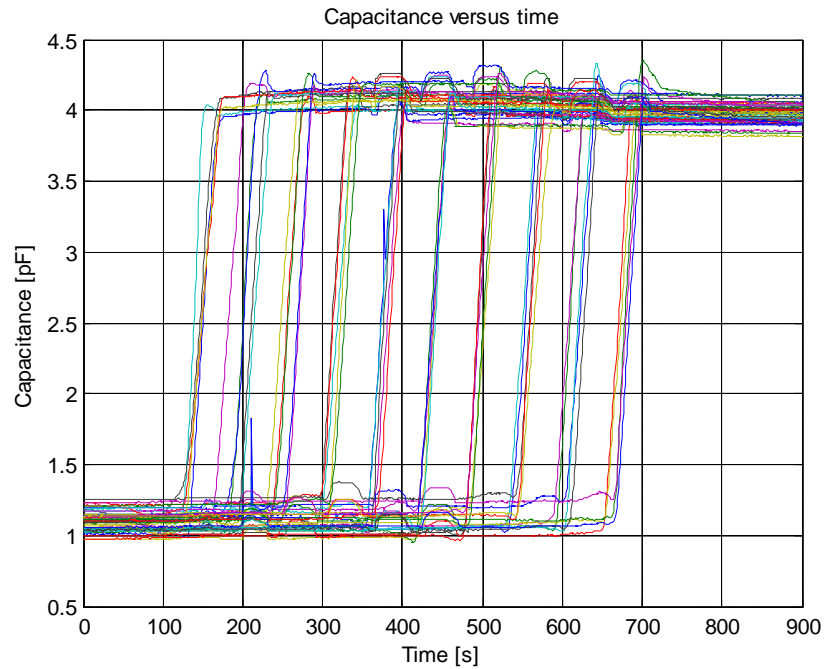


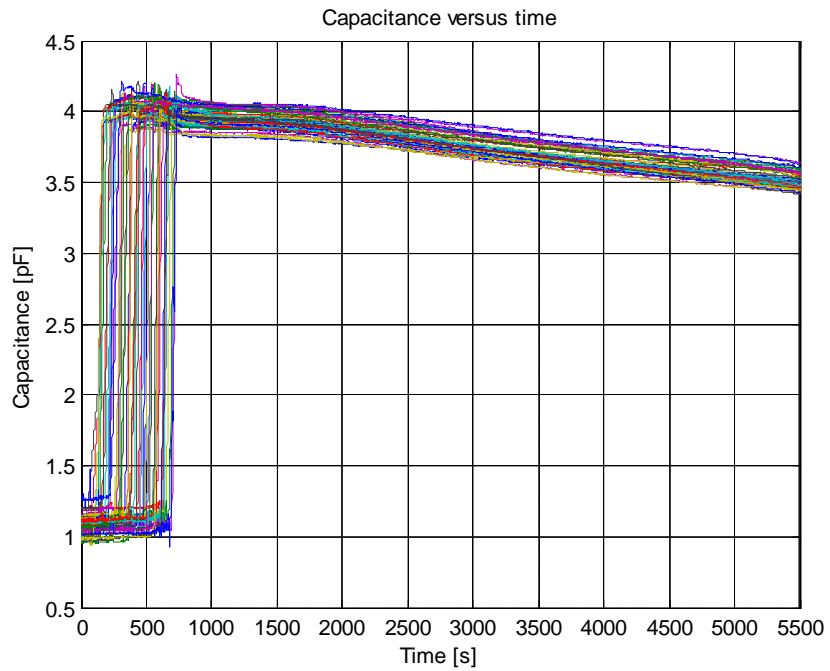
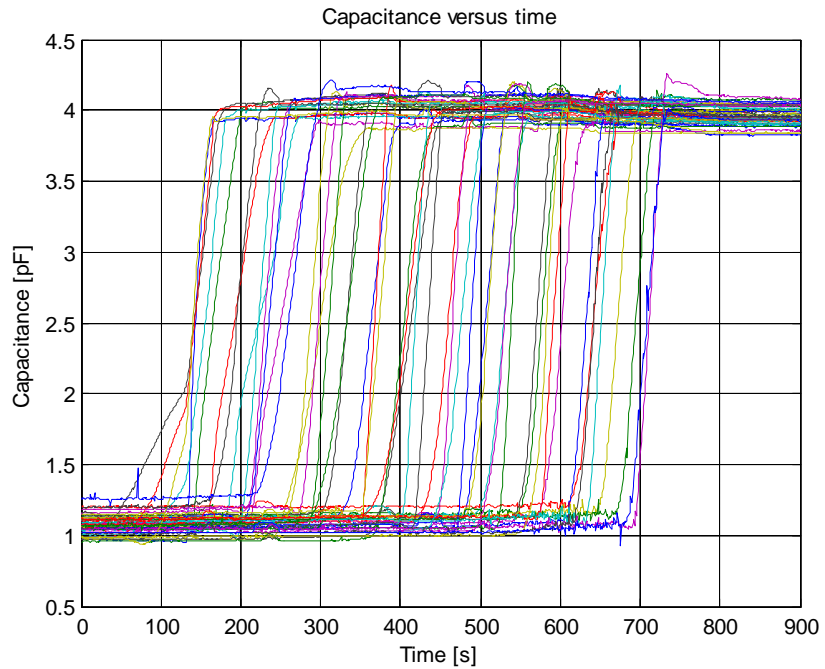
Appendix C.4. Results of Experiment 14. With modified grounded configuration.



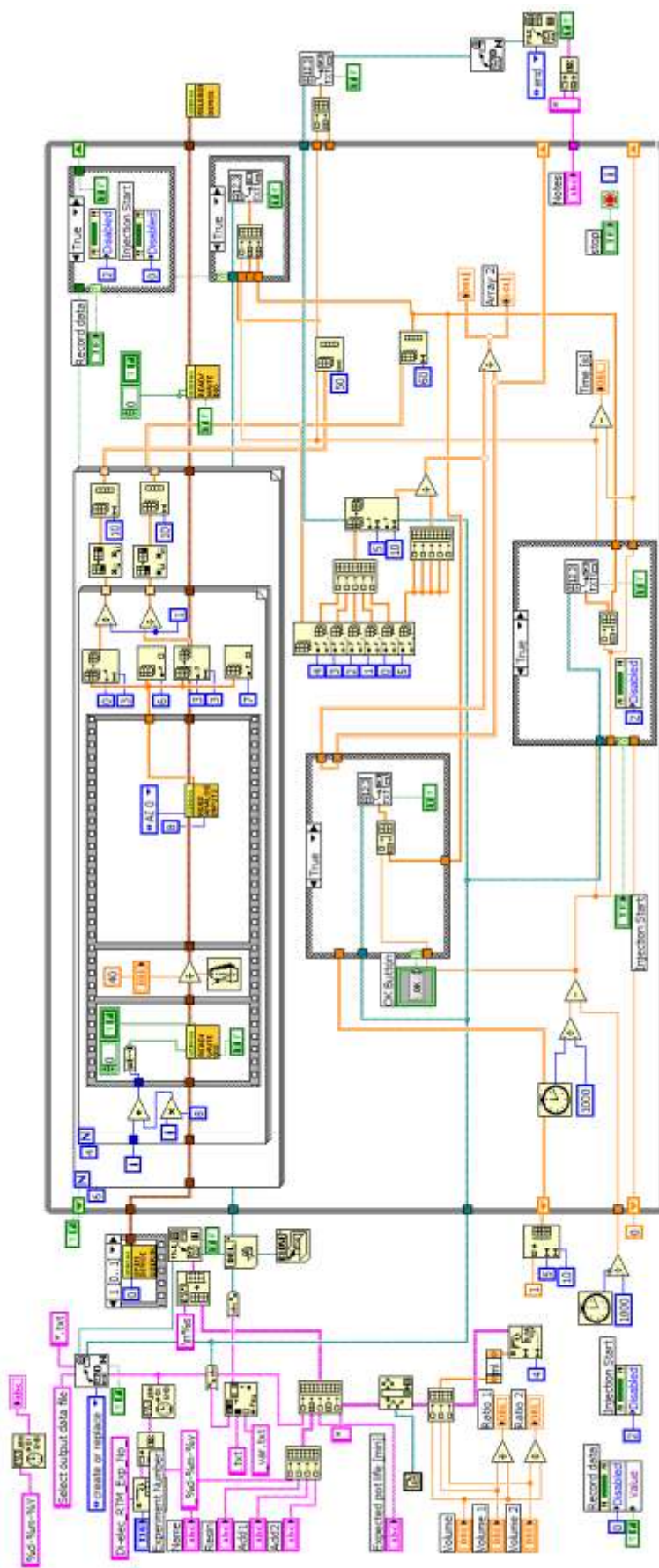
Appendix C.5. Results of Experiment 15. With modified grounded configuration.



Appendix C.6. Results of Experiment 16 – Case Study 1

Appendix C.7. Results of Experiment 17 – Case Study 2

Appendix D. Labview Diagram.



Appendix E.1. Amplifier Stage Calibration datas. Vin versus Vout

Pk-Pk In					Voltage Outputs					
40	0.982	0.958	0.929	0.982	0.947	0.982	0.891	0.952	0.927	0.940
50	1.286	1.251	1.217	1.287	1.241	1.290	1.169	1.248	1.214	1.234
60	1.557	1.512	1.474	1.558	1.504	1.563	1.416	1.511	1.470	1.497
70	1.839	1.784	1.741	1.841	1.777	1.847	1.673	1.787	1.736	1.770
80	2.063	2.001	1.954	2.067	1.994	2.074	1.877	2.004	1.948	1.987
90	2.359	2.286	2.236	2.363	2.280	2.373	2.149	2.292	2.227	2.275
100	2.639	2.555	2.499	2.643	2.551	2.654	2.403	2.564	2.492	2.545
110	2.892	2.799	2.739	2.897	2.796	2.910	2.634	2.812	2.730	2.790
120	3.157	3.055	2.991	3.163	3.053	3.180	2.878	3.069	2.982	3.047
130	3.426	3.315	3.247	3.434	3.314	3.452	3.125	3.332	3.239	3.309
140	3.726	3.606	3.531	3.733	3.605	3.754	3.400	3.626	3.525	3.600
150	3.989	3.860	3.781	3.996	3.858	4.020	3.641	3.883	3.777	3.853
Slope	36.905	38.248	38.914	36.809	38.112	36.531	40.361	37.873	38.968	38.081
Intercept	2.999	2.624	3.101	3.088	3.151	3.372	3.327	3.221	3.207	3.457
R2	0.9997	0.9997	0.9998	0.9998	0.9997	0.9998	0.9997	0.9997	0.9997	0.9997

Appendix E.2. Capacitance versus Voltage Output data.

Vout/C	0	0.9	0.9	1.3	1.3	1.9	2	2.5	2.5	2.7	2.7
1		1.057	1.002	1.417	1.395	2.008	2.056	2.738	2.78	2.943	2.962
2		0.867	0.833	1.163	1.146	1.653	1.693	2.26	2.294	2.435	2.437
3		0.739	0.716	0.996	0.98	1.427	1.467	1.957	1.983	2.098	2.105
4		0.709	0.692	0.967	0.952	1.392	1.423	1.911	1.932	2.046	2.055
5		0.62	0.599	0.843	0.832	1.219	1.25	1.67	1.701	1.808	1.805
6		0.576	0.555	0.791	0.778	1.139	1.166	1.566	1.5953	1.692	1.695
7		0.572	0.556	0.773	0.758	1.118	1.142	1.53	1.554	1.649	1.655
8		0.676	0.658	0.915	0.902	1.317	1.349	1.809	1.832	1.945	1.952
9		0.749	0.727	1.006	0.994	1.443	1.478	1.978	2.007	2.131	2.128
10		0.848	0.826	1.154	1.14	1.657	1.698	2.272	2.309	2.44	2.446
Vexc =		1.0									

Appendix E.3-5. Entire Electronic Circuit: (3) Part List, (4) Schematics and (5) PCB.

List of Materials for Di-electric Sensor

Design Title : Di-electric sensor
Author : Bekir Yenilmez
Revision : 1.0
Design Created : 16 April 2008 Wednesday
Design Last Modified : 07 August 2008 Thursday
Total Parts in Design : 239

142 Resistors

<u>Quantity:</u>	<u>References</u>	<u>Value</u>
48	R1-R3, R7, R11, R12, R17, R21, R22, R27, R31, R32, R37, R41, R42, R47, R51, R52, R57, R61, R62, R67, R71, R72, R77, R81, R82, R87, R91, R92, R97, R101, R102, R105-R108, R113-R115, R121, R122, R126-R128, R130-R132	10k
6	R4, R116-R120	1R
10	R5, R15, R25, R35, R45, R55, R65, R75, R85, R95	51k
14	R6, R16, R26, R36, R46, R56, R66, R76, R86, R96, R123-R125, R142	1k
21	R8, R13, R18, R23, R28, R33, R38, R43, R48, R53, R58, R63, R68, R73, R78, R83, R88, R93, R98, R103, R111	1M
11	R9, R19, R29, R39, R49, R59, R69, R79, R89, R99, R109	4k7
21	R10, R14, R20, R24, R30, R34, R40, R44, R50, R54, R60, R64, R70, R74, R80, R84, R90, R94, R100, R104, R112	33k
11	R110, R129, R133-R141	100k

43 Capacitors

<u>Quantity:</u>	<u>References</u>	<u>Value</u>
11	C1, C4, C7, C10, C13, C16, C19, C22, C25, C28, C31	100n
22	C2, C3, C5, C6, C8, C9, C11, C12, C14, C15, C17, C18, C20, C21, C23, C24, C26, C27, C29, C30, C32, C33	10n
10	C34-C43	1p8

22 Integrated Circuits

<u>Quantity:</u>	<u>References</u>	<u>Value</u>
1	U1	4028
1	U2	4009
2	U3, U4	4066
1	U5	4051
10	U6-U15	LF347
3	U16-U18	4052
4	U19-U22	LF353N

5 Transistors

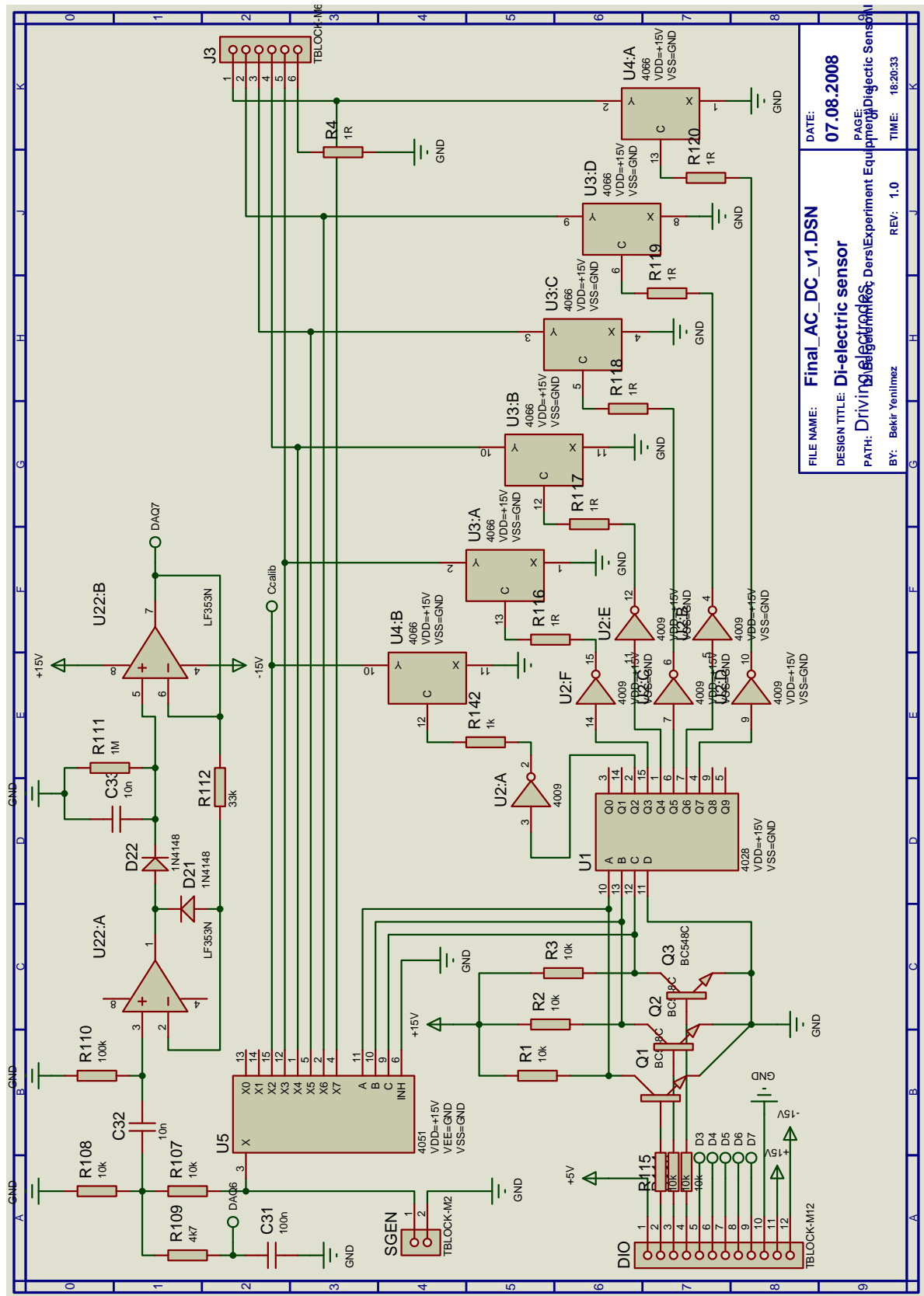
<u>Quantity:</u>	<u>References</u>	<u>Value</u>
5	Q1-Q5	BC548C

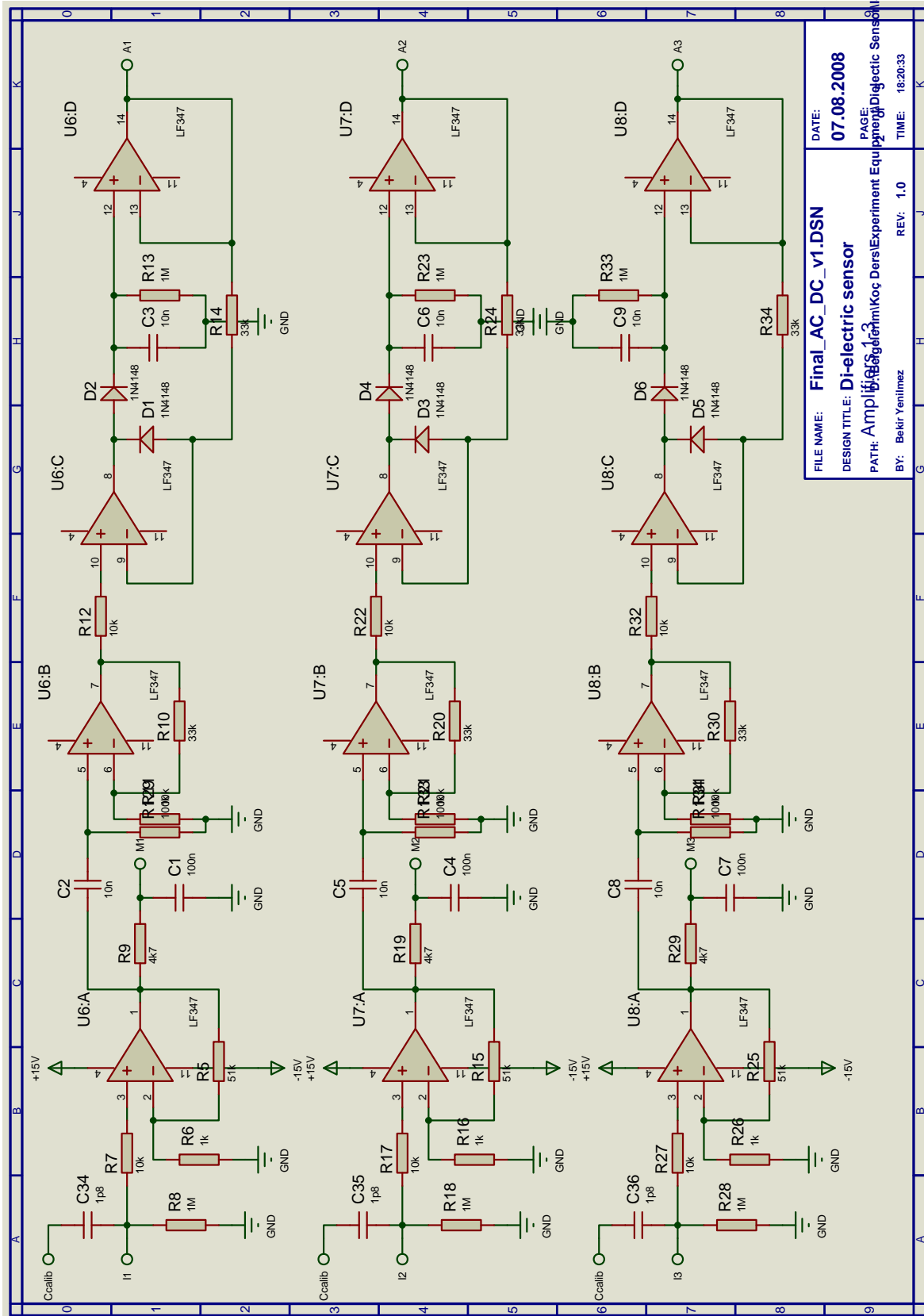
22 Diodes

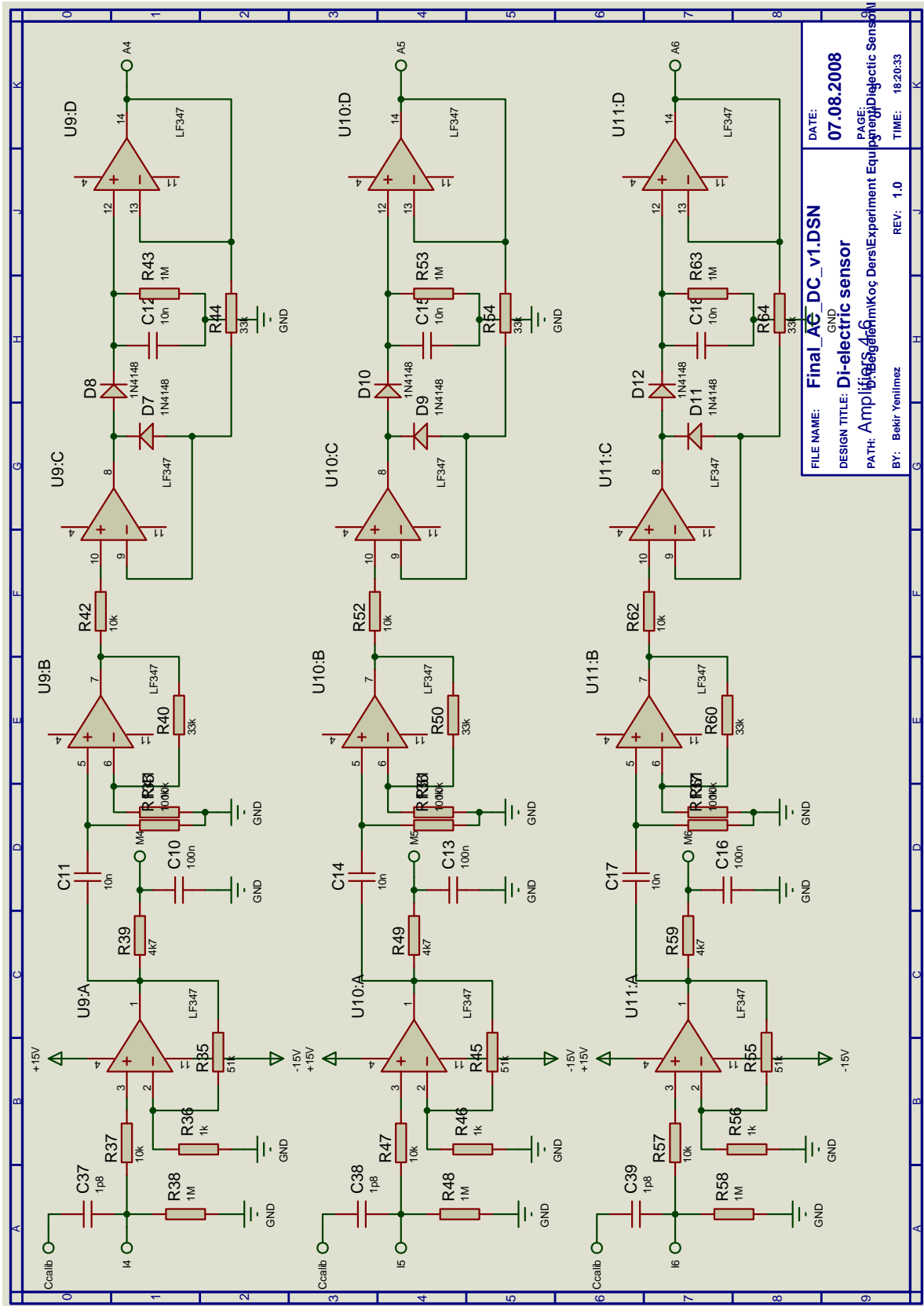
<u>Quantity:</u>	<u>References</u>	<u>Value</u>
22	D1-D22	1N4148

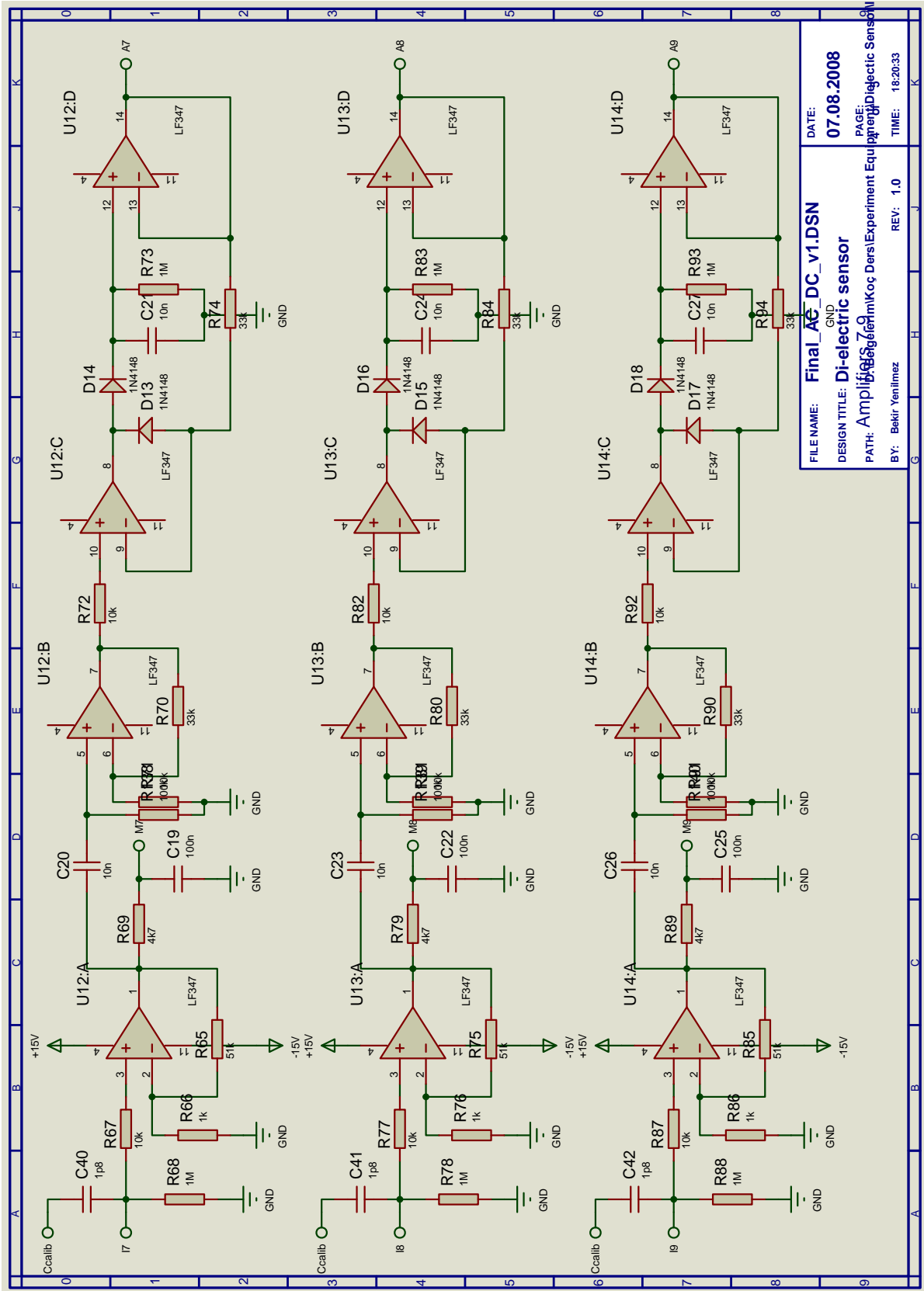
5 Miscellaneous

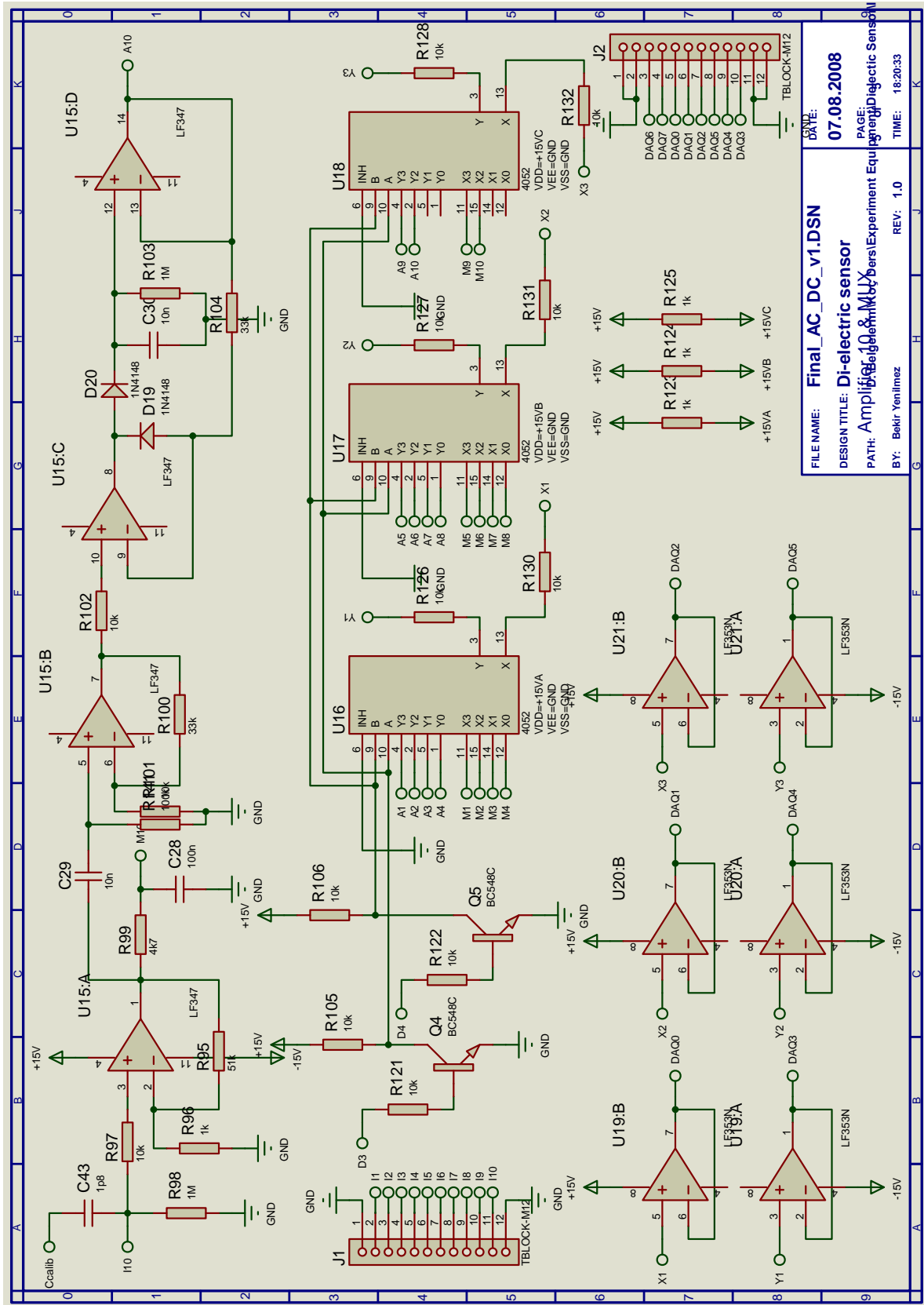
<u>Quantity:</u>	<u>References</u>	<u>Value</u>
3	DIO, J1, J2	TBLOCK-M12
1	J3	TBLOCK-M6
1	SGEN	TBLOCK-M2

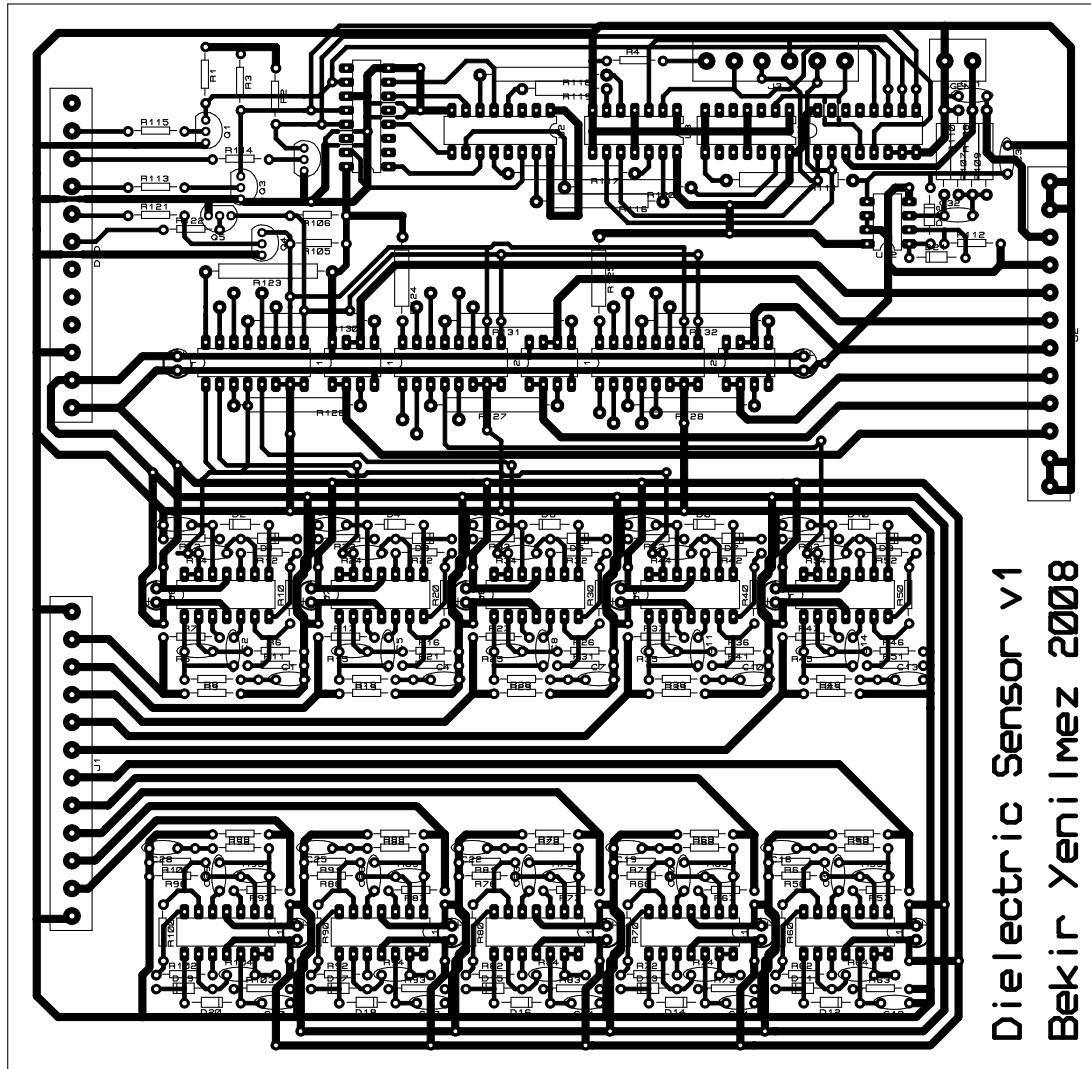




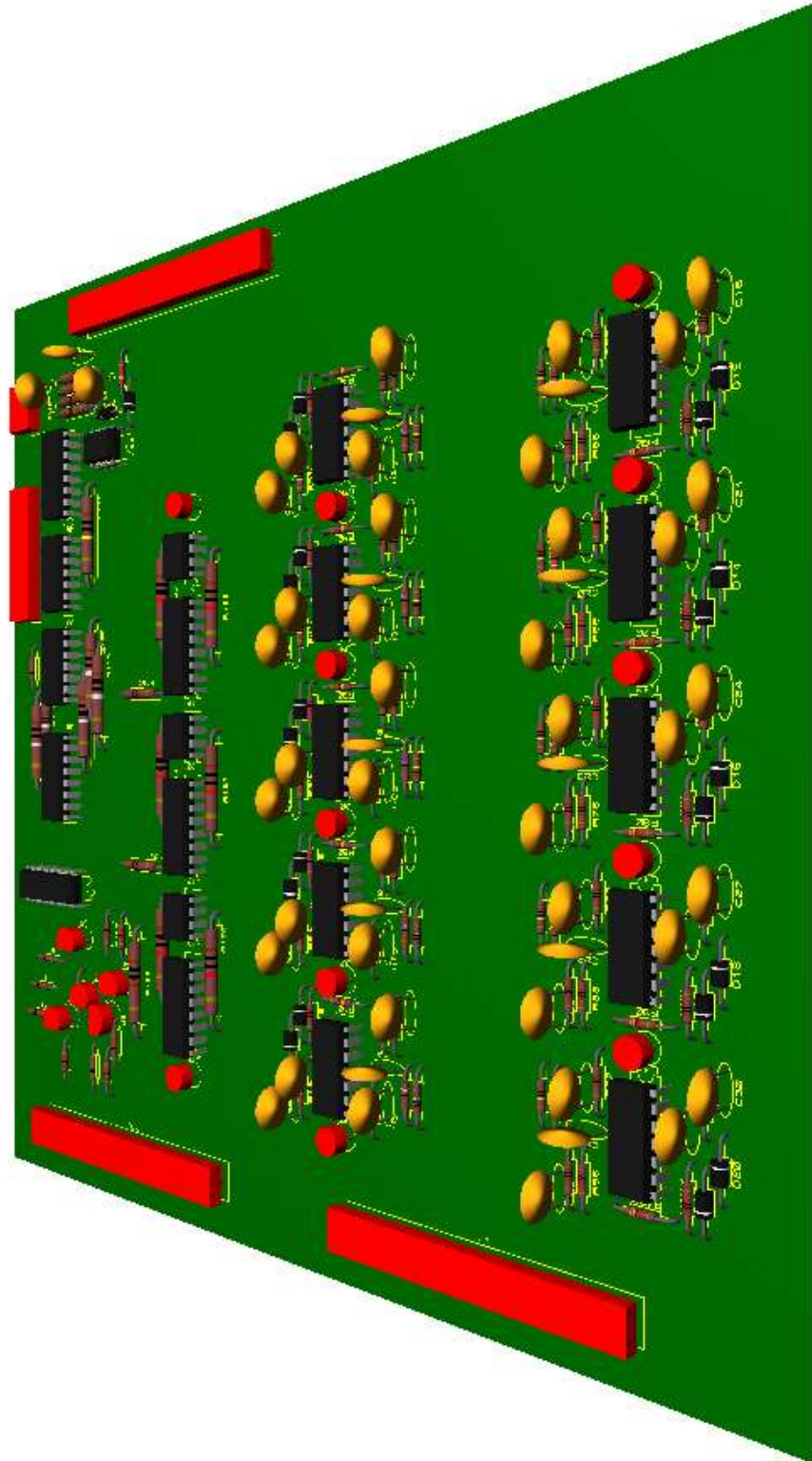


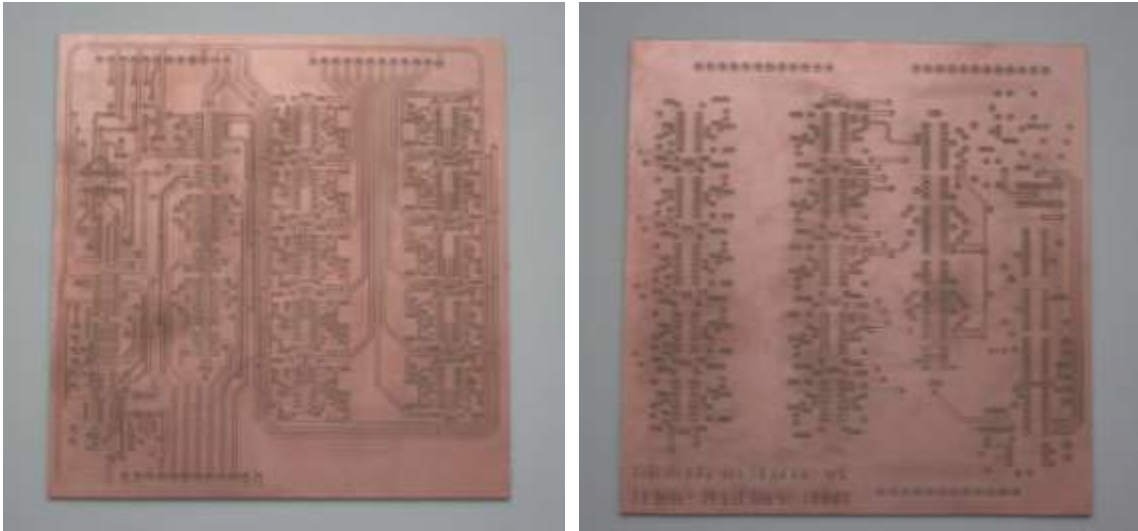
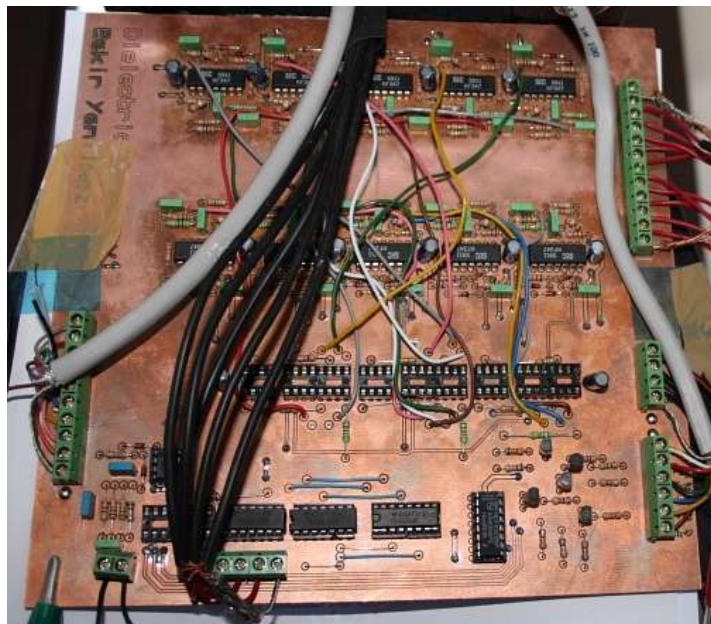




Appendix E.5.1: Double layered printed circuit board mask

Appendix E.5.2: 3D Visualization of the assembled PCB.



Appendix E.5.3: (a) Bare and (b) Assembled Photos of the PCB.**(a)****(b)**

Appendix F.1.1. Overview of The DAQ card iUSBDAQ – U120816
[From the users manual]



- USB 2.0/1.1 Full Speed Interface
- USB Bus Powered
- 8 Single-Ended, 12-Bit Analog Inputs
- 0-4.096 V Analog Input Range
- Up to 32 kSamples/Sec Throughput with Single Channel Up to 13kSamples/Second for Streaming Mode
- Supports Both Scan Mode and Continuous Streaming Mode Data Acquisition
- One Dedicated Trigger Line for Streaming Mode Data Acquisition
- Two 10-bit PWM Outputs (3kHz- 333kHz)
- 16 Bi-Directional Digital I/O Lines (125HZ update rate)
- One 16-Bit Counter
- 240 bytes EEPROM Reserved for User Data
- Multiple iUSBDAQs Can Be Connected On Same Computer
- Works with Windows 98SE, ME, 2000, or XP
- Approximately 3.5" x 3.375" x 1.125" (9cm x 8.5cm x 3cm)
- Industrial Temperature Range

Appendix F.1.2. Specifications of The DAQ card iUSBDAQ – U120816.
[From the users manual]

The spec is for 25 °C typically.

General

Parameter	Specification
Device type	USB 2.0 full speed
Device compatibility	USB 1.1, USB 2.0
Operating Temperature range	-40 to 85°C for U120816, 0 to 70°C for U1208LOG
Dimension	3.5" x 3.375" x 1.125" (9cm x 8.5cm x 3cm)
Connector Type	Screw terminal
Power Supply	USB bus powered, min 4.5V max 5.5V

Analog Input

Parameter	Min	Typical	Max	Unit	Specification
A/D converter type					Successive approximation type
Input voltage range for linear operation	0		Vref	V	
Mode					Single ended
Number of channels					8
Resolution					12 bit
Vref Voltage	4.055	4.096	4.137	V	
Accuracy	-41	1	+41	mV	Depends on the accuracy of Vref
Throughput		32k 30.1k 27k 25k 22k 19.5k 18.4k 13k 125		Samples /s	Number of channels=8 Numberof channels=7 Numberof channels=6 Numberof channels=5 Numberof channels=4 Numberof channels=3 Numberof channels=2 Numberof channels=1 Software timed scan
Maximum input voltage range	-0.6		7.6	V	

Integral Nonlinearity		+-1.0	+-2.0	LSB	
Differential Nonlinearity		+-0.5	+-1.0	LSB	No missing codes over-temperature
Offset Error		+-1.25	+-3	LSB	
Leakage Current		0.001	+-1	uA	
Trigger source					Software or Trigger line
Gain Error		+-1.25	+-5	LSB	

Digital input/output

Number of IOs	16 bi-directional
Digital type	CMOS output, TTL or Schmitt trigger input
Pull up	All pins pull up to V_s via 470 ohm, 1M to ground
Input high voltage	2.0V min, 5.5V absolute max
Input low voltage	-0.3V absolute min, 0.8V max
Output voltage	$(V_s - 0.47)$ V at 1mA
Output short circuit current	10.6mA at $V_s = 5V$
Maximum output current sunk	25mA
Maximum output current sourced	25mA
Power on states	All are inputs
Input leakage current	+-1uA

Counter

Resolution	16 bit
Maximum input frequency	1M HZ
High pulse width	0.5us min
Low pulse width	0.5us min
Input leakage current	+-1uA
Input high voltage	4.0V min, 5.5V absolute max
Input low voltage	0.8Vmax, -0.3V absolute min
Pull up	470ohm in series, 1M ohm to ground

PWM

Resolution	10 bit
Number of channels	2
Pull up	470ohm pull up to V_s , 1M ohm to ground
Period	3us – 333us
Frequency	333kHz – 3kHz

Trigger Line

Pull up/pull down	470ohm in series, 1M ohm to ground
Input leakage current	+/-1uA
Input high voltage	2.0V min, 5.5V absolute max
Input low voltage	-0.3V absolute min, 0.8V max
Trigger mode	High state will start data acquisition if used


+5V Power

Parameter	Condition	Specification
Output voltage	Connected to self-powered hub Connected to externally powered root hub	4.5V min, 5.25V max
	Connected to bus powered hub	4.1V min, 5.25Vmax
Output current	Connected to self-powered hub Connected to externally powered root hub	450mA max
	Connected to bus powered hub	50mA max

EEPROM

Size	240 bytes
Address range	0 - 239

Appendix F.2. Datasheet of the operational amplifier LF347


August 2000

LF147/LF347

Wide Bandwidth Quad JFET Input Operational Amplifiers

General Description

The LF147 is a low cost, high speed quad JFET input operational amplifier with an internally trimmed input offset voltage (BI-FET II™ technology). The device requires a low supply current and yet maintains a large gain bandwidth product and a fast slew rate. In addition, well matched high voltage JFET input devices provide very low input bias and offset currents. The LF147 is pin compatible with the standard LM148. This feature allows designers to immediately upgrade the overall performance of existing LF148 and LM124 designs.

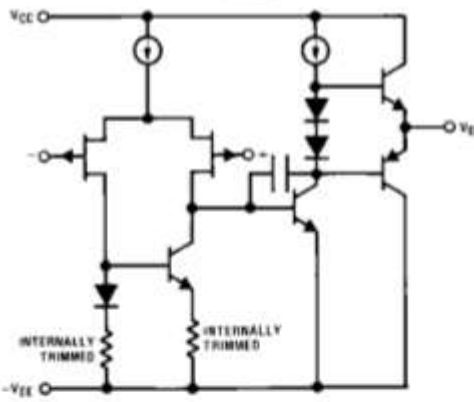
The LF147 may be used in applications such as high speed integrators, fast D/A converters, sample-and-hold circuits and many other circuits requiring low input offset voltage, low input bias current, high input impedance, high slew rate and wide bandwidth. The device has low noise and offset voltage drift.

Features

- Internally trimmed offset voltage: 5 mV max
- Low input bias current: 50 pA
- Low input noise current: 0.01 pA/√Hz
- Wide gain bandwidth: 4 MHz
- High slew rate: 13 V/μs
- Low supply current: 7.2 mA
- High input impedance: 10¹²Ω
- Low total harmonic distortion: ≤0.02%
- Low 1/f noise corner: 50 Hz
- Fast settling time to 0.01%: 2 μs

Simplified Schematic

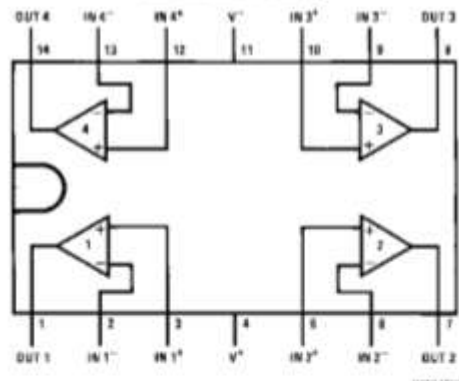
¼ Quad



00064710

Connection Diagram

Dual-In-Line Package



100064710

Note 1: LF147 available as per .B318510/11006.

Top View

Order Number LF147J, LF147J-SMD, LF347M,
LF347BN, LF347N, LF147J/883,
or JL147 BCA (Note 1)

See NS Package Number J14A, M14A or N14A

BI-FET II™ is a trademark of National Semiconductor Corporation

LF147/LF347 Wide Bandwidth Quad JFET Input Operational Amplifiers

LF147/LF347

Absolute Maximum Ratings (Note 2)

If Military/Aerospace specified devices are required, please contact the National Semiconductor Sales Office/Distributors for availability and specifications.

	LF147	LF347B/LF347
Supply Voltage	±22V	±18V
Differential Input Voltage	±38V	±30V
Input Voltage Range (Note 3)	±19V	±15V
Output Short Circuit Duration (Note 4)	Continuous	Continuous
Power Dissipation (Notes 5, 11)	900 mW	1000 mW
T _J max	150°C	150°C
θ _{JA}		
Ceramic DIP (J) Package		70°C/W
Plastic DIP (N) Package		75°C/W
Surface Mount Narrow (M)		100°C/W
Surface Mount Wide (WM)		85°C/W

	LF147 (Note 6)	LF347B/LF347 (Note 6)
Operating Temperature Range		
Storage Temperature Range	-65°C ≤ T _A ≤ 150°C	
Lead Temperature (Soldering, 10 sec.)	260°C	260°C
Soldering Information		
Dual-In-Line Package		
Soldering (10 seconds)		260°C
Small Outline Package		
Vapor Phase (60 seconds)		215°C
Infrared (15 seconds)		220°C
See AN-450 "Surface Mounting Methods and Their Effect on Product Reliability" for other methods of soldering surface mount devices.		
ESD Tolerance (Note 12)		900V

DC Electrical Characteristics (Note 7)

Symbol	Parameter	Conditions	LF147			LF347B			LF347			Units
			Min	Typ	Max	Min	Typ	Max	Min	Typ	Max	
V _{OS}	Input Offset Voltage	R _S =10 kΩ, T _A =25°C Over Temperature		1	5		3	5		5	10	mV mV
ΔV _{OS} /ΔT	Average TC of Input Offset Voltage	R _S =10 kΩ		10			10			10		μV/°C
I _{OS}	Input Offset Current	T _J =25°C, (Notes 7, 8) Over Temperature		25	100		25	100		25	100	pA nA
I _{BI}	Input Bias Current	T _J =25°C, (Notes 7, 8) Over Temperature		50	200		50	200		50	200	pA nA
R _{ife}	Input Resistance	T _J =25°C		10 ¹²			10 ¹²			10 ¹²		Ω
A _{VOL}	Large Signal Voltage Gain	V _B =±15V, T _A =25°C V _O =±10V, R _L =2 kΩ Over Temperature	50	100		50	100		25	100		V/mV V/mV
V _O	Output Voltage Swing	V _B =±15V, R _L =10 kΩ	±12	±13.5		±12	±13.5		±12	±13.5		V
V _{CM}	Input Common-Mode Voltage Range	V _B =±15V	±11	+15		±11	+15		±11	+15		V V
CMRR	Common-Mode Rejection Ratio	R _S ≤10 kΩ	80	100		80	100		70	100		dB
PSRR	Supply Voltage Rejection Ratio	(Note 9)	80	100		80	100		70	100		dB
I _S	Supply Current			7.2	11		7.2	11		7.2	11	mA

AC Electrical Characteristics (Note 7)												
Symbol	Parameter	Conditions	LF147			LF347B			LF347			Units
			Min	Typ	Max	Min	Typ	Max	Min	Typ	Max	
	Amplifier to Amplifier Coupling	$T_A=25^{\circ}\text{C}$, $f=1\text{ Hz}-20\text{ kHz}$ (Input Referred)		-120			-120			-120		dB
SR	Slew Rate	$V_{EE}=\pm 15\text{V}$, $T_A=25^{\circ}\text{C}$	8	13		8	13		8	13		V/ μs
GBW	Gain-Bandwidth Product	$V_{EE}=\pm 15\text{V}$, $T_A=25^{\circ}\text{C}$	2.2	4		2.2	4		2.2	4		MHz
e_{ni}	Equivalent Input Noise Voltage	$T_A=25^{\circ}\text{C}$, $R_L=100\Omega$, $f=1000\text{ Hz}$		20			20			20		nV/ $\sqrt{\text{Hz}}$
i_{ni}	Equivalent Input Noise Current	$T_A=25^{\circ}\text{C}$, $f=1000\text{ Hz}$		0.01			0.01			0.01		pA/ $\sqrt{\text{Hz}}$
THD	Total Harmonic Distortion	$A_V=+10$, $R_L=10\text{k}$, $V_{CE}=20\text{ Vp-p}$, $\text{BW}=20\text{ Hz}-20\text{ kHz}$		<0.02			<0.02			<0.02		%

Note 2: Absolute Maximum Ratings indicate limits beyond which damage to the device may occur. Operating Ratings indicate conditions for which the device is functional, but do not guarantee specific performance limits.

Note 3: Unless otherwise specified the absolute maximum negative input voltage is equal to the negative power supply voltage.

Note 4: Any of the amplifier outputs can be shorted to ground indefinitely, however, more than one should not be simultaneously shorted as the maximum junction temperature will be exceeded.

Note 5: For operating at elevated temperature, these devices must be derated based on a thermal resistance of θ_{JA} .

Note 6: The LF147 is available in the military temperature range $-55^{\circ}\text{C} \leq T_A \leq 125^{\circ}\text{C}$, while the LF347B and the LF347 are available in the commercial temperature range $0^{\circ}\text{C} \leq T_A \leq 70^{\circ}\text{C}$. Junction temperature can rise to $T_J \text{ max} = 150^{\circ}\text{C}$.

Note 7: Unless otherwise specified the specifications apply over the full temperature range and for $V_{CE}=\pm 20\text{V}$ for the LF147 and for $V_{CE}=\pm 15\text{V}$ for the LF347B/LF347. V_{CE} , I_Q , and I_{CE} are measured at $V_{CM}=0$.

Note 8: The input bias currents are junction leakage currents which approximately double for every 10°C increase in the junction temperature, T_J . Due to limited production test time, the input bias currents measured are correlated to junction temperature. In normal operation the junction temperature rises above the ambient temperature as a result of internal power dissipation, P_D . $T_J = T_A + \theta_{JA} P_D$ where θ_{JA} is the thermal resistance from junction to ambient. Use of a heat sink is recommended if input bias current is to be kept to a minimum.


Note 9: Supply voltage rejection ratio is measured for both supply magnitudes increasing or decreasing simultaneously in accordance with common practice from $V_{EE} = \pm 5\text{V}$ to $\pm 15\text{V}$ for the LF347 and LF347B and from $V_{EE} = \pm 20\text{V}$ to $\pm 5\text{V}$ for the LF147.

Note 10: Refer to HEETS147X for LF147D and LF147J military specifications.

Note 11: Max. Power Dissipation is defined by the package characteristics. Operating the part near the Max. Power Dissipation may cause the part to operate outside guaranteed limits.

Note 12: Human body model, 1.5 k Ω in series with 100 pF.

Appendix F.3. Datasheet of the Grounding switch CD4066.



National Semiconductor

June 1992

CD4066BM/CD4066BC Quad Bilateral Switch

General Description

The CD4066BM/CD4066BC is a quad bilateral switch intended for the transmission or multiplexing of analog or digital signals. It is pin-for-pin compatible with CD4016BM/CD4016BC, but has a much lower "ON" resistance, and "ON" resistance is relatively constant over the input-signal range.

- Extremely low "OFF" switch leakage @ $V_{DD} - V_{SS} = 10V, T_A = 25^\circ C$ 0.1 nA (typ.)
- Extremely high control input impedance $10^{12} \Omega$ (typ.)
- Low crosstalk between switches @ $f_{in} = 0.9 MHz, R_L = 1 k\Omega$ -50 dB (typ.)
- Frequency response, switch "ON" 40 MHz (typ.)

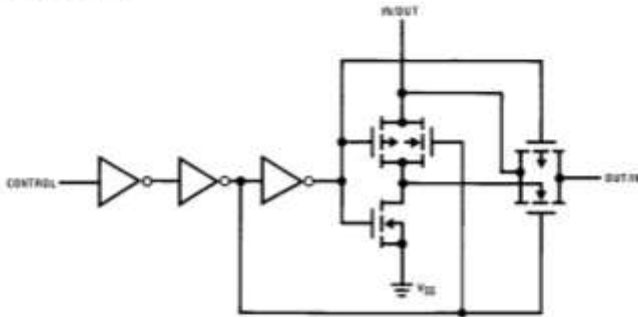
Features

- Wide supply voltage range 3V to 15V
- High noise immunity $0.45 V_{DD}$ (typ.)
- Wide range of digital and analog switching $\pm 7.5 V_{PEAK}$
- "ON" resistance for 15V operation 80 Ω
- Matched "ON" resistance $\Delta R_{ON} = 5 \Omega$ (typ.) over 15V signal input
- "ON" resistance flat over peak-to-peak signal range
- High "ON"/"OFF" output voltage ratio @ $f_{in} = 10 kHz, R_L = 10 k\Omega$ 65 dB (typ.)
- High degree linearity @ $f_{in} = 1 kHz, V_{in} = 5V_{P-P}, V_{DD} - V_{SS} = 10V, R_L = 10 k\Omega$ 0.1% distortion (typ.)

Applications

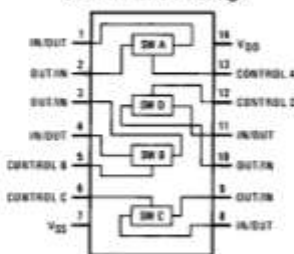
- Analog signal switching/multiplexing
 - Signal gating
 - Squelch control
 - Chopper
 - Modulator/Demodulator
 - Commutating switch
- Digital signal switching/multiplexing
- CMOS logic implementation
- Analog-to-digital/digital-to-analog conversion
- Digital control of frequency, impedance, phase, and analog-signal-gain

Schematic and Connection Diagrams



Order Number CD4066B

Dual-In-Line Package



Top View

TL/F/5665-1

CD4066BM/CD4066BC Quad Bilateral Switch

DC Electrical Characteristics (Continued) CD4066BC (Note 2)										
Symbol	Parameter	Conditions	-40°C		+25°C			+85°C		Units
			Min	Max	Min	Typ	Max	Min	Max	
SIGNAL INPUTS AND OUTPUTS										
R_{ON}	"ON" Resistance	$R_L = 10\text{ k}\Omega$ to $\frac{V_{DD} - V_{SS}}{2}$ $V_C = V_{DD}, V_{SS}$ to V_{DD} $V_{DD} = 5\text{V}$ $V_{DD} = 10\text{V}$ $V_{DD} = 15\text{V}$		650 330 210		270 120 60	1050 400 240		1200 520 300	Ω Ω Ω
ΔR_{ON}	Δ "ON" Resistance Between Any 2 of 4 Switches	$R_L = 10\text{ k}\Omega$ to $\frac{V_{DD} - V_{SS}}{2}$ $V_{CC} = V_{DD}, V_{IS} = V_{SS}$ to V_{DD} $V_{DD} = 10\text{V}$ $V_{DD} = 15\text{V}$				10 5				Ω Ω
I_{IS}	Input or Output Leakage Switch "OFF"	$V_C = 0$		± 50		± 0.1	± 50		± 200	nA
CONTROL INPUTS										
V_{ILC}	Low Level Input Voltage	$V_{IS} = V_{SS}$ and V_{DD} $V_{OS} = V_{DD}$ and V_{SS} $I_{IS} = \pm 10\mu\text{A}$ $V_{DD} = 5\text{V}$ $V_{DD} = 10\text{V}$ $V_{DD} = 15\text{V}$		1.5 3.0 4.0		2.25 4.5 6.75	1.5 3.0 4.0		1.5 3.0 4.0	V V V
V_{IHC}	High Level Input Voltage	$V_{DD} = 5\text{V}$ $V_{DD} = 10\text{V}$ (See note 6) $V_{DD} = 15\text{V}$	3.5 7.0 11.0		3.5 7.0 11.0	2.75 5.5 8.25		3.5 7.0 11.0		V V V
I_{IN}	Input Current	$V_{DD} - V_{SS} = 15\text{V}$ $V_{DD} \geq V_{IS} \geq V_{SS}$ $V_{DD} \geq V_C \geq V_{SS}$		± 0.3		$\pm 10^{-5}$	± 0.3		± 1.0	μA
AC Electrical Characteristics* $T_A = 25^\circ\text{C}$, $t_r = t_f = 20\text{ ns}$ and $V_{SS} = 0\text{V}$ unless otherwise noted										
Symbol	Parameter	Conditions	Min	Typ	Max	Units				
t_{PHL}, t_{PLH}	Propagation Delay Time Signal Input to Signal Output	$V_C = V_{DD}, C_L = 50\text{ pF}$, (Figure 1) $R_L = 200\text{k}$ $V_{DD} = 5\text{V}$ $V_{DD} = 10\text{V}$ $V_{DD} = 15\text{V}$		25 15 10	55 35 25	ns ns ns				
t_{PZH}, t_{PZL}	Propagation Delay Time Control Input to Signal Output High Impedance to Logical Level	$R_L = 1.0\text{ k}\Omega, C_L = 50\text{ pF}$, (Figures 2 and 3) $V_{DD} = 5\text{V}$ $V_{DD} = 10\text{V}$ $V_{DD} = 15\text{V}$			125 60 50	ns ns ns				
t_{PHZ}, t_{PLZ}	Propagation Delay Time Control Input to Signal Output Logical Level to High Impedance Sine Wave Distortion Frequency Response-Switch "ON" (Frequency at -3 dB)	$R_L = 1.0\text{ k}\Omega, C_L = 50\text{ pF}$, (Figures 2 and 3) $V_{DD} = 5\text{V}$ $V_{DD} = 10\text{V}$ $V_{DD} = 15\text{V}$ $V_C = V_{DD} = 5\text{V}, V_{SS} = -5\text{V}$ $R_L = 10\text{ k}\Omega, V_{IS} = 5V_{p-p}, f = 1\text{ kHz}$, (Figure 4) $V_C = V_{DD} = 5\text{V}, V_{SS} = -5\text{V}$, $R_L = 1\text{ k}\Omega, V_{IS} = 5V_{p-p}$, $20 \text{ Log}_{10} V_{OS}/V_{OS} (1\text{ kHz}) - \text{dB}$, (Figure 4)		0.1 40	125 60 50	ns ns ns % MHz				

AC Electrical Characteristics* (Continued) $T_A = 25^\circ\text{C}$, $t_r = t_f = 20\text{ ns}$ and $V_{SS} = 0\text{V}$ unless otherwise noted						
Symbol	Parameter	Conditions	Min	Typ	Max	Units
	Feedthrough — Switch "OFF" (Frequency at -50 dB)	$V_{DD} = 5.0\text{V}$, $V_{CC} = V_{SS} = -5.0\text{V}$, $R_L = 1\text{ k}\Omega$, $V_{IS} = 5.0\text{V}_{p-p}$, 20 Log_{10} , $V_{OS}/V_{IS} = -50\text{ dB}$, (Figure 4)		1.25		
	Crosstalk Between Any Two Switches (Frequency at -50 dB)	$V_{DD} = V_{C(A)} = 5.0\text{V}$; $V_{SS} = V_{C(B)} = -5.0\text{V}$, $R_L = 1\text{ k}\Omega$, $V_{IS(A)} = 5.0\text{V}_{p-p}$, 20 Log_{10} , $V_{OS(B)}/V_{IS(A)} = -50\text{ dB}$ (Figure 5)		0.9		MHz
	Crosstalk; Control Input to Signal Output	$V_{DD} = 10\text{V}$, $R_L = 10\text{ k}\Omega$, $R_{IN} = 1.0\text{ k}\Omega$, $V_{CC} = 10\text{V}$ Square Wave, $C_L = 50\text{ pF}$ (Figure 6)		150		mV _{p-p}
	Maximum Control Input	$R_L = 1.0\text{ k}\Omega$, $C_L = 50\text{ pF}$, (Figure 7) $V_{OS(f)} = \frac{1}{2} V_{OS}(1.0\text{ kHz})$ $V_{DD} = 5.0\text{V}$ $V_{DD} = 10\text{V}$ $V_{DD} = 15\text{V}$		6.0 8.0 8.5		MHz MHz MHz
C_{IS}	Signal Input Capacitance			8.0		pF
C_{OS}	Signal Output Capacitance	$V_{DD} = 10\text{V}$		8.0		pF
C_{IOS}	Feedthrough Capacitance	$V_C = 0\text{V}$		0.5		pF
C_{IN}	Control Input Capacitance			5.0	7.5	pF

*AC Parameters are guaranteed by DC correlated testing.

Note 1: "Absolute Maximum Ratings" are those values beyond which the safety of the device cannot be guaranteed. They are not meant to imply that the devices should be operated at these limits. The tables of "Recommended Operating Conditions" and "Electrical Characteristics" provide conditions for actual device operation.

Note 2: $V_{SS} = 0\text{V}$ unless otherwise specified.

Note 3: These devices should not be connected to circuits with the power "ON".

Note 4: In all cases, there is approximately 5 pF of probe and jig capacitance in the output; however, this capacitance is included in C_L wherever it is specified.

Note 5: V_{IS} is the voltage at the in/out pin and V_{OS} is the voltage at the out/in pin. V_C is the voltage at the control input.

Note 6: Conditions for V_{HC} : a) $V_{IS} = V_{DD}$, $I_{OS} = \text{standard B series } I_{OH}$ b) $V_{IS} = 0\text{V}$, $I_{CL} = \text{standard B series } I_{OL}$.

AC Test Circuits and Switching Time Waveforms

FIGURE 1. t_{pHL} , t_{pLH} Propagation Delay Time Signal Input to Signal Output


FIGURE 2. t_{pZH} , t_{pHZ} Propagation Delay Time Control to Signal Output

FIGURE 3. t_{pZL} , t_{pLZ} Propagation Delay Time Control to Signal Output

TL/F/5685-2

Appendix F.4. Datasheet of the Multiplexers CD4051 and CD4052.

October 1989



CD4051BM/CD4051BC Single 8-Channel Analog Multiplexer/Demultiplexer CD4052BM/CD4052BC Dual 4-Channel Analog Multiplexer/Demultiplexer CD4053BM/CD4053BC Triple 2-Channel Analog Multiplexer/Demultiplexer

General Description

These analog multiplexers/demultiplexers are digitally controlled analog switches having low "ON" impedance and very low "OFF" leakage currents. Control of analog signals up to 15V_{p-p} can be achieved by digital signal amplitudes of 3–15V. For example, if V_{DD} = 5V, V_{SS} = 0V and V_{EE} = –5V, analog signals from –5V to +5V can be controlled by digital inputs of 0–5V. The multiplexer circuits dissipate extremely low quiescent power over the full V_{DD}–V_{SS} and V_{DD}–V_{EE} supply voltage ranges, independent of the logic state of the control signals. When a logical "1" is present at the inhibit input terminal all channels are "OFF".

CD4051BM/CD4051BC is a single 8-channel multiplexer having three binary control inputs, A, B, and C, and an inhibit input. The three binary signals select 1 of 8 channels to be turned "ON" and connect the input to the output.

CD4052BM/CD4052BC is a differential 4-channel multiplexer having two binary control inputs, A and B, and an inhibit input. The two binary input signals select 1 or 4 pairs of channels to be turned on and connect the differential analog inputs to the differential outputs.

CD4053BM/CD4053BC is a triple 2-channel multiplexer having three separate digital control inputs, A, B, and C, and

an inhibit input. Each control input selects one of a pair of channels which are connected in a single-pole double-throw configuration.

Features

- Wide range of digital and analog signal levels: digital 3–15V, analog to 15V_{p-p}
- Low "ON" resistance: 80Ω (typ.) over entire 15V_{p-p} signal-input range for V_{DD}–V_{EE} = 15V
- High "OFF" resistance: channel leakage of ±10 pA (typ.) at V_{DD}–V_{EE} = 10V
- Logic level conversion for digital addressing signals of 3–15V (V_{DD}–V_{SS} = 3–15V) to switch analog signals to 15 V_{p-p} (V_{DD}–V_{EE} = 15V)
- Matched switch characteristics: ΔR_{ON} = 5Ω (typ.) for V_{DD}–V_{EE} = 15V
- Very low quiescent power dissipation under all digital-control input and supply conditions: 1 μW (typ.) at V_{DD}–V_{SS}–V_{DD}–V_{EE} = 10V
- Binary address decoding on chip

Connection Diagrams

Dual-In-Line Packages

CD4051BM/CD4051BC

TOP VIEW

CD4052BM/CD4052BC

TOP VIEW

CD4053BM/CD4053BC

TOP VIEW

Order Number CD4051B, CD4052B, or CD4053B

CD4051BM/CD4051BC, CD4052BM/CD4052BC, CD4053BM/CD4053BC
Analog Multiplexer/Demultiplexers

Absolute Maximum Ratings			Recommended Operating Conditions							
If Military/Aerospace specified devices are required, please contact the National Semiconductor Sales Office/Distributors for availability and specifications. DC Supply Voltage (V_{DD}) $-0.5 V_{DD}$ to $+16 V_{DD}$ Input Voltage (V_{IH}) $-0.5 V_{DD}$ to $V_{DD} + 0.5 V_{DD}$ Storage Temperature Range (T_S) -65°C to $+150^{\circ}\text{C}$ Power Dissipation (P_D) Dual-In-Line 700 mW Small Outline 500 mW Lead Temp. (T_L) (soldering, 10 sec.) 260 $^{\circ}\text{C}$			DC Supply Voltage (V_{DD}) $+5 V_{DD}$ to $+15 V_{DD}$ Input Voltage (V_{IH}) 0V to V_{DD} V_{DD} Operating Temperature Range (T_A) 4051BM/4052BM/4053BM -55°C to $+125^{\circ}\text{C}$ 4051BC/4052BC/4053BC -40°C to $+85^{\circ}\text{C}$							
DC Electrical Characteristics (Note 2)			- 55 $^{\circ}\text{C}$		+ 25 $^{\circ}$		+ 125 $^{\circ}\text{C}$		Units	
Symbol	Parameter	Conditions	Min	Max	Min	Typ	Max	Min		Max
I_{DD}	Quiescent Device Current	$V_{DD} = 5\text{V}$ $V_{DD} = 10\text{V}$ $V_{DD} = 15\text{V}$		5 10 20			5 10 20	150 300 600	μA μA μA	
Signal Inputs (V_{IS}) and Outputs (V_{OS})										
R_{ON}	"ON" Resistance (Peak for $V_{EE} \leq V_{IS} \leq V_{DD}$)	$R_L = 10\text{ k}\Omega$ (any channel selected)	$V_{DD} = 2.5\text{V}$, $V_{EE} = -2.5\text{V}$ or $V_{DD} = 5\text{V}$, $V_{EE} = 0\text{V}$	800		270	1050		1300	Ω
			$V_{DD} = 5\text{V}$, $V_{EE} = -5\text{V}$ or $V_{DD} = 10\text{V}$, $V_{EE} = 0\text{V}$	310		120	400		550	Ω
			$V_{DD} = 7.5\text{V}$, $V_{EE} = -7.5\text{V}$ or $V_{DD} = 15\text{V}$, $V_{EE} = 0\text{V}$	200		80	240		320	Ω
ΔR_{ON}	Δ "ON" Resistance Between Any Two Channels	$R_L = 10\text{ k}\Omega$ (any channel selected)	$V_{DD} = 2.5\text{V}$, $V_{EE} = -2.5\text{V}$ or $V_{DD} = 5\text{V}$, $V_{EE} = 0\text{V}$			10				Ω
			$V_{DD} = 5\text{V}$, $V_{EE} = -5\text{V}$ or $V_{DD} = 10\text{V}$, $V_{EE} = 0\text{V}$			10				Ω
			$V_{DD} = 7.5\text{V}$, $V_{EE} = -7.5\text{V}$ or $V_{DD} = 15\text{V}$, $V_{EE} = 0\text{V}$			5				Ω
	"OFF" Channel Leakage Current, any channel "OFF"	$V_{DD} = 7.5\text{V}$, $O/I = \pm 7.5\text{V}$, $I/O = 0\text{V}$		± 50		± 0.01	± 50		± 500	nA
	"OFF" Channel Leakage Current, all channels "OFF" (Common OUT/IN)	Inhibit = 7.5V $V_{DD} = 7.5\text{V}$, $V_{EE} = -7.5\text{V}$, $O/I = 0\text{V}$, $I/O = \pm 7.5\text{V}$	CD4051	± 200		± 0.06	± 200		± 2000	nA
			CD4052	± 200		± 0.04	± 200		± 2000	nA
			CD4053	± 200		± 0.02	± 200		± 2000	nA
Control Inputs A, B, C and Inhibit										
V_{IL}	Low Level Input Voltage	$V_{EE} = V_{SS}$, $R_L = 1\text{ k}\Omega$ to V_{SS} $I_{IS} < 2\text{ }\mu\text{A}$ on all OFF channels $V_{IS} = V_{DD}$ thru $1\text{ k}\Omega$ $V_{DD} = 5\text{V}$ $V_{DD} = 10\text{V}$ $V_{DD} = 15\text{V}$		1.5 3.0 4.0			1.5 3.0 4.0		1.5 3.0 4.0	V V V
V_{IH}	High Level Input Voltage	$V_{DD} = 5$ $V_{DD} = 10$ $V_{DD} = 15$		3.5 7 11		3.5 7 11		3.5 7 11		V V V
Note 1: "Absolute Maximum Ratings" are those values beyond which the safety of the device cannot be guaranteed. Except for "Operating Temperature Range" they are not meant to imply that the devices should be operated at these limits. The table of "Electrical Characteristics" provides conditions for actual device operation. Note 2: All voltages measured with respect to V_{SS} unless otherwise specified.										

DC Electrical Characteristics (Note 2) (Continued)										
Symbol	Parameter	Conditions	-40°C		+25°C			+85°C		Units
			Min	Max	Min	Typ	Max	Min	Max	
I_{IN}	Input Current	$V_{DD} = -15V, V_{IN} = 0V, V_{EE} = 0V$		-0.1		-10^{-5}	-0.1		-1.0	μA
		$V_{DD} = 15V, V_{IN} = 15V, V_{EE} = 0V$		0.1		10^{-5}	0.1		1.0	μA
I_{DD}	Quiescent Device Current	$V_{DD} = 5V$		20			20		150	μA
		$V_{DD} = 10V$		40			40		300	μA
		$V_{DD} = 15V$		60			60		600	μA
Signal Inputs (V_{IS}) and Outputs (V_{OS})										
R_{ON}	"ON" Resistance (Peak for $V_{EE} \leq V_{IS} \leq V_{DD}$)	$R_L = 10\text{ k}\Omega$ (any channel selected)	$V_{DD} = 2.5V, V_{EE} = -2.5V$ or $V_{DD} = 5V, V_{EE} = 0V$		850		270	1050	1200	Ω
			$V_{DD} = 5V, V_{EE} = -5V$ or $V_{DD} = 10V, V_{EE} = 0V$		330		120	400	520	Ω
			$V_{DD} = 7.5V, V_{EE} = -7.5V$ or $V_{DD} = 15V, V_{EE} = 0V$		210		60	240	300	Ω
ΔR_{ON}	Δ "ON" Resistance Between Any Two Channels	$R_L = 10\text{ k}\Omega$ (any channel selected)	$V_{DD} = 2.5V, V_{EE} = -2.5V$ or $V_{DD} = 5V, V_{EE} = 0V$				10			Ω
			$V_{DD} = 5V, V_{EE} = -5V$ or $V_{DD} = 10V, V_{EE} = 0V$				10			Ω
			$V_{DD} = 7.5V, V_{EE} = -7.5V$ or $V_{DD} = 15V, V_{EE} = 0V$				5			Ω
	"OFF" Channel Leakage Current, any channel "OFF"	$V_{DD} = 7.5V, V_{EE} = -7.5V$ $O/I = \pm 7.5V, I/O = 0V$		± 50		± 0.01	± 50	± 500	nA	
	"OFF" Channel Leakage Current, all channels "OFF" (Common OUT/IN)	Inhibit = 7.5V $V_{DD} = 7.5V, V_{EE} = -7.5V, O/I = 0V, I/O = \pm 7.5V$	CD4051	± 200		± 0.06	± 200	± 2000	nA	
			CD4052	± 200		± 0.04	± 200	± 2000	nA	
			CD4053	± 200		± 0.02	± 200	± 2000	nA	
Control Inputs A, B, C and inhibit										
V_{IL}	Low Level Input Voltage	$V_{EE} = V_{SS}, R_L = 1\text{ k}\Omega$ to V_{SS} $I_{IS} < 2\text{ }\mu A$ on all OFF Channels $V_{IS} = V_{DD}$ thru $1\text{ k}\Omega$ $V_{DD} = 5V$ $V_{DD} = 10V$ $V_{DD} = 15V$								
				1.5			1.5		1.5	V
				3.0			3.0		3.0	V
				4.0			4.0		4.0	V
V_{IH}	High Level Input Voltage	$V_{DD} = 5$ $V_{DD} = 10$ $V_{DD} = 15$	3.5		3.5			3.5		V
			7		7			7	V	
			11		11			11	V	
I_{IN}	Input Current	$V_{DD} = -15V, V_{IN} = 0V, V_{EE} = 0V$ $V_{DD} = 15V, V_{IN} = 15V, V_{EE} = 0V$		-0.1		-10^{-5}	-0.1		-1.0	μA
				0.1		10^{-5}	0.1		1.0	μA
<p>Note 1: "Absolute Maximum Ratings" are those values beyond which the safety of the device cannot be guaranteed. Except for "Operating Temperature Range" they are not meant to imply that the devices should be operated at these limits. The table of "Electrical Characteristics" provides conditions for actual device operation.</p> <p>Note 2: All voltages measured with respect to V_{SS} unless otherwise specified.</p>										

AC Electrical Characteristics* $T_A = 25^\circ\text{C}$, $t_r = t_f = 20\text{ ns}$, unless otherwise specified.							
Symbol	Parameter	Conditions	V _{DD}	Min	Typ	Max	Units
t _{pZH} , t _{pZL}	Propagation Delay Time from inhibit to Signal Output (channel turning on)	V _{EE} = V _{SS} = 0V	5V		600	1200	ns
		R _L = 1 kΩ	10V		225	450	ns
		C _L = 50 pF	15V		160	320	ns
t _{pHZ} , t _{pLZ}	Propagation Delay Time from inhibit to Signal Output (channel turning off)	V _{EE} = V _{SS} = 0V	5V		210	420	ns
		R _L = 1 kΩ	10V		100	200	ns
		C _L = 50 pF	15V		75	150	ns
C _{IN}	Input Capacitance Control input Signal input (IN/OUT)				5	7.5	pF
					10	15	pF
C _{OUT}	Output Capacitance (common OUT/IN)						
	CD4051	V _{EE} = V _{SS} = 0V	10V		30		pF
	CD4052		10V		15		pF
	CD4053		10V		8		pF
C _{IOS}	Feedthrough Capacitance				0.2		pF
C _{PD}	Power Dissipation Capacitance						
	CD4051				110		pF
	CD4052				140		pF
	CD4053				70		pF
Signal Inputs (V_{IS}) and Outputs (V_{OS})							
	Sine Wave Response (Distortion)	R _L = 10 kΩ f _{IS} = 1 kHz V _{IS} = 5 V _{p-p} V _{EE} = V _{SI} = 0V	10V		0.04		%
	Frequency Response, Channel "ON" (Sine Wave Input)	R _L = 1 kΩ, V _{EE} = 0V, V _{IS} = 5V _{p-p} 20 log ₁₀ V _{OS} /V _{IS} = -3 dB	10V		40		MHz
	Feedthrough, Channel "OFF"	R _L = 1 kΩ, V _{EE} = V _{SS} = 0V, V _{IS} = 5V _{p-p} 20 log ₁₀ V _{OS} /V _{IS} = -40 dB	10V		10		MHz
	Crosstalk Between Any Two Channels (frequency at 40 dB)	R _L = 1 kΩ, V _{EE} = V _{SS} = 0V, V _{IS(A)} = 5V _{p-p} 20 log ₁₀ V _{OS(B)} /V _{IS(A)} = -40 dB (Note 3)	10V		3		MHz
t _{pHL} , t _{pLH}	Propagation Delay Signal Input to Signal Output	V _{EE} = V _{SS} = 0V	5V		25	55	ns
		C _L = 50 pF	10V		15	35	ns
			15V		10	25	ns
Control inputs, A, B, C and inhibit							
	Control input to Signal Crosstalk	V _{EE} = V _{SS} = 0V, R _L = 10 kΩ at both ends of channel. Input Square Wave Amplitude = 10V	10V		65		mV (peak)
t _{pHL} , t _{pLH}	Propagation Delay Time from Address to Signal Output (channels "ON" or "OFF")	V _{EE} = V _{SS} = 0V	5V		500	1000	ns
		C _L = 50 pF	10V		160	360	ns
			15V		120	240	ns
*AC Parameters are guaranteed by DC correlated testing. Note 3: A, B are two arbitrary channels with A turned "ON" and B "OFF".							